THE UNIVERSITY OF OKLAHOMA

GRADUATE COLLEGE

The Role of Amyloid Precursor Protein in the Mitochondria

A DISSERTATION

SUBMITTED TO THE GRADUATE FACULTY

in partial fulfillment of the requirements for the

Degree of

DOCTOR OF PHILOSOPHY

By Kriti Shukla

Norman, Oklahoma

2026

THE ROLE OF AMYLOID PRECURSOR PROTEIN IN THE MITOCHONDRIA

A Dissertation approved for the

Department of Chemistry and Biochemistry

By the committee consisting of

Heather Rice, Ph.D., co-Chair

Ann West, Ph.D., co-Chair

Christina Bourne, Ph.D., Member

Elena Zgurskaya, Ph.D., Member

Jialing Lin, Ph.D., Member

Randall Hewes, Ph.D., Member

Table of contents

Abbreviations

Aβ	Amyloid β
AcD	Acidic Domain
AD	Alzheimer's Disease
ADAM	A Disintegrin and Metalloprotease
ADP	Adenosine Diphosphate
AICD	APP Intracellular Domain
ALS	Amyotrophic Lateral Sclerosis
APLP	Amyloid Precursor Like Protein
APP	Amyloid Precursor Protein
APP FL	Amyloid Precursor Protein Full Length
ATP	Adenosine Triphosphate
BCA	Bicinchoninic Acid (assay)
BCL-xL	B-cell Lymphoma-extra Large
BiP	Binding Immunoglobulin Protein
BACE1	BETA-site APP Cleaving Enzyme-1
CTF	C-terminal Fragment
CuBD	Copper Binding Domain
DNA	Deoxyribonucleic acid
DRP1	Dynamin-related Protein 1
E1	Extracellular Domain 1
E2	Extracellular Domain 2
ETC	Electron Transport Chain

ER	Endoplasmic Reticulum
ExD	Extension Domain
FACL4	Fatty Acid CoA Ligase 4
FADH2	Flavin Adenine Dinucleotide
FUNDC1	FUN14 Domain Containing Protein 1
GFLD	Growth Factor-like Domain
GSK3β	Glycogen Synthase Kinase 3 Beta
HMOX1	Heme Oxygenase 1
IP	Immunoprecipitation
ITC	Isothermal Titration Calorimetry
KBD	Keap1 Binding Domain
KEAP1	Kelch-like ECH-associated Protein 1
KLC1	Kinesin Light Chain 1
KO	Knockout
MERCS	Mitochondria-ER Contact Sites
MFN1	Mitofusin 1
MFN2	Mitofusin 2
MM	Multimerization Motif
mtDNA	Mitochondrial DNA
NAD+	Nicotinamide Adenine Dinucleotide (Oxidized)
NADH	Nicotinamide Adenine Dinucleotide Hydrogen
NRF2	Nuclear factor erythroid 2 p45-related Factor 2
NQO1	NADH:Quinone Oxidoreductase 1

OMM	Outer Mitochondrial Membrane
PARL	Presenilin-associated Rhomboid-like
PGAM5	Phosphoglycerate Mutase Family Member 5
PINK1	PTEN-induced Kinase 1
qPCR	Quantitative Polymerase Chain Reaction
RCR	Respiratory Control Ratio
ROS	Reactive Oxygen Species
sAPPα	Soluble APP Alpha
sAPPβ	Soluble APP Beta
TOM20	Translocase of Outer Mitochondrial Membrane 20
TCA	Tricarboxylic Acid
WT	Wild Type

Acknowledgements

I would like to express my deepest gratitude to my Ph.D. committee members- Dr. Heather Rice, Dr. Ann West, Dr. Christina Bourne, Dr. Elena Zgurskaya, Dr. Jialing Lin, and Dr. Randall Hewes for their guidance, support, and invaluable feedback throughout the course of my doctoral studies. Their collective expertise and encouragement have been instrumental in shaping both this dissertation and my development as a scientist.

I am especially grateful to Dr. Heather Rice and Dr. Ann West for their mentorship, patience, and unwavering support. Your belief in my abilities has made a profound impact on my academic journey and personal growth. I could not have asked for better mentors.

I would like to thank my lab mates- Samah, Casandra, Dominika, Yvonne and Dylan for creating a collaborative and supportive environment. Your camaraderie and shared experiences made even the most challenging days enjoyable.

I would like to thank Dr. Bart De Strooper and Dr. Joris de Wit for providing APP plasmids and Dr. Apirat Chaikuad for PGAM5 plasmids. I highly appreciate the support and assistance from Dr. Philip Bourne and The University of Oklahoma Protein Production and Characterization Core (OU PPC) for all the help with protein purification and ITC experiments. I would also like to thank Dr. Yishi Jin and Dr. Michael Lenardo for sending us the PGAM5 KO mice.

I am extremely thankful to the contributions from the members of Humphries lab (OMRF), Plafker lab (OMRF) and Lin lab (OUHSC) towards my published doctoral work.

My special thanks to Anna Faakye, Kendra S. Plafker, Zhi Zhang and Satoshi Matsuzaki for their crucial contributions in the manuscript.

This work was supported by the National Institutes of Health (R35GM142726, P20GM125528 to H.C.R.), Institutional Development Award (IDeA) from the National Institute of General Medical Sciences (NIGMS) of the National Institutes of Health (NIH) (P20GM103640 to J.L. as a junior investigator), and the Presbyterian Health Foundation (Pilot Research Funding to H.C.R.; Bridge Funding to J.L..), IDeA from the NIGMS of NIH (P20GM103640 and P30GM145423), the OU Vice President for Research and Partnerships, and the OU College of Arts and Sciences.

To my parents, thank you for your unconditional love and sacrifices that made this journey possible. You have always believed in me, even when I doubted myself, and your support has been my foundation. To my sister and greatest friend, Shruti Shukla, thank you for being a constant source of strength and grounding. I am incredibly fortunate to have you by my side.

Finally, a very special thank you to Jeff Gruenbaum, my (almost) husband. Your love, patience and constant support have carried me through the highs and lows of this past year in my Ph.D. journey. Day to day, you have been my anchor and my greatest cheerleader. I am endlessly grateful to share this milestone with you.

Abstract

The amyloid precursor protein (APP) is widely recognized for its central role in the generation of amyloid-β (Aβ) peptides and the pathogenesis of Alzheimer's disease (AD). However, its normal physiological function, particularly in the mitochondria, remains incompletely understood. This study addresses this gap by investigating a novel protein-protein interaction of APP with the mitochondrial phosphatase phosphoglycerate mutase family member 5 (PGAM5) and proposes a role of this interaction on the mitochondrial respiration.

PGAM5 is a mitochondrial membrane protein and acts as a serine-threonine phosphatase towards various protein substrates. Through its substrates and binding partners, PGAM5 regulates mitochondrial mobility, mitophagy, redox homeostasis, respiration, and cell death. In this work, I demonstrate a direct, domain-specific interaction of PGAM5 with APP. My data provides evidence for an endogenous interaction between these proteins in the mouse brain. I show that both APP and PGAM5 localize and likely interact at the mitochondria-ER contact sites (MERCS). Using qPCR on isolated mitochondrial samples from mouse brains, I show that this domain-specific interaction can lead to modulation of a well-established Nrf2-dependent stress response pathway in the mitochondria by APP.

Moreover, functional experiments using APP KO mouse model reveal that the absence of APP leads to significant impairments in mitochondrial function. Specifically, mitochondria isolated from APP deficient brains exhibit reduced substrate-specific respiration and compromised activity of the electron transport chain (ETC). These

findings indicate that APP is necessary for maintaining efficient oxidative phosphorylation and ATP production in the brain mitochondria.

Mitochondrial dysfunction is often observed in AD, but the molecular pathways are poorly defined. This study demonstrates a significant reduction in PGAM5 proteolytic cleavage in AD mice. The observed decrease in PGAM5 cleavage in AD mice suggests impaired PARL activity and consequent deficits in mitophagy.

In summary, I present APP as a regulator of mitochondrial respiration while PGAM5 as a key player for impaired mitophagy seen in AD. Moreover, the novel APP-PGAM5 interaction described in this study provides a new mechanistic insight into how APP may influence mitochondrial physiology beyond its established role in amyloidogenic processing. By adding mitochondrial respiration to the repertoire of physiological functions of APP and proposing a role of PGAM5 in AD, the findings suggest a new direction for understanding and treating Alzheimer’s disease.

List of Figures

Chapter 1: Introduction

1.1 Alzheimer's Disease

Alzheimer's disease (AD) is a progressive neurodegenerative disorder and the most common cause of dementia, a condition characterized by declines in memory, thinking, and the ability to perform everyday activities[1,2]. The disease develops gradually as damage occurs to nerve cells in the brain, disrupting communication between neurons and leading to the loss of cognitive function over time[3]. Early symptoms often include difficulty remembering recent conversations, names, or events, while later stages involve more severe impairments such as confusion, disorientation, communication difficulties, and loss of the ability to perform everyday tasks. The disease develops gradually over many years, with underlying brain changes occurring long before noticeable symptoms appear. These changes ultimately cause widespread brain damage and severe cognitive decline in later stages of the illness[3].

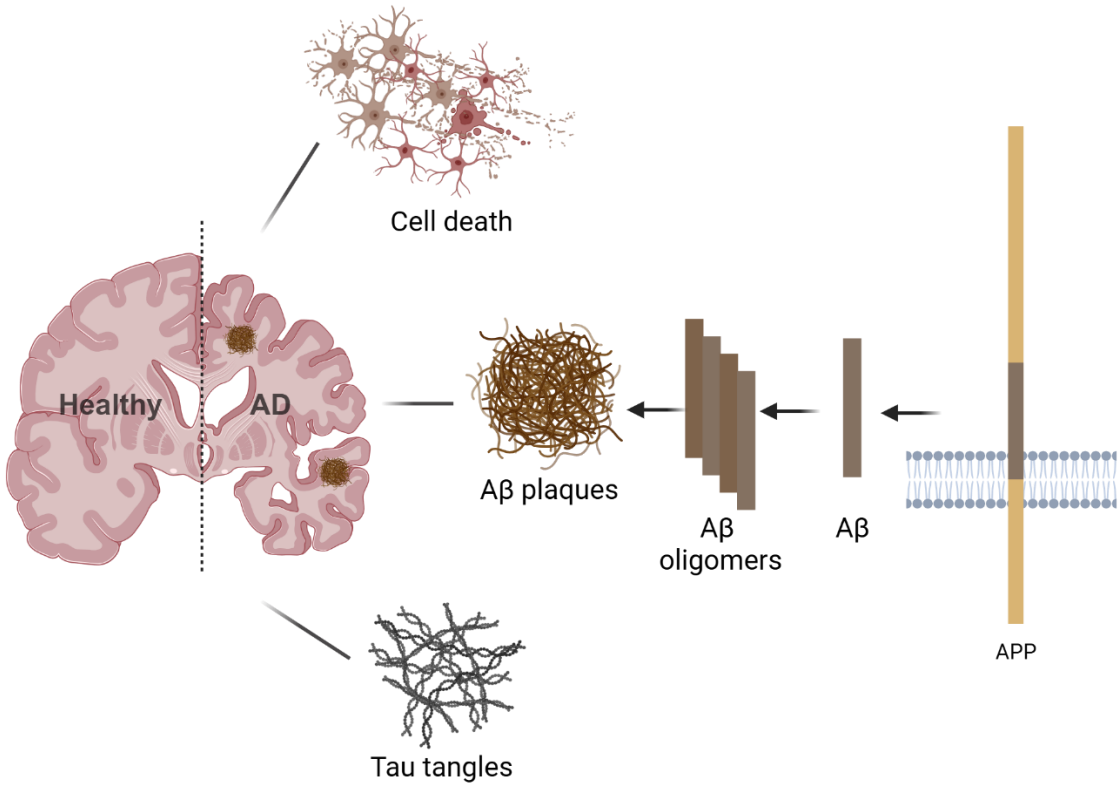

Figure 1. Overview of Alzheimer's disease pathology. A. Schematic representation of pathological features in Alzheimer's disease (AD) shown by accumulation of amyloid-β (Aβ) plaques, neurofibrillary tau tangles and cell death resulting in shrinkage of brain tissue in AD. B. The Aβ plaques are formed by aberrant oligomerization of Aβ peptides, produced by proteolytic cleavage of APP. Created in BioRender. Shukla, K. (2026) https://BioRender.com/5b9yw71.

The pathological hallmarks of Alzheimer's disease include cell death, extracellular accumulation of beta-amyloid (Aβ) plaques and neurofibrillary tangles composed of tau protein within neurons[4,5]. These abnormal protein deposits disrupt neuronal communication and lead to widespread brain tissue damage. Amyloid-beta (Aβ) is produced during the proteolytic cleavage of the Amyloid Precursor Protein (APP)[6,7]

(discussed in detail in chapter 1.3). This peptide, being sticky in nature, oligomerizes and gets deposited as plaques in the extracellular spaces in the brain (Figure 1). Because Alzheimer's disease progressively worsens and currently has no cure, it represents a major public health concern, with millions of individuals affected and the number expected to increase as population ages[8]. In addition to the medical impact, the disease places a major burden on families and healthcare systems due to the long-term care needs of affected individuals. Although the exact cause of Alzheimer's disease is complex and involves multiple factors such as age, genetics, and biological processes in the brain, understanding these mechanisms has been essential for advancing research and developing potential treatments.

Beyond the above-mentioned hallmarks, mitochondrial dysfunction is also a crucial contributor to the development and progression of AD, expanding AD pathology beyond amyloid-β and tau tangles. Studies from as early as 1990s have shown that mitochondrial function is significantly disrupted in AD (Figure 2), leading to widespread neuronal damage[9,10]. Several others have since then tightly linked mitochondrial dysfunction to both the onset and progression of AD[11–16].

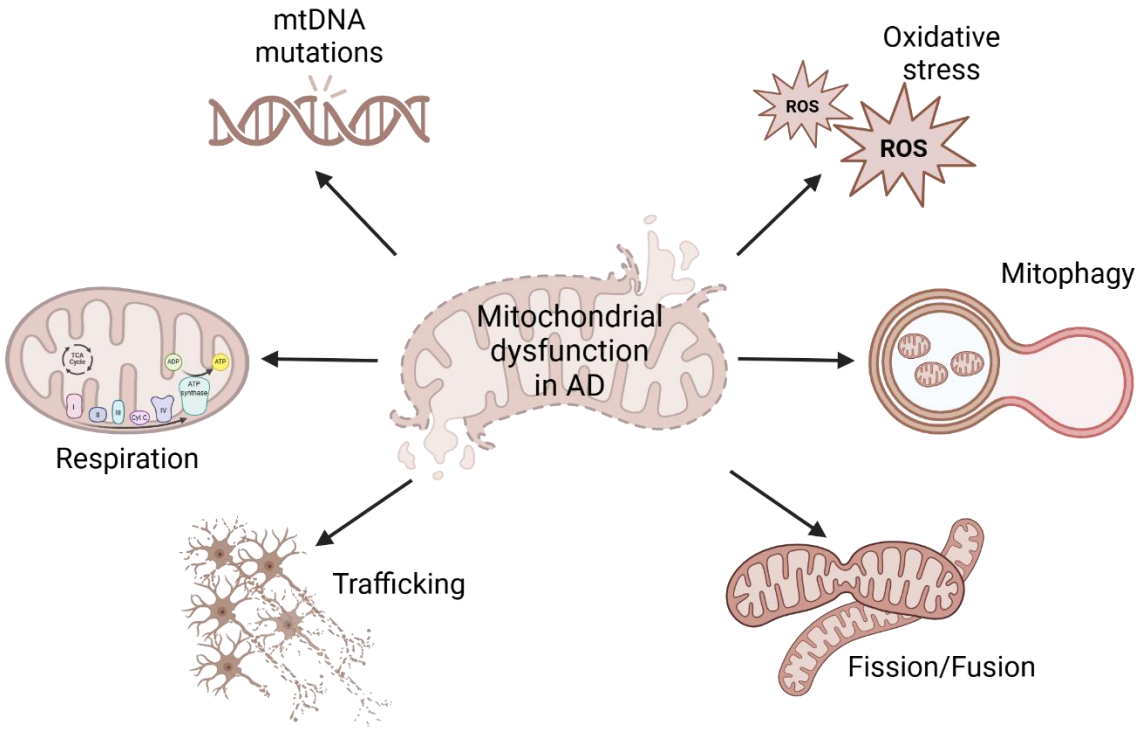

Figure 2. Mitochondrial dysfunction in Alzheimer's Disease. Schematics showing processes in the mitochondria that are altered in Alzheimer's Disease. Clockwise- excessive reactive oxygen species (ROS) generation leading to oxidative stress conditions, impaired clearance of defective mitochondria via mitophagy, fission and fusion imbalances, impairment in mitochondrial trafficking in neuronal compartments, defective oxidative phosphorylation resulting in poor respiration and mutations in mitochondrial DNA (mtDNA). Created in BioRender. Shukla, K. (2026) https://BioRender.com/p55kw1r.

One of the primary alterations is impaired energy production, as defects in the electron transport chain reduce ATP generation, leaving neurons without sufficient energy to maintain normal function[17,18]. At the same time, mitochondria produce excessive reactive oxygen species, increasing oxidative stress and damaging mitochondrial

DNA[13,19–21]. Additionally, mitochondrial dynamics are altered[22,23], with increased fragmentation and reduced fusion, resulting in smaller, less efficient mitochondria that are poorly distributed within neurons[24,25]. In healthy neurons, mitochondria are transported to areas of high energy demand, such as synapses, but this movement is disrupted in Alzheimer's disease, contributing to early synaptic failure[26].

Another key mitochondrial process, mitophagy, is also altered in AD. Mitophagy is a process where dysfunctional or damaged mitochondria are targeted for degradation by lysosomes. It acts as a crucial mitochondrial quality control mechanism, ensuring cellular homeostasis by preventing the accumulation of toxic or damaged organelles. In AD, the clearance of damaged mitochondria is reduced, leading to cellular stress[12,27]. Disrupted calcium signaling is also often seen in AD which is exacerbated by the presence of amyloid-β and tau, which directly impair mitochondrial structure and function[28–30]. Together, these alterations in normal mitochondrial biology contribute to progressive neurodegeneration and cognitive decline seen in AD.

1.2 Mitochondria-ER Contact Sites (MERCS) in Alzheimer's Disease

Mitochondria are essential organelles responsible for energy production, cellular metabolism, and maintaining cellular homeostasis. These dynamic structures are often described as the "powerhouses" of the cell due to their critical role in oxidative phosphorylation and ATP synthesis. Beyond their classical functions in energy metabolism, mitochondria are also deeply involved in a wide range of cellular processes, including cell death, calcium signaling, and reactive oxygen species (ROS) regulation. One emerging area of mitochondrial research focuses on mitochondrial interactions with other cellular organelles, particularly the endoplasmic reticulum (ER). Mitochondria and the ER are spatially and functionally interconnected through specialized regions known as Mitochondria-Endoplasmic Reticulum Contact Sites (MERCS). These two organelles are intricately connected, and many of their biological processes overlap, particularly mitophagy, lipid trafficking, ROS cross signaling[31,32] and mitochondrial protein quality control (usually affecting mitochondrial dynamics through trafficking, fission and fusion) (Figure 3). These overlapping processes are crucial for maintaining cellular health, and their dysregulation contributes significantly to the pathogenesis of Alzheimer's disease[33]. Mitophagy is an example that highlights the importance of inter-organelle communication between mitochondria and MERCS as upon mitophagy induction, crucial mitophagy related proteins like PINK1 and BCL-1 re-localize to the MERCS to promote autophagosome formation. MERCS have gained significant attention for their role in mediating cellular responses to stress and disease, with emerging evidence linking these contact sites to neurodegenerative diseases like AD.

Increasing contacts between mitochondria and the ER has been implicated in Alzheimer's disease[34–36]. Studies on AD mice have shown changes in the structure and function of MERCS in the early stages of amyloid accumulation that predate symptoms of AD, such as memory loss[37]. This leads to the hypothesis that MERCS dysregulation may impact the progression of AD. This is plausible as many functions of MERCS are prerequisites for neurodegeneration[38]. Altered levels of MERCS-resident proteins in AD brains further support the idea that dysregulated mitochondria-ER communication is central to disease progression. Overall, MERCS dysfunction appears early in both familial and sporadic AD and may contribute to multiple pathological features, making it a promising target for therapeutic intervention[12]. Pharmacological agents, small molecules, and transcriptional modulators, including microRNA-based approaches, demonstrate the capacity to restore MERCS function, improve mitochondrial dynamics, and mitigate oxidative stress, although specificity and off-target effects remain significant challenges[39-41]. Beyond conventional drug design, emerging strategies such as mitochondrial transplantation and peptide-mediated delivery systems further highlight the therapeutic potential of restoring mitochondrial function and MERCS integrity[42,43]. These approaches have shown encouraging results in preclinical models, including improved bioenergetics, reduced reactive oxygen species, and enhanced neuronal survival and regeneration[43]. There is also emerging evidence that MERCS influence amyloid precursor protein (APP) processing, potentially affecting amyloid-beta production, a hallmark of AD[44].

Despite these advances, the complexity of MERCS regulation, variability across disease states, and incomplete understanding of their mechanistic roles present ongoing limitations. Future studies targeting more MERCS-resident proteins is necessary to fully define the role of this inter-organelle compartment in AD. Comprehensive *in vivo* studies across multiple stages of both familial and sporadic AD is required to fully define the temporal dynamics of MERCS remodeling and to identify optimal therapeutic windows.

Lastly, MERCS functions are largely governed by tethering proteins as discussed in this section. Dysregulation of these proteins contributes to the pathogenesis of Alzheimer's disease (AD) and other neurodegenerative disorders[45]. This shows that altered MERCS integrity and protein expression are potential hallmarks of disease progression. Consequently, targeting MERCS-resident proteins and pathways has emerged as a promising therapeutic strategy[46-49]. As more MERCS-resident proteins are being recognized to play a role in Alzheimer's Disease, roles of several others are still unexplored.

Dysregulation of key MERCS proteins (MFN1, MFN2 and TOM70) has been observed in both SAD and FAD, implicating MERCS dysfunction in AD pathology[23,50,51]. Before the formation of tau tangles in a mouse model of Alzheimer's disease (JNPL3 mice expressing mutant tau P301L), researchers found a significant increase in physical contact between rough endoplasmic reticulum membranes and mitochondria in affected neurons compared to wild-type mice[52]. MERCS associated proteins, PACS2 and Sig1R, were shown to be essential for neuronal survival. These MERCS proteins were

upregulated in the AD brain and $APP_{Swe/Lon}$ mouse model where up-regulation was observed before the appearance of plaques[53]. This study showed that nanomolar concentrations of amyloid β-peptide increased the expression of MERCS-resident proteins- inositol-1,4,5-triphosphate receptor and voltage-dependent anion channel (VDAC) protein expression[53]. Additionally, PS2 mutations increase the ER–mitochondria connection in the fibroblasts of patients with sporadic AD[54]. In APPswe cells, analysis revealed altered tethering protein levels: MFN1 increased at MERCS, while MFN2 decreased across all subcellular fractions[55]. Transmission electron microscopy showed a mild reduction in close ER-mitochondria contacts (≤25 nm) and a significant decrease in mitochondria per cell. Confocal microscopy confirmed a ~25% reduction in mitochondrial mass and perinuclear localization in APPswe cells[55]. Levels of MERCS resident proteins MFN1, MFN2 and TOM70 are decreased in human post-mortem cortex from FAD APP^{swe} patients[50].

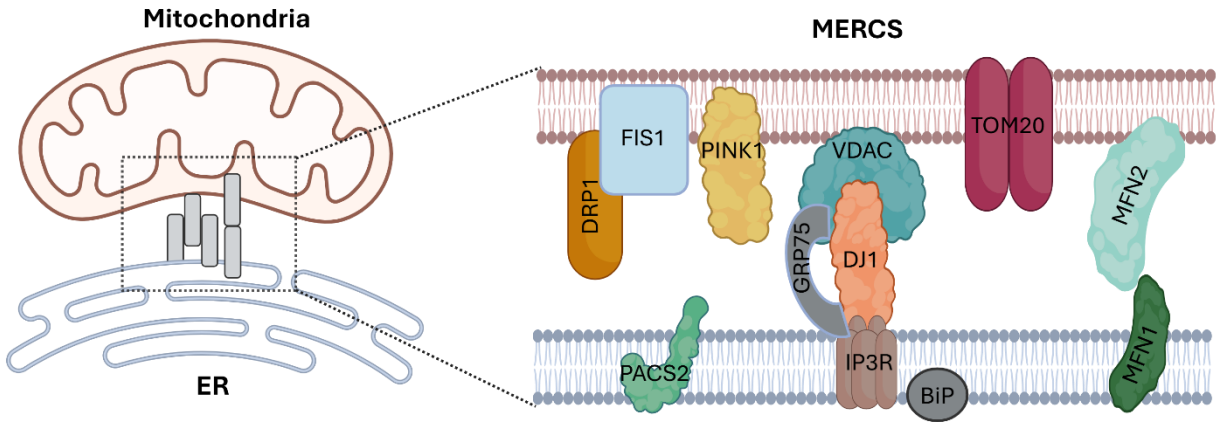

Figure 3. Mitochondria-ER contact sites. Schematics showing proteins crucial to maintain Mitochondria-ER contact sites (MERCS) structure and function.

1.2.1 Mitochondrial dynamics (fission and fusion)

Mitochondria-ER contact sites (MERCS) play a central role in cellular aging by regulating mitochondrial function, dynamics, and quality control. As mitochondrial dysfunction is a key hallmark of aging, MERCS contribute by coordinating mitochondrial fission and fusion processes that maintain a healthy mitochondrial network[12,56]. They act as physical platforms where fission is initiated through recruitment of key proteins like Drp1[57,58], while also supporting fusion through proteins such as Mfn2 that tether mitochondria to the ER[59]. This dynamic interaction ensures damaged mitochondria can be removed and functional ones maintained, helping cells adapt to stress and prevent degeneration.

Immunoblot analysis of AD hippocampus samples revealed decreased expression of DRP1. DRP1 overexpression prevented oligomeric Aβ-induced synaptic loss in primary neurons[23,60]. This suggests that an altered balance in mitochondrial fission and fusion is an important mechanism leading to synaptic dysfunction in the AD brain. More recent work in Drp1+/− x APP mice revealed that mitochondrial dysfunction is reduced in these mice relative to APP mice. These results were replicated with Drp1+/− x Tau mice relative to Tau mice[61]. Sandwich ELISA assay revealed that soluble Aβ levels were significantly reduced in Drp1+/− x APP mice relative to APP mice, indicating that reduced Drp1 decreases soluble Aβ production in AD progression. In a study, frontal cortices from patients at all stages of AD development (Braak stage I/II [early AD], III/IV [definite AD], and V/VI [severe AD]), there was an increased expression of Drp1[24]. IHC data also showed increased Drp1 in these AD patients.

In mammals, mitochondrial fusion is coordinated by dynamin-related GTPases, with mitofusin-1 (Mfn1) and mitofusin-2 (Mfn2) mediating outer mitochondrial membrane (OMM) fusion and OPA1 facilitating inner membrane fusion. Mfn2 also supports MERCS functions[62]. Dysfunctions in Mfn1, Mfn2, or OPA1 are linked to neurodegenerative diseases like Alzheimer's disease. Recent evidence indicates that Tau overexpression impairs fusion-fission balance and disrupts mitochondrial dynamics, possibly by stabilizing Actin and inhibiting Drp1-mediated fission[63,64]. Another study showed that AD neurons exhibit reduced levels of key fusion proteins (OPA1, Mfn1, Mfn2) leading to abnormal mitochondrial distribution in axons and neuronal processes[23]. In APPswe cells, Western blot analysis showed a significant decrease in the fusion protein MFN2, while MFN1 was unchanged, indicating impaired mitochondrial dynamics[55].

1.2.2 Lipid homeostasis

MERCS are also a location for the synthesis of sphingolipids, and contain high levels of these lipids, including cholesterol[65,66]. Recently, cholesterol levels have been tied to PINK1 biology and to defective mitophagy in Alzheimer's disease[67]. Both PS1 and PS2 are enriched in the MERCS[68] and mutations in PS2 increase MERCS formation and enhance cholesteryl ester and phospholipid synthesis in the cellular models[54,69]. Exposure of oligomeric Aβ in primary hippocampal neurons increases MERCS and alters Ca^{2+} homoeostasis[53]. Individuals carrying the ε4 allele of apolipoprotein E (ApoE4) have increased risk for developing AD compared to the ones carrying ApoE3, the most common isoform. Cells treated with ApoE4 containing astrocyte conditioned media (ACM) have increased synthesis of phospholipids and of cholesteryl esters compared to those

treated with ApoE3 containing ACM, suggesting an upregulated MERCS functions in the cells[70,71]. Moreover, familial or sporadic AD patient fibroblasts were found to have increased ER-mitochondria coupling and MERCS function, including phospholipid and cholesterol metabolism[35].

1.2.3 Ca^{2+} signaling

Experimental studies show that oligomeric Aβ42 increases ER-mitochondria connectivity and ER to mitochondria Ca^{2+} transfer in hippocampal neurons[72]. Disruption in MERCS function also reduces γ-secretase activity, while defects in PS1 and PS2 can increase ER-mitochondria contacts and Ca^{2+} transfer[54,73]. Mutations in these proteins also enhance calcium release from the ER, promoting further APP cleavage, and amyloid-β itself can increase ER-mitochondria coupling[53]. In a healthy cell, a MERCS-resident protein Sig-1R forms a Ca^{2+}-sensitive chaperone complex with Bip/GRP78 and promotes Ca^{2+} release from the ER by stabilizing IP3R3. It has been proposed that Sig-1R forms part of the endogenous defense system against AD[74]. Reportedly, compounds with Sig-1R agonist activity possess neuroprotective abilities. These findings have highlighted the importance of Ca^{2+} signaling as a promising therapeutic target for AD[47,75]. A recent study indicates that Aβ accumulation induces *in vivo* mitochondrial Ca^{2+} overload via increased ER-mitochondria crosstalk[72], leading to neuronal death[30].

1.2.4 Redox homeostasis

Oxidative stress is a common feature of the aging process and of many neurodegenerative disorders, including Alzheimer's disease[13,14,21]. A study found local

increase in the Aβ42 levels upon direct infusion of oxidizing agents into the hippocampus of wild type mice[76]. MERCS are an important site for regulating oxidative stress in the cell. Unfolded Protein Response (UPR), originating in the ER, often due to misfolding of proteins signals downstream of ER stress, through the MERCS to re-establish homeostasis. The UPR stress receptor kinases, PERK and IRE1, are found to be located at MERCS[77]. Mitohermis is a process where moderate mitochondrial stress activates beneficial signaling pathways to improve mitochondrial function and stress resistance. Mitohermis is triggered by the presence of ROS at the MERCS[78] and activates the PERK-ATF4-Nrf2 pathway which helps regulate redox balance and mitochondrial respiration[79,80]. Studies show that disrupting this pathway (deleting Nrf2) impairs the adaptive response. Consistent with this, reduced Nrf2 activity failed to counter the high levels of ROS, facilitating AD progression[20,81]. Additionally, Nrf2 expression in the nucleus of neurons and astrocytes, is reduced in the CA1 region of hippocampus in the AD patients[82]. Studies show that removing or reducing Nrf2 genetically increases accumulation, interferon-gamma (IFNγ) levels, and exacerbates cognitive deficits in AD mouse models[81,83,84].

1.3 Amyloid Precursor Protein

Amyloid precursor protein (APP) belongs to a highly conserved family of type I (N-terminal outside the cell and C-terminal inside the cell) transmembrane proteins that are found across a wide range of species, from invertebrates to mammals. Members of this family include APL-1 in C. elegans, APPL in Drosophila, and in mammals[85,86], APP itself along with its homologs APP-like proteins 1 and 2 (APLP1 and APLP2)[85,87]. The

presence of these homologous proteins across evolution highlights their fundamental biological importance. Evidence for functional conservation across species comes from experiments showing that human APP can partially rescue behavioral defects in fruit flies lacking APPL[86]. In terms of expression, APP family proteins are particularly abundant in the nervous system. In mammals, APLP1 is expressed almost exclusively in neurons[88]. APP and APLP2 are also highly enriched in the brain, but unlike APLP1, they are more widely expressed and can be detected in many other tissues throughout the body. This broader distribution suggests that APP and APLP2 may have both neural and non-neural functions, while APLP1 may play a more specialized role in neuronal biology[89].

The human APP gene is located on chromosome 21 and spans approximately 240 kilobases[90,91]. It contains at least 18 exons and undergoes alternative splicing, a process that allows a single gene to produce multiple protein variants. As a result, several APP isoforms are generated, ranging in size from 365 to 770 amino acids. Among these, the most well-studied isoforms are APP695, APP751, and APP770[92]. These isoforms differ in their structure and tissue distribution, which likely reflects differences in their biological roles. For example, in the central nervous system, neurons primarily express the APP695 isoform, while the longer isoforms are more broadly distributed across tissues[93].

By getting sequentially cleaved by enzymes, APP serves as the parent protein of Aβ peptides, which aggregate into brain plaques and are a defining feature of Alzheimer's disease[7,94]. APP undergoes a process known as regulated intramembrane proteolysis, in which it is sequentially cleaved by different enzymes to produce various fragments.

This processing occurs through two main pathways: the non-amyloidogenic and amyloidogenic pathways[95] (Figure 3). In the non-amyloidogenic pathway, APP is first cleaved by α-secretase within the Aβ region, preventing the formation of Aβ. This produces a soluble fragment called sAPPα and a membrane-bound fragment that is later cleaved by γ-secretase (an enzyme complex composed of multiple proteins including presenilin, nicastrin, APH1, and PEN2) to generate a smaller peptide (P3) and the AICD[96]. This pathway is considered protective and is the predominant route under normal physiological conditions. In contrast, the amyloidogenic pathway involves initial cleavage by β-secretase, producing sAPPβ. sAPPβ is then cleaved by γ-secretase, leading to the production of Aβ peptides. In neurons, the primary β-secretase is BACE1[97], a transmembrane aspartyl protease. In contrast, α-secretase activity is carried out by several enzymes, including members of the ADAM (A Disintegrin and Metalloproteinases) family such as ADAM10 and ADAM17[96]. A shift in balance between these two pathways increases Aβ production and leads to aggregation of Aβ into extracellular plaques, a key pathology of Alzheimer's disease. Interestingly, APP-like proteins (APLP1 and APLP2) undergo similar processing but do not produce Aβ, instead generating non-pathological fragments, emphasizing that Aβ production is a unique and disease-related feature of APP and highlights the importance of further studying this protein[98].

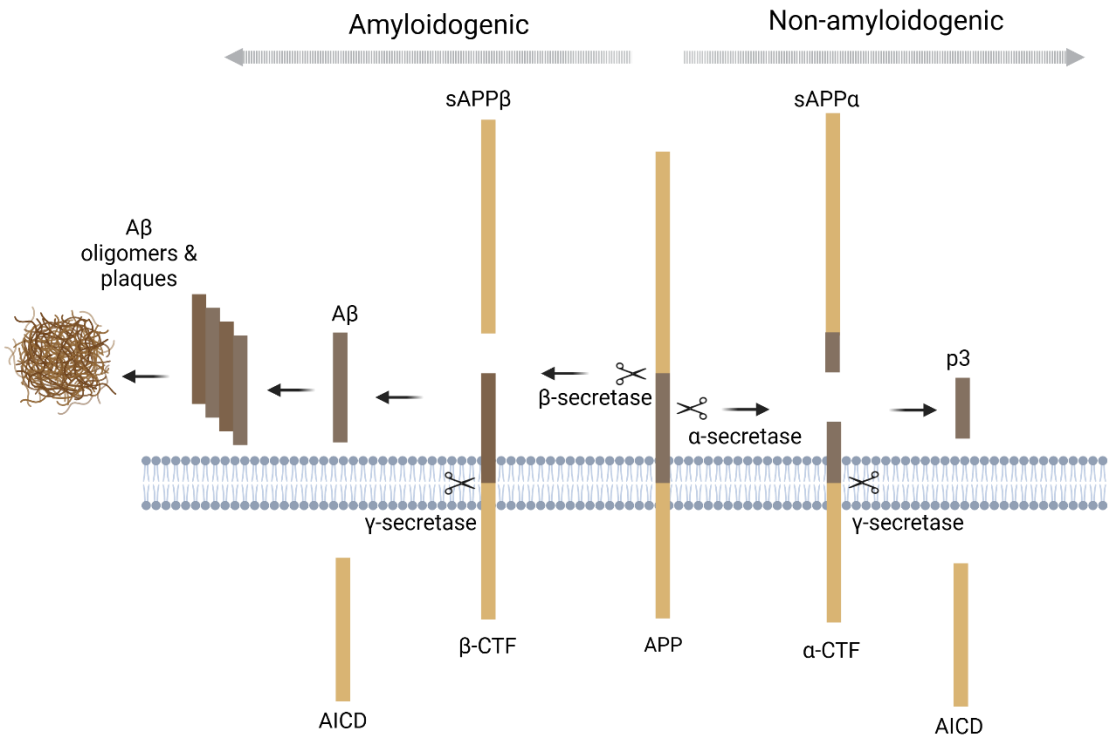

Figure 4. APP processing. Schematics showing proteolytic cleavage pathways of Amyloid Precursor Protein.

APP is a type I transmembrane protein composed of three main parts: a large extracellular N-terminal region, a single membrane-spanning region, and a short intracellular C-terminal tail[99,100] (Figure 4). The extracellular region of APP is composed of several distinct domains that contribute to its diverse functions. These include extracellular domains followed by a juxta membrane segment linking them to the transmembrane domain. Within these regions there are specialized subdomains, such as a growth factor-like domain (GFLD) and copper-binding domains (CuBD) (formerly known as E1), and a heparin-binding domain in E2[101]. APP751 and APP770 isoforms also contain additional domains, including the Kunitz protease inhibitor (KPI) domain and the Ox-2 antigen domain, which may influence interactions with extracellular

molecules[102]. These KPI-containing isoforms are expressed in a wide variety of tissues, suggesting they may have more general physiological functions. In contrast, APP695 lacks the KPI domain and is predominantly expressed in neurons[103]. This neuron-specific expression pattern implies that APP695 may be particularly important for brain-specific processes such as synaptic activity or neural development[90].

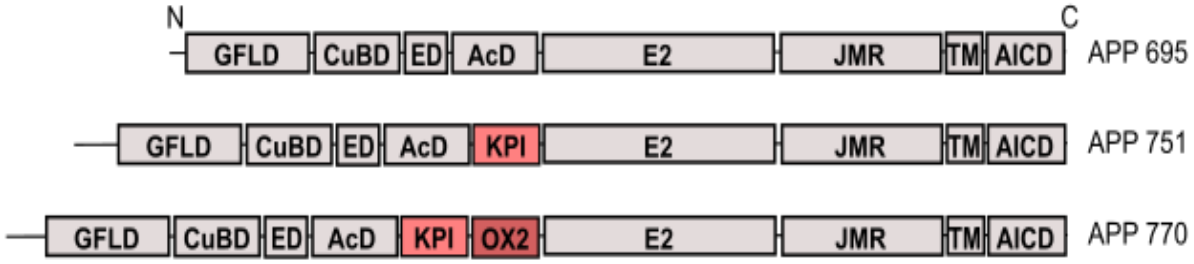

Figure 5. Mammalian isoforms of APP. Schematics showing differences in domain arrangements between different mammalian isoforms of Amyloid Precursor Protein. GFLD- Growth-factor like domain; CuBD- Copper binding domain; ED- Extension domain; AcD- Acidic domain; E2- Ectodomain 2; JMR- Juxtamembrane region; TM- Transmembrane; AICD- APP intracellular domain.

APP also undergoes phosphorylation at multiple sites in both its extracellular and intracellular domains[104,105]. Most studied phosphorylation site in APP is threonine 668 (Thr668) in the intracellular VT668PEER motif. Kinases such as CK1/2, CDK5, JNK1/3, CDK1/CDC2, and GSK3β mediate this phosphorylation[106], which influences APP biology, but less is known about the phosphatases of APP with only one study suggesting that Protein phosphatase 1 can modulate APP phosphorylation[107]. Studies

have shown that Thr668 phosphorylation directs APP to growth cones and nerve terminals, contributes to Aβ generation, protects APP from caspase cleavage and alters interactions with adaptor proteins like Fe65 and Mint-1/X11a, affecting APP's nuclear signaling and trafficking[108]. Thr668 phosphorylation also influences APP processing and endocytic trafficking. Another study showed that Thr668 phosphorylation enables the Pin1-mediated cis/trans isomerization of the Thr668-Pro669 bond, impacting APP conformation and possibly accelerating Alzheimer's disease pathology[109].

Structural analyses of APP reveal a high degree of heterogeneity, with the full-length protein comprising both well-structured domains and intrinsically disordered regions. This structural complexity indicates that APP likely performs multiple functions mediated by distinct regions of the protein, potentially through interactions with a variety of macromolecules. A full-length three-dimensional structure of APP has not yet been resolved. This is largely due to the inherent difficulty of studying membrane proteins at atomic resolution. While structural information is available for several isolated domains, the functional outcome from the intact protein remains poorly characterized[100–102,110]. Existing evidence suggests that the cytoplasmic C-terminal region lacks a stable tertiary structure, whereas the transmembrane segment is likely α-helical[111]. The extracellular soluble domain of APP (sAPP) represents a particularly important focus of study in the field, as it is capable of independent folding, exhibits significant biological activity, and is more experimentally accessible than the full transmembrane protein[99,112].

Several domains within the APP protein have been structurally and functionally characterized. These include the protease inhibitory (Kunitz-type) domain present in certain isoforms, which functions as an independent folding unit and mediates

interactions with receptors such as the LDL receptor-related protein[102]. The N-terminal region contains binding sites for molecules such as heparin, copper, and zinc, although these segments likely do not function as fully independent structural units within the intact protein[101]. Further along the extracellular region, central domains include a well-conserved α-helical structure involved in binding extracellular matrix components such as collagen and laminin, as well as other ligands[99,111,112]. In contrast, regions closer to the membrane appear to lack defined secondary structure and are highly susceptible to proteolytic cleavage, consistent with their role in processing by α- and β-secretases[113].

APP engages in a wide range of interactions including cations, extracellular ligands and intracellular partners, supporting roles in cell adhesion, signaling, and extracellular matrix interactions[114,115]. Importantly, these interactions are not independent; binding events at one site can influence the affinity or activity at others, indicating coordinated interdomain communication[116]. Post-translational modifications, including glycosylation[117] and phosphorylation[105], further regulate APP function and demonstrate crosstalk between extracellular and cytoplasmic regions. Additionally, like other cell surface receptors, APP has been shown to undergo dimerization, which may serve as a mechanism for transducing signals across the membrane[103]. Small-angle X-ray scattering data showed that these can be homodimers or dimers with APLP1 and APLP2[118,119]. This dimerization can be influenced by metal ions such as copper and may play a role in regulating APP function.

1.3.1 APP functions

The physiological roles of Amyloid Precursor Protein go far beyond its involvement in Alzheimer's disease. During neuronal development and connectivity, APP regulates neurite outgrowth[114,120,121] and axonal generation[122] by interacting with extracellular receptors[115]. APP and its soluble cleavage products also support neuronal differentiation and migration[123]. APP expression is upregulated during brain development and after injury, suggesting a role in circuit formation and repair[124]. APP also functions as a cell adhesion molecule, helping stabilize cell-to-cell contacts that are crucial for synaptogenesis. This was shown by a study where neurons from APP KO mice had reduced dendritic spine density, impaired synaptic structure and neuromuscular junction defects[125]. This synaptic role is further supported by evidence that soluble APP fragments such as sAPPα have neurotrophic effects, promoting dendritic complexity and synaptic plasticity underlying learning and memory[89,115,126]. Knock-out studies also highlight the biological importance of APP as compared to its mammalian homologues APLP1 and APLP2. While APP KO produces clear neuronal and functional deficits, APLP1/2-KO are largely mild or phenotypically silent unless combined with APP loss[127,128]. These studies show that APP has unique, non-redundant role in maintaining synaptic functions whereas APLPs might provide compensatory support that becomes critical only in the absence of APP.

Beyond development, APP may also be involved in gene expression, especially through its intracellular domain, AICD[129]. APP can also act as a membrane cargo receptor for kinesin-I[130]. APP binds directly to the kinesin light chain 1 (KLC1) subunit of the kinesin-1 motor, which drives fast anterograde transport and absence of functional APP leads

to reduced axonal transport rates[131,132]. APP functions to regulate neuronal iron content by stabilizing ferroportin, which is the only iron exporter channel of cells[133]. Consistent with this, a study found that brain ferroportin levels were decreased in APP KO mice[134]. These multifaceted roles highlight that proper APP expression and processing are essential for maintaining neuronal homeostasis, synaptic integrity, and functional plasticity in the healthy brain.

1.3.2 Subcellular localization of APP and its fragments

APP is synthesized in the endoplasmic reticulum (ER), trafficked through the Golgi apparatus, and localized primarily at the cell surface/plasma membrane[135]. It undergoes several post-translational modifications along the way, including N- and O-linked glycosylation, phosphorylation, and tyrosine sulfation[108,117,136]. Once matured, full-length APP gets cleaved by either α- or β-secretase within its extracellular domain and results in the release of soluble fragments (sAPPα and sAPPβ) in the inter-cellular space[97,137]. This process leaves behind membrane-bound carboxyl-terminal fragments (CTFs) which are further processed by γ-secretase. This cleavage occurs at the carboxyl-terminal end of the Aβ region and generates either a small peptide known as P3 (when preceded by α-secretase cleavage) or the amyloid-β (Aβ) peptide (when preceded by β-secretase cleavage), along with the APP intracellular domain (AICD). These processing events can take place in various parts of the cell, including the cell surface and intracellular organelles including trans-Golgi network, ER and mitochondria-ER contact sites (MERCS)[44]. Moreover, full-length APP that reaches the cell surface is rapidly internalized through a conserved sequence motif known as YENPTY, after which it is either directed to endosomes for further processing or recycled back to the

plasma membrane[135,138]. However, the mechanisms by which APP and γ-secretase traffic to MERCS after maturation in the Golgi and endosomes remain unclear.

Although APP is mostly known to localize at the plasma membrane and ER, studies over the past two decades have consistently reported its localization to mitochondria across multiple models and human tissues. Initial studies demonstrated that APP contains an N-terminal mitochondrial targeting domain[139] and that specific positively charged amino acids regulate its mitochondrial import in human cortical neurons and PC12 cells[140]. Postmortem human brain studies further confirmed mitochondrial localization of APP, with early reports suggesting its presence predominantly in AD cases, where it appeared associated with mitochondrial outer and inner translocases (TOMM40 and TIM23, respectively) and possibly impaired mitochondrial protein import[141]. APP and its proteolytic products have been shown to localize at the mitochondria in both normal and AD samples[140,142]. The extracellular domains of APP as well as Aβ bind directly to the ATP synthase α-subunit at the cell surface of neurons and astrocytes[143]. Expressing APP increased cell-surface ATP synthase levels, suggesting APP helps recruit ATP synthase to the membrane[143]. Research also shows that γ-secretase components including presenilin 1/2, Nicastrin, APH1, and PEN2 are present in mitochondria and MERCS, where they may process APP fragments to generate AICD and potentially Aβ[44].

1.3.3 APP in Mitochondria and MERCS

Although APP functions in the brain are well-established, the studies examining the roles of APP at the mitochondria are limited and have produced mixed results across various cell types and in vivo models[144]. Within mitochondria, both full-length APP and

its proteolytic fragments appear to have context-dependent effects[145,146] although their precise roles are not fully defined yet. Overexpression of APP in HCN1A, SH-SY5Y, PC12, and HEK cells has been reported to induce bioenergetic stress, including reduced ATP production, decreased cytochrome oxidase activity, altered mitochondrial membrane potential, increased reactive oxygen species (ROS), and changes in apoptosis, although effects vary by cell type and experimental conditions[147–149]. Accumulation of full-length APP and its fragments in mitochondria and MERCS has been linked to impaired mitochondrial respiration, increased cytochrome c release, altered lipid composition, and DNA damage, with modulation of BACE activity reducing these effects[64,141,145,150,151]. On the other hand, APP loss-of-function studies highlight its crucial role in maintaining mitochondrial health. APP knockout mice exhibit behavioral deficits, increased gliosis, altered astrocytic calcium signaling, reduced mitochondrial calcium handling, and fragmented mitochondrial morphology, all of which can be partially rescued by restoring APP expression[152]. Similarly, in HeLa cells, loss of mitochondrial-localized APP leads to increased ROS, ATP depletion, membrane depolarization, and mitochondrial fragmentation[153]. Evidence also suggests that APP may participate in autophagy and mitophagy, potentially acting as a recognition receptor for ubiquitination of proteins critical for synaptic function[154].

Abnormal processing of amyloid precursor protein (APP) is a key feature of Alzheimer's disease (AD), with mutations in PS1 and PS2 (components of the γ-secretase complex) playing a major role in familial AD. These proteins along with BACE (β-secretase) and APP are enriched at MERCS[155], highlighting the importance of mitochondria-ER interactions in APP processing[68,156]. Our preliminary subcellular fractionations of HeLa

cells show localization of APP and its cleavage products across distinct subcellular compartments (Figure S2). Consistent with the literature, full-length APP (APP-FL) was found to be highly enriched in plasma membranes, but a significant amount was also present at MERCS (Figure S2A). Interestingly, although mitochondria had the highest levels of APP C-terminal fragments (APP-CTF) (Figure S2B), multiple amyloid-beta (Aβ) species, including Aβ38, Aβ40, and the pathogenic Aβ42, were found at markedly elevated levels within MERCS (Figure S2C-E). Notably, the enrichment of Aβ42, strongly implicated in AD pathogenesis highlights the pathological significance of this organelle. Together, these findings support that MERCS are key subcellular hubs for APP processing and suggest that their dysfunction may directly contribute to the development and progression of Alzheimer's disease.

Since APP contains multiple binding domains as discussed earlier, its diverse functions at the mitochondria can be a result of its ability to interact with a wide range of other proteins. Understanding these interactions is key to clarifying how APP contributes to normal mitochondrial functions. It can also provide valuable insight into potential therapeutic targets, as disrupting harmful interactions or enhancing beneficial ones could influence disease progression.

1.4 Phosphoglycerate Mutase Family Member 5

Phosphoglycerate Mutase (PGAM) is a class of enzymes that catalyze the reversible conversion of 3-phosphoglycate to 2-phosphoglycate during glycolysis. Although most members of this family (like PGAM1 and PGAM4) mediate phosphate transfer through a highly conserved phosphohistidine signature motif in the PGAM domain, PGAM5 instead acts as a GTPase activator and a serine-threonine phosphatase[157]. PGAM5 represents a unique adaptation within the phosphoglycerate mutase family, combining ancestral structural features with a specialized regulatory phosphatase function critical for mitochondrial biology[158].

PGAM5 is a structurally complex protein composed of three main regions: an N-terminal mitochondrial targeting sequence, a central region with functional motifs, and a C-terminal phosphatase domain (Figure 4). The N-terminus contains a conserved WDXNWD motif that promotes multimer formation and enzyme stability. PGAM5 can be present as dimers or dodecamers (12-mer). The N-terminus also includes a transmembrane helix that anchors the protein to mitochondria. Cleavage at this helix (aa 24-25) by PARL can release part of PGAM5 into the cytoplasm[159]. Its C-terminal domain houses a conserved catalytic center that can adopt different structural states depending on phosphate binding[158,160]. PGAM5 can form dimers through intermolecular interactions, though these are less active, while dodecamerization is essential for maximal enzymatic activity[158].

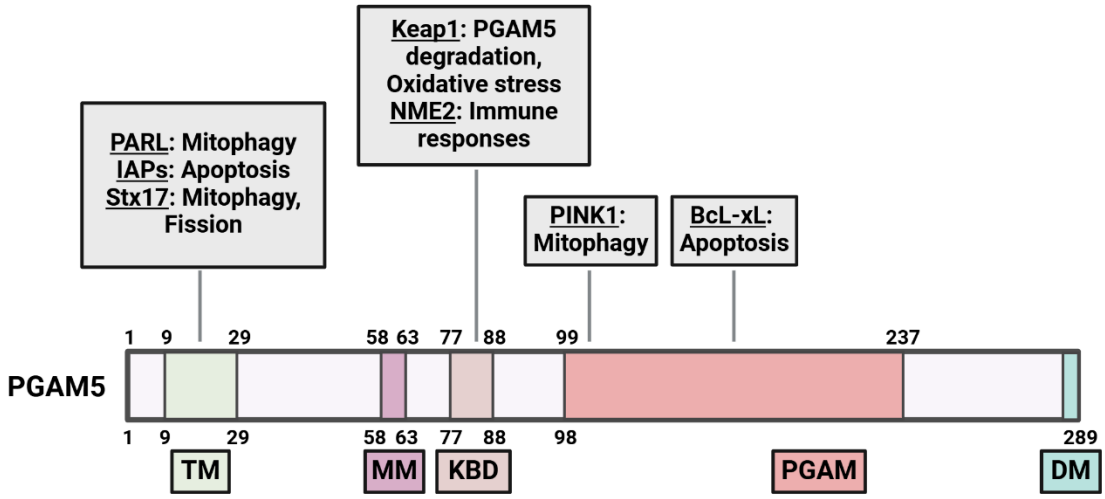

Figure 6. PGAM5 domain arrangement and interactions. Schematics showing domains in PGAM5 protein, its known protein interactions with specific domains and their functional implications. TM- Transmembrane; MM- Multimerization motif; KBD- Keap1-binding domain; PGAM- Phosphoglycerate mutase domain; DM- Dimerization motif.

1.4.1 PGAM5 in the Mitochondria and MERCS

PGAM5 primarily localizes to the mitochondria, with evidence indicating association with mitochondrial membranes, particularly the inner mitochondrial membrane and cristae[161]. Some studies have also shown that PGAM5 interacts with cytoplasmic signaling proteins suggesting that PGAM5 can also localize to the cytoplasm, outer mitochondrial membrane and MERCS[162]. PGAM5 regulates critical mitochondrial functions through its protein-protein interactions[163–165] (Figure 4).

PGAM5 plays a central role in regulating mitochondrial dynamics (fission and fusion)[164]. It activates the fission protein Drp1 by modifying its phosphorylation state, enabling

Drp1 to move to the mitochondrial membrane and drive mitochondrial division through interactions with ER and actin polymerization[166]. In addition to its direct effect on Drp1, PGAM5 dephosphorylates FUNDC1, which induces the mitochondrial localization of Drp1 and hence mitochondrial fission [164,167]. While PGAM5-mediated fission is essential, excessive fragmentation can damage mitochondria, reduce mitochondrial DNA, and increase harmful reactive oxygen species. At the same time, PGAM5 also supports mitochondrial fusion by dephosphorylating Mfn2, helping maintain mitochondrial integrity, DNA stability, and overall cellular health[168].

Mitochondrial biogenesis is essential for maintaining mitochondrial function and restoring cellular balance after damage. PGAM5 contributes to this process by activating the Wnt/β-catenin signaling pathway, particularly under stress conditions such as mitochondrial membrane potential loss or mitophagy[169]. When translocated to the cytoplasm, PGAM5 interacts with components like Axin-1 and β-catenin, leading to β-catenin dephosphorylation and activation of Wnt signaling independently of external ligands, thereby promoting the formation of new mitochondria[169]. Additionally, PGAM5 is associated with increased expression of key regulators of mitochondrial biogenesis, including PGC-1α, NRF1, and TFAM, which coordinate mitochondrial DNA replication and overall mitochondrial mass[170].

PGAM5 also plays a key role in major mitophagy pathways: PINK1-Parkin-mediated and receptor-mediated mitophagy[171]. During mitochondrial stress, PGAM5 helps stabilize PINK1 on the outer mitochondrial membrane, leading to Parkin activation, ubiquitination of mitochondrial proteins, and recruitment of autophagy machinery to

degrade damaged mitochondria[159,172]. PGAM5 also regulates receptor-mediated mitophagy by dephosphorylating FUNDC1 and promoting mitochondrial clearance[173].

Apoptosis, or caspase- dependent (programmed) cell death, is tightly regulated by apoptotic BCL-2 family proteins, and PGAM5 plays a context-dependent role in this process. In healthy cells, PGAM5 helps prevent apoptosis by maintaining Bcl-xL in an unphosphorylated state and inhibiting proapoptotic protein activation and mitochondrial translocation[167]. However, under cellular stress, PGAM5 shifts from a low-activity dimer to a more active dodecameric form, promoting Bcl-xL phosphorylation and enabling proapoptotic factors like BAX to act. PGAM5 can also directly activate apoptosis by dephosphorylating BAX, facilitating its movement to mitochondria, increasing membrane permeability, and triggering the release of apoptotic signals such as cytochrome c[174].

Necroptosis is a caspase-independent cell death driven by the RIPK1/RIPK3/MLKL complex, with PGAM5 acting as an important downstream effector[163,175,176]. Activated by RIPK3, PGAM5 promotes mitochondrial dysfunction primarily by regulating Drp1, enhancing its activity through phosphorylation or dephosphorylation, which leads to mitochondrial fission and contributes to cell death in conditions such as liver injury and pulmonary fibrosis[175]. PGAM5 also participates in necroptosis through the RIPK3/PGAM5/CypD pathway, increasing mitochondrial permeability transition pore opening and further driving cellular damage. Inhibition of this pathway reduces necroptosis, highlighting the importance of PGAM5-Drp1 signaling[177].

Pyroptosis is a form of inflammatory programmed cell death distinct from necroptosis. It is usually triggered by infections and is characterized by inflammasome activation, caspase-1 activity, and the release of proinflammatory cytokines such as IL-1β and IL-18, while the nucleus remains intact. PGAM5 has been shown to play a significant role in regulating pyroptosis by promoting inflammasome activation, particularly through the NLRP3 pathway and caspase-1-mediated processing of IL-1β[178,179].

Oxeiptosis is a recently identified form of ROS-induced programmed cell death that depends on PGAM5 and functions independently of other pathways like apoptosis or necroptosis, helping limit excessive inflammation caused by oxidative stress[180]. PGAM5 regulates this process through interactions with key molecules such as KEAP1, NRF2, and AIFM1. At low ROS levels, the KEAP1/PGAM5/NRF2 complex allows NRF2 to activate antioxidant defenses, promoting cell survival[181,182]. In contrast, high ROS levels disrupt this complex, enabling PGAM5 to dephosphorylate AIFM1 and trigger cell death[183]. This mechanism plays an important role in responses to infections and inflammation, where controlled cell death can be protective. Additionally, PGAM5 influences the balance between different cell death pathways, and its deficiency can worsen inflammation and viral infection outcomes, underscoring its central role in regulating oxidative stress responses[170,184,185] and immune defense.

1.4.2 The PGAM5-Keap1-Nrf2 Pathway

Lo & Hannink identified PGAM5 as a previously unrecognized substrate of the Keap1-Cul3 ubiquitin ligase[186]. They showed that PGAM5 contains a conserved Keap1-binding domain and is targeted for Kelch-dependent ubiquitination and proteasomal degradation under basal conditions. Oxidative stress or electrophilic agents inhibit

Keap1's ubiquitination activity and stabilizes PGAM5, suggesting Keap1 regulates PGAM5 abundance[186]. Keap1 also acts in a similar manner towards NRF2, a transcription factor crucial for regulating expression of genes affecting mitochondrial respiration[187]. Later studies showed that PGAM5-KEAP1 complex is required for mitochondrial localization of NRF2[181]. In this complex, PGAM5 can tether NRF2 to mitochondria and influence its cellular distribution and transcription activity. Only under oxidative stress conditions, is this complex disrupted leading to Nrf2 accumulation in the cytoplasm and its eventual nuclear translocation where it activates expression of antioxidant and pro-respiratory genes (*Hmox1 and Nqo1*)[188].

Interestingly, disruption of NRF2 or PGAM5 (but not KEAP1) impairs mitochondrial retrograde trafficking due to aberrant degradation of mitochondrial adapter Miro2[188]. Moreover, under mitochondrial stress, disruption of PGAM5 was shown to decrease NRF2's mitochondrial localization, increase its nuclear translocation, and enhance gene expression, highlighting a mechanism between PGAM5 sequestration of NRF2 and mitochondrial functions[182]. These studies show that PGAM5 might be directly regulating Nrf2-mediated mitochondrial functions independent of Keap1.

Collectively, these studies reveal that the PGAM5-Keap1-Nrf2 axis represents a complex signaling network integrating oxidative stress sensing, mitochondrial quality control, and cellular antioxidant responses.

1.5 Concluding remarks

As discussed in the preceding sections, both APP and PGAM5 are emerging as novel proteins to be localized at the mitochondria-ER contact sites (MERCS), which have been strongly implicated in the pathogenesis of Alzheimer's disease. Although APP is well established in its association with Alzheimer's disease, the role of PGAM5 remains comparatively limited. One study has reported that PGAM5 protein levels are elevated in the hippocampal tissues of Alzheimer's disease mouse models, linking this increase to mitochondrial damage and subsequent neuronal death[183]. More recent research has identified PGAM5 as a diagnostic gene associated with mitochondrial autophagy in Alzheimer's disease, suggesting its potential utility as a biomarker for clinical diagnosis[189].

Given this context, the mechanisms by which PGAM5 may contribute to mitochondrial and/or MERCS dysfunction can be further elucidated through the study of its protein-protein interactions[163,164,175]. In this study, we identified a novel interaction between APP and PGAM5, potentially occurring at MERCS, and further investigated its functional implications.

Chapter 2: Amyloid precursor protein interacts with the mitochondrial phosphatase PGAM5 and regulates mitochondrial respiration

Kriti Shukla[1,2], Zhi Zhang[3], Kendra S. Plafker[1], Satoshi Matsuzaki[1], Casandra Salinas-Salinas[1], Yvonne Thomason[1], Samah Houmam[1,3,4], Dylan Barber[1,5], Anna Faakye[1,3], Kenneth M. Humphries[1,3], Scott M. Plafker[1], Jialing Lin[3], Heather C. Rice[1,2,3,4]

[1]Aging & Metabolism Research Program, Oklahoma Medical Research Foundation, Oklahoma City, OK, 73104, USA
[2]Department of Chemistry and Biochemistry, University of Oklahoma, Norman, OK, 73072, USA
[3]Department of Biochemistry & Physiology, University of Oklahoma Health Center, Oklahoma City, OK, 73104, USA
[4]Center for Geroscience and Healthy Brain Aging, University of Oklahoma Health Sciences Center, Oklahoma City, OK 73104
[5]Neuroscience Program, University of Oklahoma Health Center, Oklahoma City, OK, 73104, USA

Author Contributions

Kriti Shukla: Conceptualization of project, Data collection and analysis for figures 7-9 (except 8c), Investigation, Methodology, Writing- Original Draft, Writing- Reviewing and Editing

Zhi Zhang: Data collection for figure 8c, Investigation

Kendra S. Plafker: Supervision in data collection and analysis for figures 9 and 11, Writing- Reviewing and Editing

Satoshi Matsuzaki: Data collection for figure 10B

Casandra Salinas-Salinas: Protein purification and cell cultures for data collected towards figures 8 and 9, Writing- Reviewing and Editing

Yvonne Thomason: Animal colony management for the project, Writing- Editing

Samah Houmam: Writing- Reviewing and Editing

Dylan Barber: Writing- Reviewing and Editing

Anna Faakye: Supervision in data collection for figure 10A, Writing- Reviewing and Editing

Kenneth M. Humphries: Resources, Supervision, Writing- Reviewing and Editing

Scott M. Plafker: Resources, Supervision, Writing – review & editing

Jialing Lin: Conceptualization, Funding acquisition, Resources, Supervision, Writing – review & editing

Heather C. Rice: Conceptualization, Formal Analysis, Funding acquisition, Resources, Supervision, Writing- Original Draft, Writing- review & editing

2.1 Abstract

Amyloid Precursor Protein (APP) has been reported to partially localize to mitochondria, and mitochondrial dysfunction is a key feature of Alzheimer's disease; however, the mechanisms linking APP to mitochondrial functions remain incompletely defined. In this study, we identified an interaction between APP and phosphoglycerate mutase family member 5 (PGAM5), a mitochondrial protein phosphatase. We confirmed their endogenous interaction in mouse brain tissue and determined that APP and PGAM5 are both present at mitochondria-ER contact sites (MERCS) and. Using in vitro binding assays, we demonstrate a direct interaction between the linker region of APP and a region of PGAM5 that includes the Kelch-like ECH-associated protein 1 (Keap-1) binding domain. PGAM5 is known to anchor a portion of nuclear factor erythroid 2 p45-related factor 2 (Nrf2) through Keap1 at the outer mitochondrial membrane and regulates mitochondrial respiration and stress responses. We found that the Nrf2-regulated genes Hmox1 (Heme oxygenase-1) and Nqo1 (NADH:quinone oxidoreductase 1), which are involved in mitochondrial respiration, are downregulated in APP KO astrocytes. Accordingly, mitochondria isolated from the brains of APP knockout (KO) mice have impaired substrate-specific respiration and electron transport chain (ETC) function. Together, these findings suggest that APP supports mitochondrial respiration by binding to PGAM5 and modulating Keap1-Nrf2 signaling.

2.2 Introduction

Mitochondrial dysfunction is a prominent feature of Alzheimer's disease (AD) and is thought to contribute to disease progression[13,190–192]. Multiple studies report increased oxidative stress[19,21], decreased ATP levels[193], and impaired brain metabolism in AD[194–196]. Amyloid Precursor Protein (APP) is the parent protein of Aβ peptides that aggregate to form plaques in Alzheimer's disease.[4,94] Although primarily localized to the secretory pathway, cell surface, and endocytic compartments, a portion of APP has been shown to be present at mitochondria and mitochondria-ER contact sites (MERCS)[54,122,139,141], which are also sites of APP processing[44,197]. Several studies have suggested a role of APP in mitochondrial functions[95,198–200]. Notably, APP alters mitochondrial mass[151], bioenergetics[17,198], mitophagy[201,202] and mitochondrial respiration[18,202]. The mechanisms by which APP affects mitochondrial function remain unclear, but understanding its protein-protein interactions at the mitochondria can help define its role[115].

Phosphoglycerate mutase family member 5 (PGAM5) emerged as a candidate interactor of the APP extracellular domain in an unbiased proteomics screen performed by Rice et al.[115]. PGAM5 is a mitochondrial phosphatase, with substrates that include B-cell lymphoma-extra-large (Bcl-XL)[186], Dynamin-related protein 1 (DRP1)[164,203], FUN14 domain-containing protein 1 (FUNDC1)[167] and Mitofusin 2 (MFN2)[168], which are involved in mitochondrial mobility, mitophagy, redox homeostasis, respiration, or cell death.[163,164,167,176,182,186,203]. PGAM5 also regulates mitochondrial respiration and stress response through the Keap1-Nrf2 pathway[181,182,188,204–206]. Under homeostatic conditions, Nrf2 is constitutively translated, ubiquitylated by Keap1/Cul3, and degraded

by the proteasome[172,207]. In response to oxidative stress, modification of cysteines on Keap1 render it enzymatically inactive leading to a halt of the constitutive degradation of Nrf2. Nrf2 accumulates in the cytoplasm and then translocates to the nucleus, where it induces the transcription of antioxidant genes (e.g. *Hmox1 and Nqo1*) to restore redox homeostasis and support mitochondrial respiration[172,182,207]. A subset of Nrf2 is tethered to the outer mitochondrial membrane through a ternary complex with PGAM5 and Keap1. Knockdown of PGAM5 or Keap1 activates Nrf2 target gene expression [181,182]. The PGAM5-Keap1-Nrf2 complex has been implicated in both stress-induced mitochondrial retrograde trafficking[188] and mitochondrial respiration[182] .

In this study, we establish an interaction between APP and PGAM5 that is mediated by a region of PGAM5 that includes the Keap1-binding domain. Consistent with disrupted PGAM5-Keap1-Nrf2 signaling, expression of the Nrf2 target genes *Hmox1 and Nqo1* are reduced in APP KO astrocytes. We show that mitochondria from APP KO mouse brains have impaired substrate-specific respiration and electron transport chain (ETC) function. Together, these findings suggest a role for APP in regulating mitochondrial respiration by binding to PGAM5 and modulating Keap1-Nrf2 signaling pathway.

2.3 Results

2.3.1 APP and PGAM5 interact endogenously and are both present at mitochondria-ER contact sites

To investigate a potential mechanism underlying APP function in mitochondria, we followed up on a prior proteomics screen performed by Rice et. al. [115] identifying the mitochondrial phosphatase PGAM5 as a candidate interactor of the APP ectodomain[4]. To determine whether APP and PGAM5 interact endogenously, PGAM5 was immunoprecipitated (IPed) from brain extracts of wild-type (WT) mice or PGAM5 knockout (KO) mice, as a negative control. APP co-IPed with PGAM5 in WT but was not detected in IPs from PGAM5 KO extracts, indicating that APP and PGAM5 interact endogenously in mouse brain (Figure 4A). To confirm that a portion of APP and PGAM5 localize to common subcellular compartments, we performed subcellular fractionation of WT mouse brains to isolate mitochondria, ER, and mitochondria-ER contact sites (MERCS). Both young (3mo) and old (12mo) mice showed similar subcellular distribution of APP and PGAM5, so both ages were plotted together. Consistent with the literature, APP was found to be localized at the ER but interestingly, a significant amount was also present at MERCS (Figure 4B,C). On the other hand, PGAM5 was also found to be present at MERCS while predominantly being present at the mitochondria (Figure 4B,D). This data showed that both APP and PGAM5 can be found at MERCS (Figure 4B-D), suggesting MERCS as a potential site for their interaction.

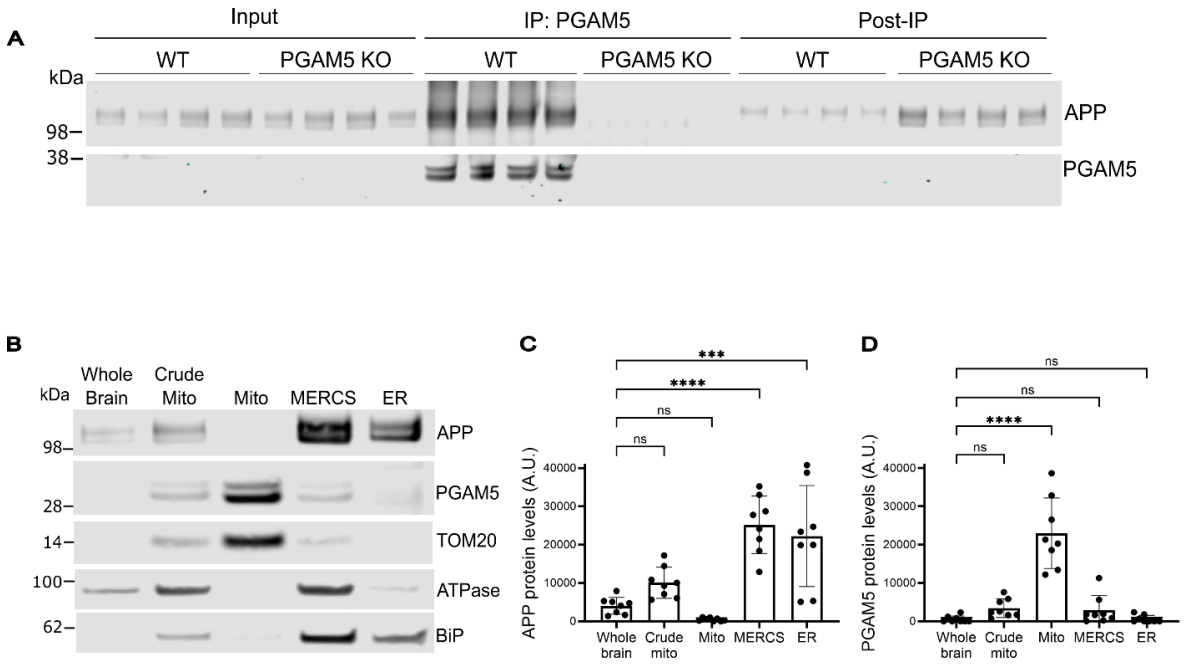

Figure 7. APP and PGAM5 interact endogenously and are both present at MERCS. (A). Western blot showing immunoprecipitated PGAM5 and co-immunoprecipitated APP in WT and PGAM5 KO (4mo, males) mouse brains. **(B).** Western blot showing subcellular localization of PGAM5 and APP in WT (C57Bl6, 3-12 months old, females) mouse brains. The cellular compartments shown are Whole brain, Crude mitochondria, Mitochondria, Mitochondria-ER contact sites (MERCS) and Endoplasmic reticulum (ER). The purity of each sample was validated by its marker protein (TOM20 (Translocase of Outer Mitochondrial Membrane 20), Mitochondria; ATPase (Adenosine Triphosphatase), MERCS; BiP (Binding Immunoglobulin Protein), ER). **(C-D).** Graphs showing western blot quantification indicating levels of C. APP protein and D. PGAM5 protein. Values shown are band intensity means ± SD (n =7). One-way ANOVA tests were performed for each graph, *** ($P < 0.001$), **** ($P < 0.0001$), ns (non-significant).

2.3.2 APP interacts with a region of PGAM5 containing the Keap1 binding domain

Next, we used *in vitro* binding assays to determine whether APP and PGAM5 can directly interact and to narrow the binding regions responsible for this interaction. Since both APP and PGAM5 full-length proteins have transmembrane domains (TM), we used the recombinant soluble APP (sAPPα, aa1-496) (Figure 5A) and truncated PGAM5 constructs (Figure 5B). Amino acids 1-54 (TM domain) of PGAM5 were removed to make PGAM5Δ54 while PGAM5Δ90 had additional 36 amino acids (containing the multimerization motif;MM and Keap1-binding domain;KBD) removed[4734,36,48]. We used Protein G Sepharose beads to pull down Fc-tagged sAPPα incubated with either PGAM5Δ54 or PGAM5Δ90. PGAM5Δ54 but not PGAM5Δ90 was pulled-down with sAPPα-Fc, indicating that the interaction requires the N-terminal region of PGAM5 containing the KBD and MM (Figure 5C). Isothermal titration calorimetry (ITC) with sAPPα (without an Fc tag) and PGAM5Δ54, revealed a dissociation constant (K_d) of 3.45 μM and a binding stoichiometry of N = 0.114 (Figure 5D). A preliminary ITC run with sAPPα (without an Fc tag) and PGAM5Δ90 showed no binding (Figure S1). Then, to narrow down the domain in APP required for binding to PGAM5, we used Protein G Sepharose beads to pull down individual Fc-tagged domains of APP (Growth factor-like domain;GFLD-Fc, Copper binding domain;CuBD-Fc, Extension domain;ExD-Fc, Acidic domain;AcD-Fc and Extracellular 2;E2-Fc) incubated with PGAM5Δ54. PGAM5Δ54 was most efficiently pulled-down with ExD-Fc followed by AcD-Fc (Figure 5E-F). Together, these results suggest that the linker region of APP (constituted by AcD and

ExD) and the N-terminal amino acids (aa55-89) of PGAM5 (containing Keap1 binding domain) are critical for binding between these two proteins.

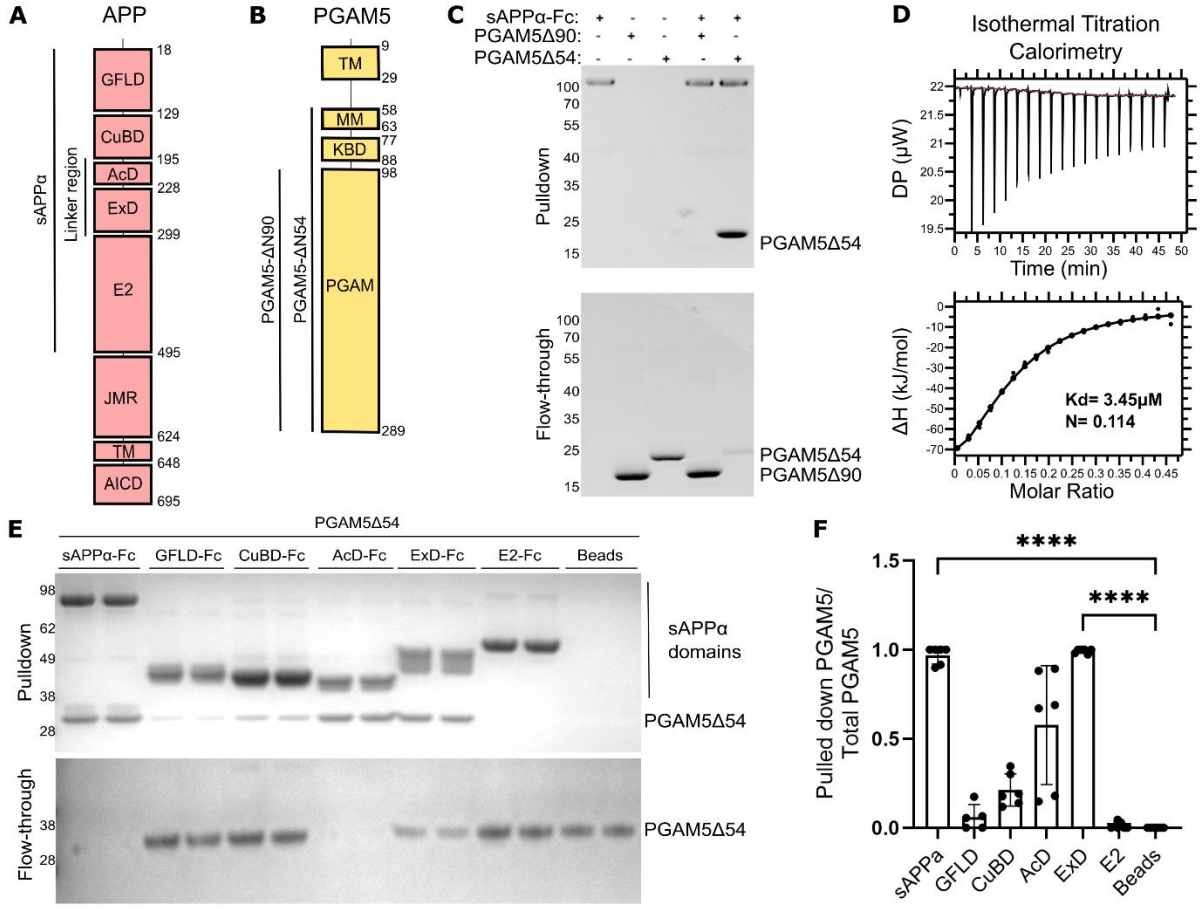

Figure 8. APP interacts with a region of PGAM5 containing the Keap1 binding domain. (A-B). Schematics showing domains (GFLD; Growth-like factor domain, CuBD; Copper-binding domain, AcD; Acidic domain, ExD; Extension domain, E2, JMR; Juxtamembrane Region, TM; Transmembrane, AICD; APP intracellular domain, MM; Multimerization motif, KBD; Keap1 binding domain, PGAM; Phosphoglycerate mutase) and recombinant protein constructs (sAPPα, PGAM5-Δ90 and PGAM5-Δ54) of APP (pink) and PGAM5 (yellow). **C.** Coomassie stained SDS-PAGE gels of bound and unbound material from Fc-pulldowns of sAPP-Fc with PGAM5Δ54 or PGAM5Δ90

purified proteins, **D.** Binding curve from ITC done using the sAPPα and PGAM5-Δ54 purified proteins (n=3). **(E-F).** D. Coomassie stained SDS-PAGE gels of bound and unbound material from Fc-pulldowns of sAPP-Fc, GFLD-Fc, CuBD-Fc, ExD-Fc, AcD-Fc, E2-Fc and beads with PGAM5Δ54 purified protein and E. Quantification of pull-down assays showing net PGAM5Δ54 bound and pulled down with each Fc-tagged sAPPα domain. Values shown are means ± SD (n =5 - 6) and the statistics were performed using Dunnett's multiple comparison test. **** ($P < 0.0001$).

2.3.3 Transcription of Nrf2-regulated genes is altered in APP KO astrocytes

To understand the functional implications of binding of APP to the N-terminal region of PGAM5 containing the Keap-1 binding domain, we investigated whether the Keap1-Nrf2 pathway is affected by the presence of APP. We examined Nrf2-dependent gene expression in primary astrocytes isolated from the brains of WT or APP KO mice. Astrocytes were chosen based on prior literature demonstrating a critical role for APP in mitochondrial function in astrocytes[152]. Total RNA was isolated from WT or APP KO astrocytes and transcript levels of established Nrf2 target genes (*Hmox1, Nqo1, Gclc, Gclm, and Txnrd1*) were quantified by qPCR. Both *Hmox1* and *Nqo1* transcripts were significantly reduced in APP KO astrocytes compared to WT controls. No significant differences were observed for *Gclc*, *Gclm*, or *Txnrd1* (Figure 6). This selective modulation of gene expression was interesting since a previous study shows that mitochondrial functions of HMOX1 are mediated by PGAM5[170].

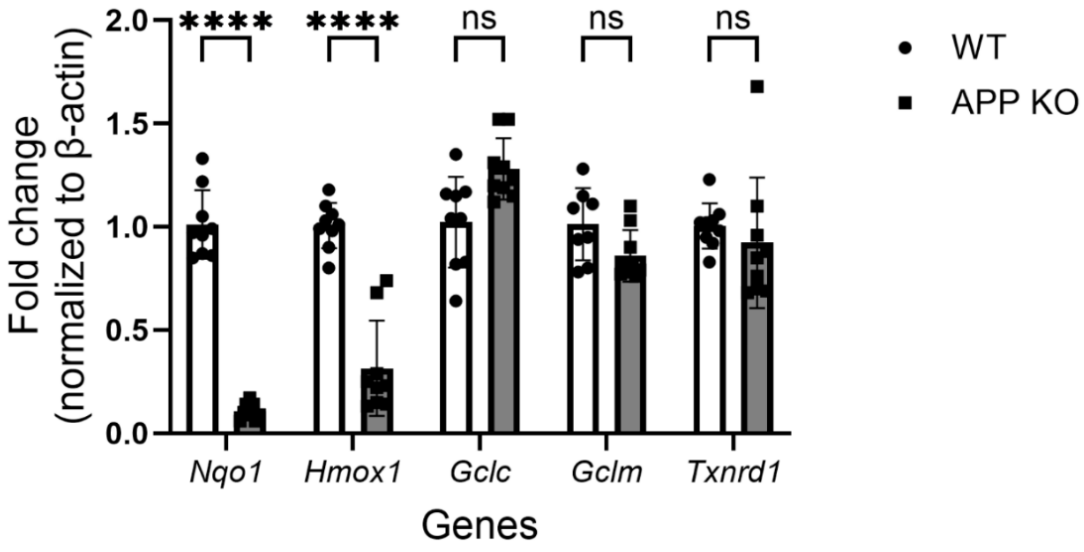

Figure 9. APP affects Nrf2-regulated gene expression. Plot showing relative mRNA

expression of Nrf2-regulated genes in cultured primary astrocytes isolated from WT and APP KO mouse brains, measured by RT-qPCR. Values shown are the means ± SD (n = 8-9) and the statistics were performed using two-way ANOVA, followed by Tukey's multiple comparison test. ***** ($P < 0.0001$), ns (non-significant).

2.3.4 Mitochondria isolated from APP KO mouse brains have impaired respiration

Since the basal expression of *Nqo1* and *Hmox1* was decreased in APP KO conditions and both these genes are essential for maintaining redox homeostasis that permit efficient NADH oxidation at Complex I[208,209], we investigated if loss of APP also affects mitochondrial respiration and ETC. We performed respiratory measurements in freshly isolated mitochondria from WT vs APP KO mouse brains. APP KO mitochondria showed significantly decreased pyruvate (Figure 7A) and glutamate-mediated (Figure 7B) respiration with no changes observed in succinate-mediated respiration (Figure 7C) as compared to WT, indicating an impairment in maximal NADH-linked mitochondrial respiration whereas Complex II–dependent respiration (succinate) remains intact. Additionally, we measured the effect of APP KO on Complex I activity, the rate limiting step of the ETC and NADH oxidase activity as a measure of total ETC activity. Our findings showed a significant decrease in NADH oxidase activity in APP KO mitochondria (Figure 7D) and a decreasing but non-statistically significant trend in complex I activity (Figure 7E). Taken together, these findings highlight a crucial physiological role of APP in maintaining Complex I function and NADH-linked respiration in brain mitochondria.

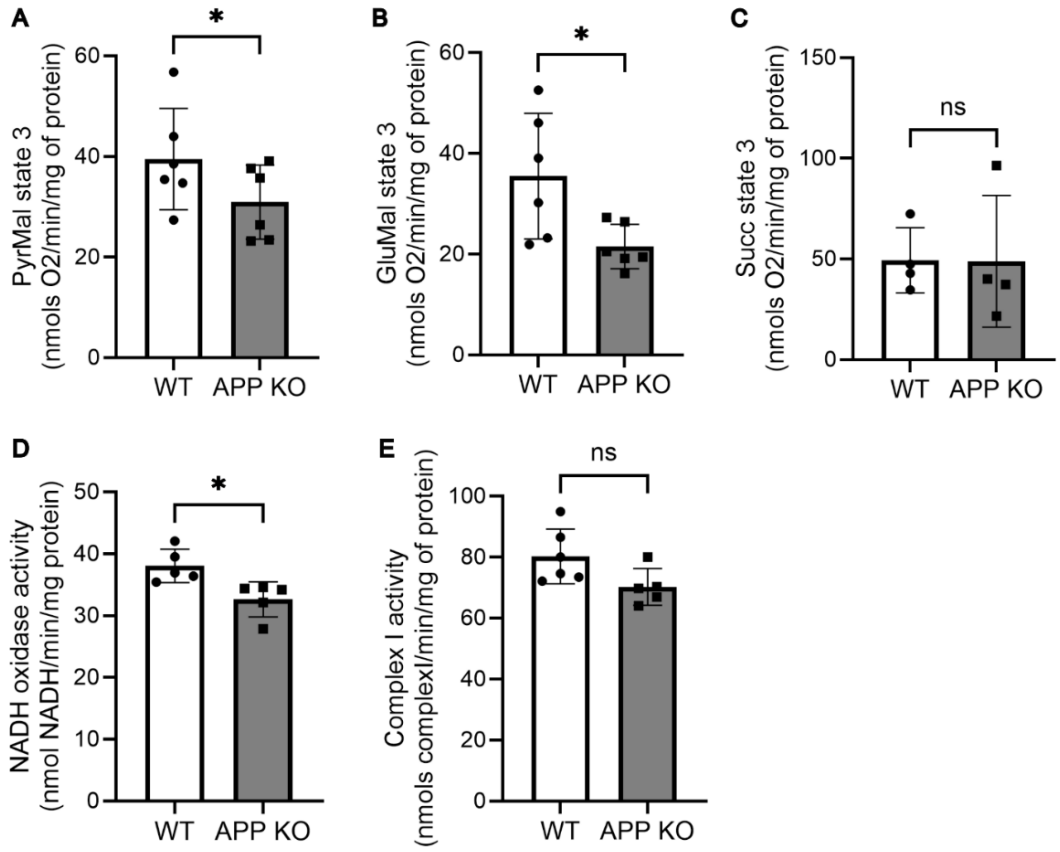

Figure 10. Isolated mitochondria from APP KO mice brain have impaired respiration. (A-C). Graphs showing maximum respiration by utilizing different oxidizable substrates (A. Pyruvate/malate, B. glutamate/malate, C. Succinate), in the mitochondria isolated from 6-8 months old APP KO mouse brains. Values shown are the means ± SD (n =4 - 6). Two-tailed paired t-tests were performed for each graph. **(D-E).** Graphs showing impaired ETC in APP KO mitochondria as indicated by D. decreased Complex I activity and E. NADH oxidase activity. Values shown are means ± SD (n =5 - 6). Two-tailed paired t-test was performed for each graph, * ($P < 0.05$), ns (non-significant).

2.4 Discussion

In this study, we identify the mitochondrial protein phosphatase PGAM5 as an interactor of APP. Both APP and PGAM5 were found to interact endogenously, and both were present at MERCS. Interestingly, the amount of APP present at MERCS was comparable to the amount at ER, suggesting a crucial role of APP at these inter-organelle sites. Previous studies have identified MERCS as an APP processing site [44,197], and our findings suggest a functional role for APP localized to MERCS[23,24]. Our ITC data showed binding between APP and PGAM5 with a binding stoichiometry (N) of 0.114, which is consistent with a dodecameric PGAM5 complex associated with an APP dimer. APP is known to form homodimers through its E1 and transmembrane domains, which has been implicated in its processing and function[119]. PGAM5, on the other hand, assembles into higher-order oligomers, predominantly forming dodecamers as well as dimers, that are critical for its functions[158,167,203]. The APP-PGAM5 interaction requires a region of PGAM5 containing the Keap1-binding domain, suggesting that APP may compete with Keap1 for its binding to PGAM5. PGAM5 is known to tether Nrf2 at the outer mitochondrial membrane through Keap1 and regulates the amount of Nrf2 translocating into the nucleus for gene expression[181]. Consistent with this, we find that transcription of Nrf2 target genes, *Nqo1* and *Hmox1,* is significantly reduced in APP KO primary astrocytes under physiological conditions. Both NQO1 and HMOX1 are critical components of the Nrf2 antioxidant network that preserve mitochondrial redox homeostasis and regulate respiration[184,210,211]. NQO1 limits quinone redox cycling and supports respiration by maintaining NAD^+/NADH balance[212,213], while HMOX1 helps mitigate oxidative stress and supports ETC[185,214]. Taken together, these findings

suggest that the APP-PGAM5 interaction at MERCS may regulate mitochondrial respiration and stress response through modulation of Keap1-Nrf2 signaling.

We further show that APP deficiency leads to a selective reduction in glutamate- and pyruvate-driven respiration. This substrate-specific defect points to a dysfunction upstream of or at Complex I, rather than a global failure of the electron transport chain or mitochondrial integrity. Consistent with this interpretation, we observe a reduction in NADH oxidase activity and a downward trend in Complex I enzymatic activity in APP KO mitochondria. Together, these results position APP as a regulator of NADH-linked respiration in the brain and suggest that impaired NADH-dependent respiration may not only limit electron transport capacity but also promote oxidative imbalance and bioenergetic insufficiency. In this context, diminished Complex I function could enhance electron leak and reactive oxygen species generation while simultaneously constraining ATP synthesis. When considered alongside previous evidence that manipulation of APP alters ETC activity, ATP levels, and mitochondrial biogenesis[153,202], our findings strengthen the conclusion that APP is an essential contributor to mitochondrial bioenergetics.

Based on our findings, we propose a model in which APP helps maintain Nrf2-dependant gene regulation by competing with Keap1 to bind to PGAM5 at MERCS. In WT conditions, APP binding to PGAM5 may promote displacement of Keap1-bound Nrf2, enabling Nrf2 accumulation at the cytoplasm and eventual nuclear translocation that in turn leads to gene expression (Figure 8A). On the other hand, in the absence of

APP, Keap1-bound Nrf2 is constantly tethered to PGAM5 and is unable to translocate to the nucleus to turn on the gene transcription and hence the expression of genes required to maintain mitochondrial respiration and redox balance is reduced (Figure 8B). This model provides a mechanistic basis for mitochondrial bioenergetic deficits often observed upon APP loss[61–63] and warrants future studies to determine whether mitochondrial dysfunction observed in AD arises from loss of normal APP function.

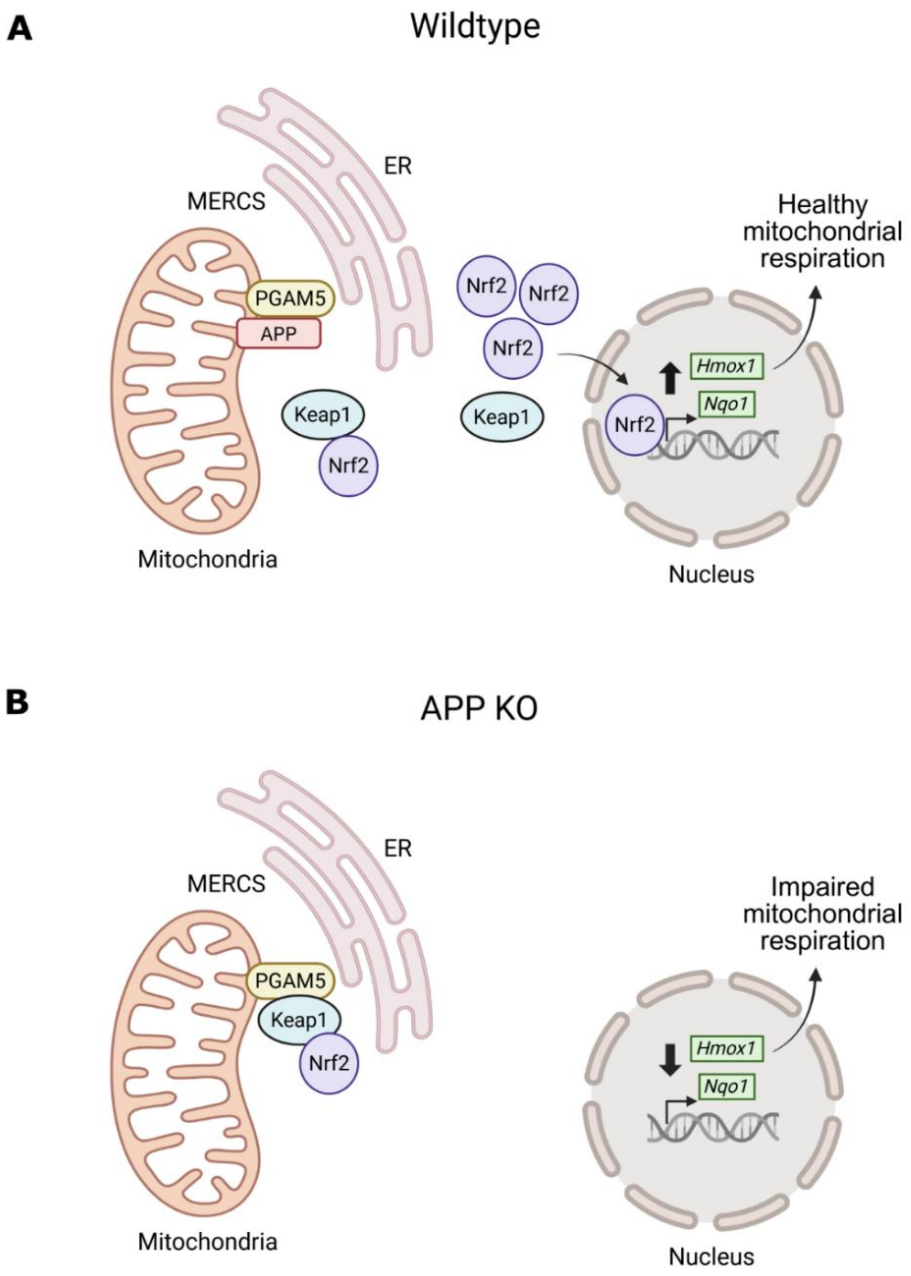

Figure 11. Proposed model by which APP affects mitochondrial respiration. A. In WT cells, APP localized to MERCS can bind to PGAM5 and displace Keap1. This releases Keap1-bound Nrf2 to the cytoplasm where Nrf2 dissociates from Keap1, accumulates, and subsequently translocates to the nucleus to activate transcription of genes that maintain normal mitochondrial respiration. B. In APP KO cells, Nrf2

remains bound to PGAM5 at the mitochondria, leading to reduced Nrf2 translocation to the nucleus and reduced transcription of its target genes. This reduced Nrf2 signaling in the absence of APP leads to impaired mitochondrial respiration. The schematic was created in BioRender. Rice, H. (2026) https://BioRender.com/ftsycbt.

2.5 Materials and Methods

Mouse models

Wild-type mouse strain used in this study was C57/Bl6 (starin 000664, The Jackson Laboratory) and genetically modified mouse strains were APP KO (strain 004113, B6.129S7-App/J, The Jackson Laboratory) and PGAM5 KO (MGI:4432458, $Pgam5^{tm1a(EUCOMM)Wtsi}$, received by Dr. Yishi Jin, University of California San Diego and originally developed by Dr. Michael Lenardo, National Institute of Health)[215]. All the mice were group-housed in the AALAS-accredited OMRF vivarium on a 14:10 h light/dark cycle with *ad libitum* access to water and food. The homozygosity of the APP KO and PGAM5 KO strains was confirmed by genotyping ear-punch biopsies via Transnetyx. Genotyping of all progenies was performed by Transnetyx Inc., which utilizes duplicate sample processing using real-time PCR, ensuring the accuracy of each mutation. Additionally, Transnetyx stores all samples for a minimum of 4 months, should re-probing be necessary. This ensures that in all studies, authentication of mouse lines is performed before use and at regular intervals by a reputable, outside party. For APP KO model, two TaqMan assays, Neomycin (binds within generic neomycin and detects the mutant allele) and App-3 WT (binds within the region deleted by neomycin and provides zygosity), are used to detect the mutant and WT alleles, respectively. For PGAM5 KO

model, the probes Pgam5-1 WT and L1L2-Bact-P TA were used. Each assay runs alongside an internal housekeeping gene, Cjun, to ensure there is enough DNA for a reaction and that all other quality controls are passed.

Co-immunoprecipitation

Whole mouse brains were homogenized in T-PER buffer supplemented with protease and phosphatase inhibitors, or previously prepared and aliquoted brain lysates (WT and PGAM5 KO) were thawed on ice. Lysates were pre-cleared with Protein A Sepharose 4 Fast Flow beads (cat. No. P9424, Sigma-Aldrich) (washed 3X in T-PER with inhibitors) for 3 h at 4°C on a nutator. Samples were centrifuged at 3,000xg for 30 s at 4°C, and the supernatant (pre-cleared lysate) was collected. A part of this pre-cleared lysate was saved as input. Rest was incubated overnight at 4°C with 1.5 µg PGAM5 rabbit polyclonal antibody (Abcam, ab126534) and 30 µL washed Protein A Sepharose 4B beads on a nutator. The following day, beads were pelleted (3,000xg, 30 s, 4°C), and the supernatant was collected as the post-IP fraction. The protein present in post-IP sample was acetone precipitated as described below. Beads were washed three times with 200–300 µL T-PER (with inhibitors), rotating 30 min at 4°C for each wash. After the final wash, residual buffer was removed, and beads were resuspended in 4X loading dye supplemented with 10X reducing agent, heated at 95°C for 10 min, and centrifuged to pellet beads. The supernatant was collected as the IP sample. Input and post-IP samples were prepared in parallel and analyzed by Western blot (described below).

Acetone Precipitation

Required volume of acetone was placed at -20°C. 4 volumes of this chilled acetone were added to 1 volume of proteins sample in acetone-compatible tube. The tube was vortexed and incubated for 60 minutes at -20°C. Afterwards, the tube was centrifuged for 10 min at 13,000-15,000×g. Supernatant was properly and carefully discarded, being careful not to dislodge the protein pellet. Acetone was allowed to evaporate from the uncapped tube at room temperature for 30 minutes. Making sure not to over-dry the pellet, the pellet was resuspended in the T-Per buffer and 4x dye and 10x reducing agent was added to prepare the samples for Western blotting.

Western blotting

Samples obtained from subcellular fractionation were quantified using the BCA protein assay (Thermo Fisher Scientific). 12 µg of protein sample was loaded on each lane, mixed with 10x reducing agent and 4X Laemmli sample buffer, boiled for 5 minutes at 95°C, and resolved on NuPAGE™ 4-12% Bis-Tris Midi gels with MES SDS running buffer. Proteins were transferred onto nitrocellulose membranes (BioRad) using Criterion Blotter (BioRad) at 400mA for 80 minutes. Membranes were blocked with 5% BSA in water for 1 hour at room temperature and then incubated overnight at 4°C with primary antibodies diluted 1:1000 in 0.05% Tween-20 in PBS (PBST)- APPY188 (rabbit, abcam, ab32136), PGAM5 (rabbit, abcam, ab126534), TOM20 (rabbit, Thermo-Fisher, 11802-1-AP), ATPase (mouse, Sigma-Aldrich, 05-369-25UG), BiP (rabbit, abcam, ab108613). After washing three times with PBST, membranes were incubated with secondary antibodies (Alexa Fluor™ Donkey anti-Rabbit 800 and Donkey anti-Mouse

680) for 1 hour at room temperature. Protein bands were visualized using Odyssey CLx detection system (Licor). The gel image was converted to grayscale, and the protein and background band intensities were obtained using ImageJ software The background intensity was then used to normalize the protein band intensity, and these values were plotted as protein levels in each subcellular compartment.

Protein pull-down assays

3 µg of Fc-tagged sAPPα (~95KD) was incubated with either 3 µg PGAM5-ΔN90 (~25kDa) or PGAM5-ΔN54 (~30kDa) in 500 µL binding buffer (10mM HEPES pH 7.4, 150mM NaCl, 2mM $CaCl_2$, 1mM $MgCl_2$, 0.1% Tween-20) at 4 °C for 1 hour with gentle rotation. For pull-down, 20ml of protein G Sepharose 4 Fast Flow beads (cat. 17061805, Cytiva), pre-equilibrated with cold binding buffer, were added and incubated for an additional 2 hours at 4 °C. Afterwards, flow-through was collected and the beads were washed 3–4 times with 500µl cold binding buffer followed by centrifugation at 3000rpm for 2 min to remove non-specifically bound proteins. Proteins bound to the beads were eluted in 25ml of SDS sample buffer, supplemented by 10% β-mercaptoethanol, heated at 95°C for 5 minutes and resolved on 13% SDS-PAGE gels, along with the flow-through samples. Gels were then incubated for 1 hour at room temperature with the Coomassie stain solution followed by destain solution and then washed with deionized water (3 times, 15 min each). The gels were then imaged using white light in Syngene apparatus to visualize the protein bands. Same protocol was followed to narrow down the interacting domain in APP by using 3 µg of Fc-tagged

Growth factor-like domain;GFLD, Copper binding domain;CuBD, Extension domain;ExD, Acidic domain;AcD and Extracellular 2;E2, with 3 µg of PGAM5-ΔN54.

Subcellular fractionation

Brain mitochondria and mitochondria-ER contact sites (MERCS) were isolated from 3-12 mo old female C57/Bl6mouse brains using a modified version of the protocol by Wieckowski et al. (2009)[216]. Briefly, freshly dissected brains were homogenized in ice-cold isolation buffer containing 0.25 M sucrose, 10 mM HEPES (pH 7.4), and protease inhibitors. For each replicate, the homogenate from 3-5 mouse brains was pooled and was subjected to sequential centrifugation to remove nuclei and debris, followed by differential centrifugation steps to separate crude mitochondria. A Percoll density gradient was used to purify mitochondria, and the post-mitochondrial supernatant was further processed to isolate MERCS. All steps were performed at 4°C to preserve organelle integrity.

Plasmids

These were provided by Dr. Bart De Strooper and Dr. Joris de Wit (VIB-KU Leuven, Belgium)[115]. These were previously generated by PCR-amplifying the following regions of mouse APP_{695}: sAPPα (aa18-612); GFLD (aa18-128); CuBD (aa129-194); AcD-Exd (aa195-298); ExD (aa195-227); AcD (aa228-298); and E2 (aa299-494). Each of the PCR fragments were inserted in frame between the prolactin signal peptide and human Fc sequence in the pCMV6-XL4 vector using Gibson Assembly (NEB). PGAM5 plasmids were provided by Dr. Apirat Chaikuad (Institute for Pharmaceutical Chemistry,

Johann Wolfgang Goethe-University and Buchmann Institute for Molecular Life Sciences,Germany)[158].

Purification of recombinant soluble APP proteins

APP fragments with a C-terminal Fc tag were expressed by transfection in HEK293T cells using polyethylenimine (PEI) (Kyfora Bio 23966) and collected in serum-free Opti-MEM media (Gibco 31985088). For Fc-tagged proteins used for *in vitro* binding assays, the conditioned medium was applied to an affinity column packed with Protein-G Sepharose Fast Flow resin (Cytiva 17061802) at 4 °C at a flow rate ~50mL/hr, washed with 250 mL wash buffer (50 mM HEPES pH 7.4, 300 mM NaCl) and eluted with 10 mL of IgG elution buffer (Pierce). For non-Fc-tagged proteins used in ITC, the conditioned medium was passed through a Protein-G Sepharose Fast Flow column, followed by washing with 250 mL of wash buffer (50 mM Tris pH 8.0, 450 mM NaCl, 1 mM EDTA). The Fc tag was cleaved by overnight incubation with GST-tagged 3C PreScission Protease (Cytiva 27084301) in cleavage buffer (50mM Tris pH 8.0, 150 mM NaCl, 1 mM EDTA, 1 mM DTT). Cleaved protein was collected in the eluate and the protease separated from the eluted proteins using a Glutathione Sepharose (Cytiva 17513201) column collecting in TNE buffer (50mM Tris pH 8.0, 150 mM NaCl, 1 mM EDTA). Proteins were dialyzed against suitable buffer, concentrated using centrifugal filter units (Millipore Sigma UFC9010), and depleted of endotoxin with Pierce™ High-Capacity Endotoxin Removal Spin Columns (Thermo Scientific 88274). Protein concentration was determined by BCA Protein Assay (Thermo Scientific 23227) and verified by Coomassie SDS-PAGE.

Purification of recombinant soluble PGAM5 proteins

PGAM5 plasmids were transfected in BL21 Rosetta competent *E. coli* cells for expression and plated on LB+Kanamycin$^{25ug/ml}$ plate and left overnight at 37°C. Next day, 25ml of LB+Kanamycin$^{25ug/ml}$ was inoculated with a few bacterial colonies from this overnight plate and left in a shaker incubator (37°C, 250rpm) overnight. Next day, 10ml of this culture was used to inoculate 500ml of LB+Kanamycin$^{25ug/ml}$ (37°C, 250rpm) for a few hours until the OD reached 0.6-0.8. Protein expression was induced by adding 0.5mM IPTG and incubating for 18hrs (18°C, 225rpm). Cells were harvested by centrifugation and re-suspended in 15ml of lysis buffer (50mM Hepes-KOH pH7.5, 500mM NaCl, 5mM Imidazole, 5% glycerol with fresh 0.5mM TCEP, 1XPIM (200X: 976ml of H_2O, 20ml of 1.5mg/ml-Aprotinin, 2ml of 10mg/ml-Pepstatin, 2ml of 10mg/ml-Leupeptin, 0.5mM PMSF). Cells were then sonicated (60% power, 3min/cycle, total 4-5 cycles) in the presence of 40mg/ml of DNAse. Supernatant was collected and incubated with 1ml of 50% Nickel(II)-NTA agarose (Ni^{2+}-beads) (rock, 4°C, 2-3 hours). Ni^{2+}-beads/supernatant mixture was settled in a column. The Ni^{2+}-beads and bound His_6-tagged PGAM5 proteins were washed with lysis buffer (10mM imidazole pH 7.4 with 0.5mMTCEP, 1XPIM, 0.2mMPMSF). Protein was eluted with lysis buffer containing higher imidazole concentration (250mM imidazole with 0.5mM TECP). Protein was concentrated to OD280 ~10-15 by using MWCO 10kDa concentrator and quantified using BCA assay. The purified proteins were dialyzed in 1X PBS, pH 7.4 and aliquots of the protein solution were frozen in liquid nitrogen and stored at -80°C after adding glycerol to a final concentration of 20% (v/v), for subsequent experiments.

Isothermal Titration Calorimetry

All ITC experiments were performed on a MicroCal PEAQ-ITC system at OU Protein Production and Characterization Core. For experiments involving APP constructs expressed in HEK293T cells, the purified PGAM5 and sAPPα constructs were dialyzed into a buffer containing 20 mM Na-HEPES pH 7.0, 150 mM NaCl, and 5 mM $MgCl_2$. Dialyzed samples were concentrated and degassed prior to the experiment. In these experiments, sAPPα were placed in the sample cell, with matching buffer in the reference cell. PGAM5 constructs were loaded into the syringe and injected into the sample cell in a series of 1 µL injections at 25°C. The raw ITC data were fitted to a single binding site model using the MicroCal PEAQ-ITC analysis software provided by the manufacturer.

Primary Mouse Astrocyte Culture

Primary astrocytes were isolated from whole brains of postnatal day 0-5 (P0-P5) C57BL/6J mice using a differential adhesion-based protocol[217]. All dissections were performed under sterile conditions. Brains were rapidly removed, transferred to ice-cold Hank's Balanced Salt Solution (HBSS), and meninges were carefully stripped to minimize contamination from fibroblasts and endothelial cells. Cortical tissue was mechanically dissociated and enzymatically digested to generate a single-cell suspension. Briefly, 0.05% DNase I was added to the tissue, followed by gentle trituration 10–15 times. Subsequently, 0.05% trypsin was added, and the tissue was further triturated 20–30 times using a 10 mL pipette before incubation at room temperature (22–25 °C) for 20 min. Cells were centrifuged for 10 min at 150×g,

resuspended in complete Dulbecco's Modified Eagle Medium (DMEM) supplemented with 10% fetal bovine serum and penicillin–streptomycin, and plated. The cells were cultured in the astrocyte media and maintained at 37°C with 5% CO_2. Media was changed on day 2 and subsequently every 2–3 days until they reached desired confluency. These were then either used for experiments or flash frozen for future use.

qPCR

Total RNA was extracted from WT and APP KO mice primary astrocytes using the Direct-zol micro-RNA isolation kit (Zymo Research) and quantified using a Nanodrop 1000 spectrophotometer. 0.25 µg RNA was used to synthesize cDNA using qScript (Quanta) according to manufacturer instructions in a BioRad T100 thermocycler. Real-time quantitative PCR was performed using PowerUp™ SYBR® Green PCR Master Mix (Applied Biosystems) and the primers for the genes- *Hmox1, Nqo1, Gclc, Gclm*, *Txnrd1* and *Actb.* The mRNA levels of target genes were normalized to *ActB* by untreated WT sample values.

Respiratory measurements with isolated mitochondria

Freshly isolated mouse brain mitochondria were resuspended in mitochondrial resuspension buffer (250 mM mannitol, 5 mM HEPES, pH 7.4, and 0.5 mM EGTA) as previously described.[216] The protein quantification was done via BCA assay. Mitochondrial respiration measurements were performed according to established protocols.[218] Briefly, mitochondria were diluted to a final concentration of 0.25 mg/mL in respiration buffer containing 210 mM mannitol, 70 mM sucrose, 10 mM MOPS, and 5

mM KH_2PO_4 (pH 7.4). Substrate-driven respiration was assessed using either 0.1 mM pyruvate plus 1 mM malate, 10 mM glutamate plus 1 mM malate, or 1 mM succinate. Oxygen consumption was measured using a fluorescence lifetime–based dissolved oxygen monitoring system (Instech) at 20°C. State 3 respiration was initiated by the addition of ADP (0.5 mM) at 2 min, and oxygen consumption was monitored until complete conversion of ADP to ATP, corresponding to state 4 respiration.

ETC enzyme activity assays

NADH oxidase activity was measured as previously described.[219] Briefly, isolated and protein quantified mitochondria were snap frozen in 25 mM MOPS (pH 7.4) at 0.025 mg/mL and kept in liquid nitrogen until ready to be used. To this frozen-thawed solution, 150 µM NADH was added and the rotenone-sensitive rate of NADH oxidation (ε_{340} = 6200 M^{-1} cm^{-1}) in the presence of 10mM KCl was measured spectrophotometrically via an Agilent 8453 diode array UV−Vis spectrophotometer. To measure Complex 1 activity, 50nM antimycin A and 100uM UQ1 were added to the frozen-thawed mitochondria, followed by 150uM NADH. Complex I activity was then monitored spectrophotometrically as the rate of NADH oxidation. Rotenone (100 nM) was used as an inhibitor to ensure NADH utilization was dependent on complex I activity.

2.6 Acknowledgements

This work was supported by the National Institutes of Health (R35GM142726, P20GM125528 to H.C.R.), Institutional Development Award (IDeA) from the National Institute of General Medical Sciences (NIGMS) of the National Institutes of Health (NIH) (P20GM103640 to J.L. as a junior investigator), and the Presbyterian Health Foundation (Pilot Research Funding to H.C.R.; Bridge Funding to J.L..). APP plasmids were provided by Dr. Bart De Strooper and Dr. Joris de Wit (VIB-KU Leuven, Belgium)[115]. PGAM5 plasmids were provided by Dr. Apirat Chaikuad (Institute for Pharmaceutical Chemistry, Johann Wolfgang Goethe-University and Buchmann Institute for Molecular Life Sciences, Germany)[158]. The ITC experiments were done at OU Protein Production and Characterization Core facility, supported by IDeA from the NIGMS of NIH (P20GM103640 and P30GM145423), the OU Vice President for Research and Partnerships, and the OU College of Arts and Sciences. PGAM5 KO mouse strain was provided by Dr. Yishi Jin with permission from Dr. Michael Lenardo who originally developed the mice[215]. Data analysis was supported by the OMRF Center for Biomedical Data Sciences. Figure 5 schematic was created in Biorender-https://BioRender.com/ftsycbt

Chapter 3: Characterization of brain mitochondria isolated from APP KO and PGAM5 KO mice

3.1 Introduction

Since we observed impaired brain mitochondria function in the absence of APP, we investigated other parameters to fully analyze the mitochondrial behavior in these APP KO mouse brains. We also wanted to see if a similar change in mitochondrial function will be observed in the PGAM5 KO mouse brain mitochondria. We harvested the PGAM5 KO brain mitochondria using the same protocol as we did for APP KO mentioned in chapter 2 and analyzed the substrate specific respiration as well as electron transport chain efficiency. We also further dissected the data obtained from respiratory assays done with both APP KO and PGAM5 KO mitochondria and looked at other parameters like P/O ratio, state 4 respiration and Respiratory Control Ratio (RCR). These analyses are described below.

3.2 WT vs APP KO mouse brain mitochondria

3.2.1 P/O ratios

P/O ratio measures the number of ATP molecules produced per oxygen atom (ATP/O atom) during respiration in the mitochondria. Both pyruvate and glutamate generate NADH which feeds into the ETC to pump out 10 protons while it takes 4 protons to make an ATP (P/O = 2.5). Succinate only results in 6 protons being pumped out of the mitochondria, but it still takes 4 protons to make an ATP (P/O = 1.5). When we calculated the P/O ratios from our respiration data, based on state 3 ratios (Figure 9), we expected to see a lower ratio for pyruvate and glutamate with no differences in succinate. Surprisingly, we saw that the pyruvate/malate P/o ratios were increased in the pyruvate/malate respiration in the absence of APP.

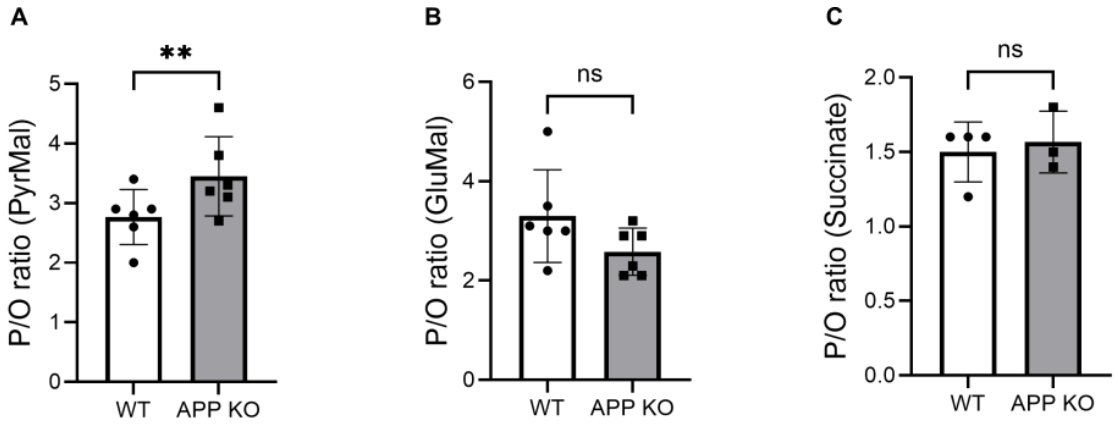

Figure 12. P/O ratios in APP KO mouse brain mitochondria. Graphs showing the P/O (phosphate/oxygen) ratios for different oxidizable substrates (A. Pyruvate/malate, B. glutamate/malate, C. Succinate), in the mitochondria isolated from 6-8 months old APP KO mouse brains. Values shown are the means ± SD (n =4 - 6). Two-tailed paired t-tests were performed for each graph,** ($P < 0.01$), ns (non-significant).

3.2.2 State 4 respiration

State 4 respiration (resting respiration) measures the oxygen consumption of isolated mitochondria after ADP has been converted to ATP, indicating the rate of proton leak across the inner mitochondrial membrane[219,220]. We also quantified the state 4 respiration for these mitochondria and found no significant differences between WT and APP KO in any of the substrates (Figure 10).

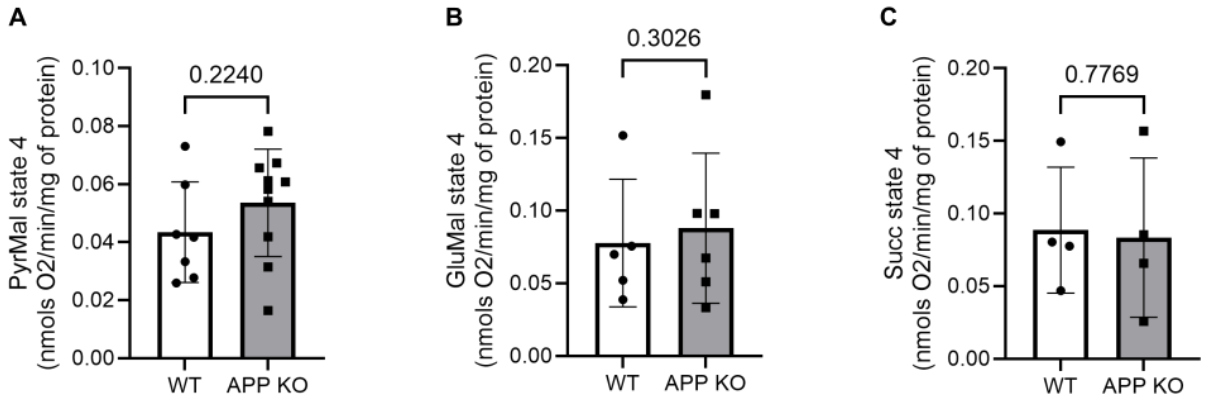

Figure 13. Resting (state 4) respiration in APP KO mouse brain mitochondria. Graphs showing the state 4 respiration for different oxidizable substrates (A. Pyruvate/malate, B. glutamate/malate, C. Succinate), in the mitochondria isolated from 6-8 months old APP KO mouse brains. Values shown are the means ± SD (n =4 - 6). Two-tailed paired t-tests were performed for each graph. P-value showed non-significant changes.

3.2.3 Respiratory Control Ratios (RCR)

In mitochondrial respiratory measurements, an RCR (Respiratory Control Ratio) value above 5 indicates healthy, well-coupled, and fully functional mitochondria. A high RCR signifies efficient conversion of oxygen consumption into usable energy (i.e. ATP). The RCR is a critical indicator of mitochondrial health and function, calculated as the ratio of State 3 respiration (with ADP, maximal phosphorylation rate) to State 4 respiration (without ADP, basal leak rate). A low RCR (below 5) indicates a proton leak and hence reduced ATP synthesis, often due to injury, disease, or toxic effects. Our data showed no difference in the RCR between WT and APP KO mitochondria (Figure 11). Moreover, we found that the isolated mitochondria from both genotypes had an RCR of below 5 (y-axis), irrespective of the substrate (Figure 11).

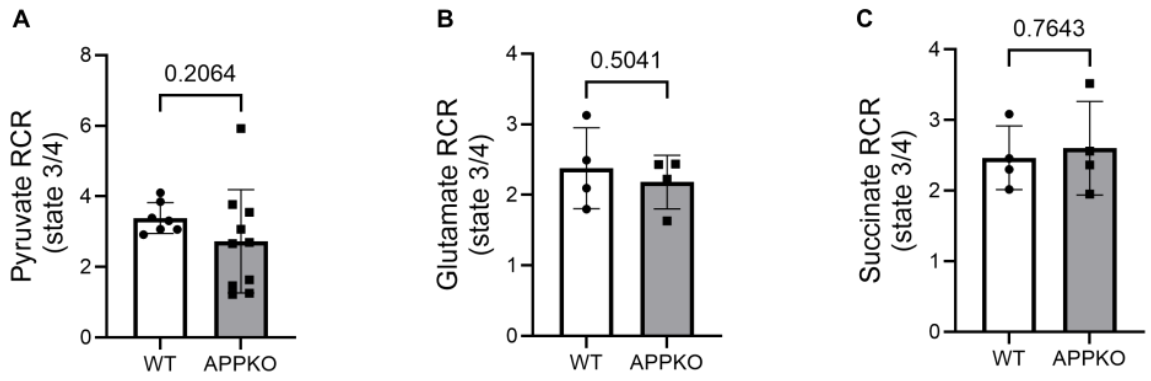

Figure 14. Respiratory Control Ratio in APP KO mouse brain mitochondria. Graphs showing the RCR (Respiratory Control Ratio) for different oxidizable substrates (A. Pyruvate/malate, B. glutamate/malate, C. Succinate), in the mitochondria isolated from 6-8 months old APP KO mouse brains. Values shown are the means ± SD (n =4 - 6). Two-tailed paired t-tests were performed for each graph. P-value showed non-significant changes.

3.3 WT vs PGAM5 KO mouse brain mitochondria

3.3.1 Maximal respiration and ETC

Being an interacting protein of APP in the mitochondria, we hypothesized that PGAM5 mediated the effect of APP in mitochondrial respiration (chapter 2). We isolated brain mitochondria from PGAM5 KO mouse and measured substrate-specific respiration in a similar manner as described above (chapter 2). Upon analysis, we did not see any changes in the respiration in the absence of PGAM5 when compared to wild-type (WT) mitochondria in any of the substrates used (Figure 12A-C). Since APP KO mitochondria did not show any changes in Palmitoyl carnitine (PC) mediated respiration, we did not look at the PC-mediated fatty-acid metabolism or fatty-acid oxidation (FAO) in these mitochondria either. Hence it is inconclusive if PGAM5 affects respiration in these mitochondria via FAO. We also looked at the NADH oxidase activity and Complex I activity as a measure of overall electron transport chain efficiency (ETC). We again found no difference in ETC efficiency in the absence of PGAM5 as compared to WT (Figure 12D-E).

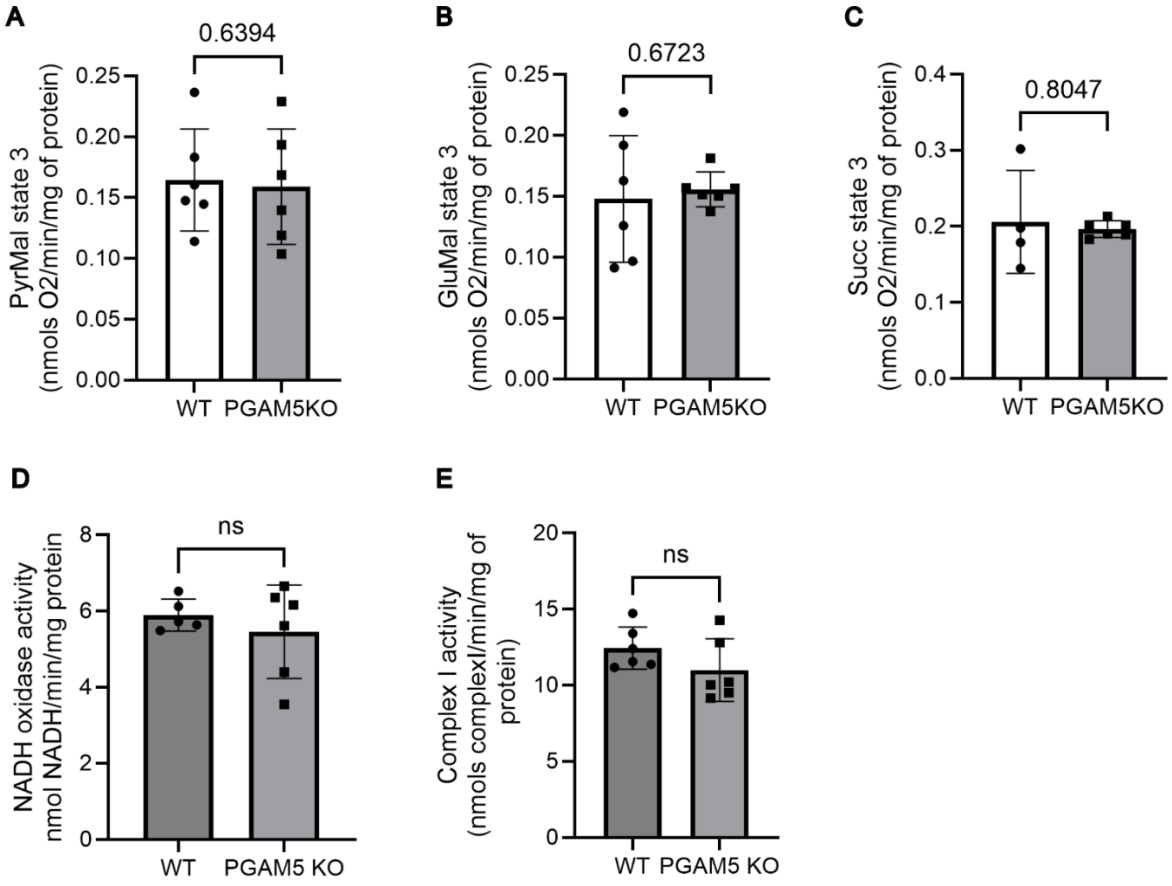

Figure 15. Maximal respiration and ETC enzyme activities in PGAM5 KO mouse brain mitochondria. (A-C). Graphs showing maximum respiration by utilizing different oxidizable substrates (A. Pyruvate/malate, B. glutamate/malate, C. Succinate), in the mitochondria isolated from 6-8 months old PGAM5 KO mouse brains. Values shown are the means ± SD (n =4 - 6). Two-tailed paired t-tests were performed for each graph. **(D-E).** Graphs showing electron transport chain efficiency as indicated by D. Complex I activity and E. NADH oxidase activity. Values shown are means ± SD (n =5 - 6). Two-tailed paired t-test was performed for each graph, ns (non-significant).

3.3.2 P/O ratios

We found that ADP to ATP conversion efficiency was unaltered in the PGAM5 KO mitochondria when Pyruvate or Glutamate were used as substrates (Figure 13A-B). Surprisingly, we saw an increased phosphorylation efficiency in these PGAM5 KO mitochondria with succinate being the substrate (Figure 13C). This indicates that FADH2-mediated respiration is improved in these mitochondria.

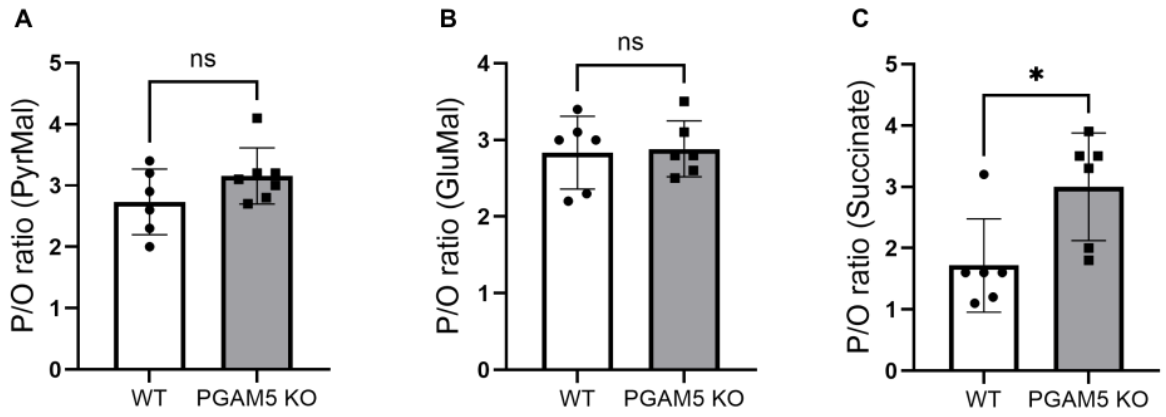

Figure 16. P/O ratios in PGAM5 KO mouse brain mitochondria. Graphs showing the P/O (phosphate/oxygen) ratios for different oxidizable substrates (A. Pyruvate/malate, B. glutamate/malate, C. Succinate), in the mitochondria isolated from 6-8 months old APP KO mouse brains. Values shown are the means ± SD (n =4 - 6). Two-tailed paired t-tests were performed for each graph,* ($P < 0.05$), ns (non-significant).

3.3.3 State 4 respiration

We also assessed whether the absence of PGAM5 affected the resting respiration of mitochondria and found no significant difference with any of the substrates when compared to WT mouse brain mitochondria (Figure 14).

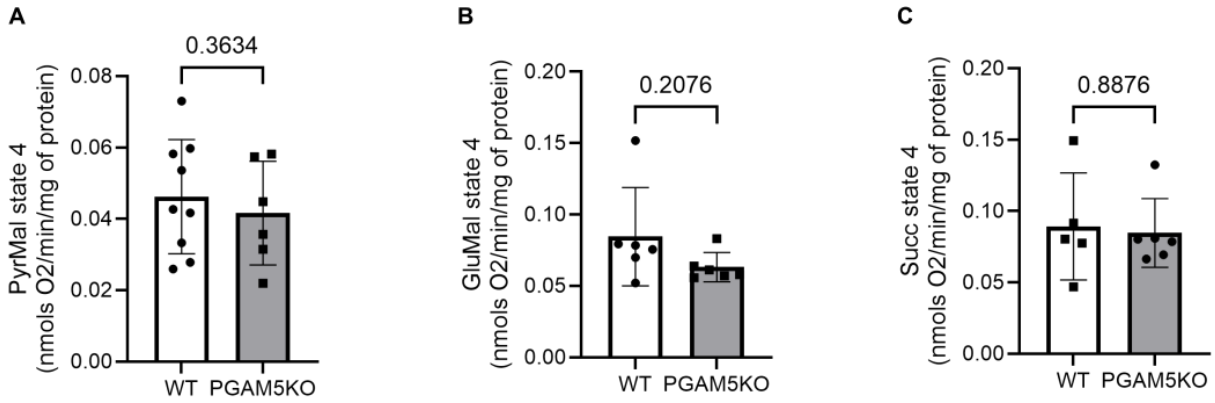

Figure 17. Resting (state 4) respiration in PGAM5 KO mouse brain mitochondria. Graphs showing the state 4 respiration for different oxidizable substrates (A. Pyruvate/malate, B. glutamate/malate, C. Succinate), in the mitochondria isolated from 6-8 months old PGAM5 KO mouse brains. Values shown are the means ± SD (n =4 - 6). Two-tailed paired t-tests were performed for each graph. P-value showed non-significant changes.

3.3.4 Respiratory Control Ratios (RCR)

We also saw no significant changes in the quality of mitochondria isolated from PGAM5 KO brain mitochondria as compared to WT, indicated by RCR values (Figure 15). Similar to the isolated mitochondria from APP KO brain, PGAM5 KO brain mitochondria also showed a low RCR value (below 5) indicating a baseline impairment in their functions due to isolation process.

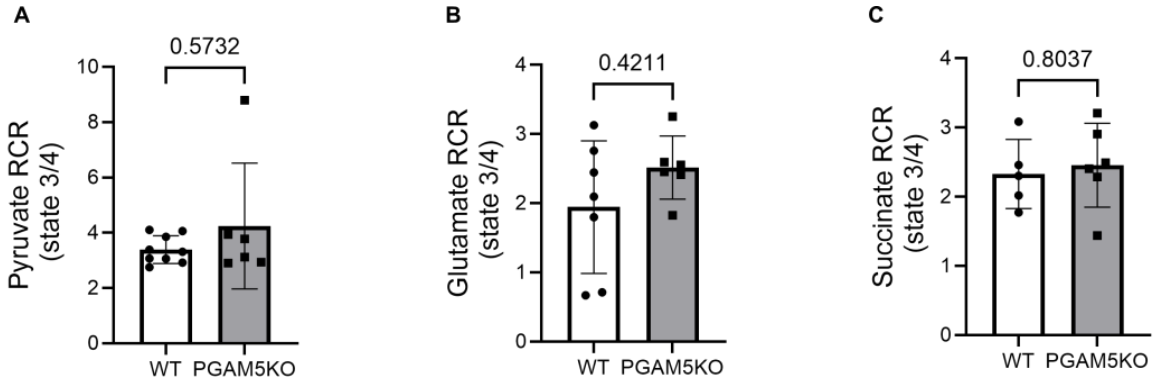

Figure 18. Respiratory Control Ratio in PGAM5 KO mouse brain mitochondria. Graphs showing the RCR (Respiratory Control Ratio) for different oxidizable substrates (A. Pyruvate/malate, B. glutamate/malate, C. Succinate), in the mitochondria isolated from 6-8 months old PGAM5 KO mouse brains. Values shown are the means ± SD (n =4 - 6). Two-tailed paired t-tests were performed for each graph. P-value showed non-significant changes.

3.4 Conclusions

In APP KO brain mitochondria, the unexpected increase in P/O ratios for pyruvate/malate respiration suggests that mitochondria may be compensating for the reduced maximal respiration rates (Chapter 2, Figure 7) by increasing ATP production efficiency. Such compensation could reflect an adaptive response aimed at maintaining energy output under conditions of impaired substrate oxidation. However, the lack of differences in state 4 respiration and respiratory control ratio (RCR) between wild-type and APP knockout mitochondria indicates that coupling efficiency and proton leak are not significantly altered by APP loss. Notably, the uniformly low RCR values (below 5) across all samples, points to a broader methodological limitation i.e. the mitochondrial isolation process itself may induce a baseline level of dysfunction. This suggests that

while relative comparisons between genotypes remain valid, the absolute functional capacity of the mitochondria is likely underestimated. Therefore, interpretations of mitochondrial efficiency and coupling should be made cautiously, as the in vitro system may not fully recapitulate the physiological state of mitochondria in intact brain tissue.

The increased phosphorylation efficiency, indicated by P/O ratios, observed with succinate in PGAM5 KO mitochondria points to a shift in metabolic preference toward FADH2-linked respiration. This enhancement may reflect increased Complex II activity or upregulation of pathways that generate FADH2, such as the TCA cycle or fatty acid β-oxidation. Another possible explanation of increased FADH2-mediated respiration can be drawn from the fact that PGAM5 is involved in mitophagy and in its absence, cells are left with a larger population of mitochondria that are reliant on Complex II respiration. Overall, this data represents a compensatory metabolic adaptation that maintains ATP production in the absence of PGAM5-mediated quality control mechanisms. Overall, while PGAM5 loss does not broadly disrupt mitochondrial respiration, it appears to subtly reprogram mitochondrial substrate utilization, particularly enhancing $FADH_2$-dependent energy metabolism.

Chapter 4: Investigating PGAM5 in Alzheimer's disease: Role in APP processing, localization and mitochondrial dysfunction

Although PGAM5 has been implicated in other neurological disorders[221,222], it is currently unknown whether PGAM5 contributes to the development or progression of Alzheimer's disease. Various studies have shown a direct effect of the substrates of PGAM5 in disease progression. This includes mitochondrial proteins like DRP1[223,224], MFN2[225] and PINK1[226]. Since our study showed that APP interacts with PGAM5, we set to investigate whether PGAM5 affects APP processing and localization. We also tested if PGAM5 protein levels are altered in the AD mouse brain mitochondria, to determine if PGAM5 can play a role in mitochondrial dysfunction seen in AD.

4.1 Role of PGAM5 in APP processing and subcellular localization

We first assessed the distribution of full-length amyloid precursor protein (APP) across subcellular compartments in brains from PGAM5 knockout (KO) mice. Consistent with previous reports, APP was predominantly localized to the endoplasmic reticulum (ER). In agreement with our earlier findings (Chapter 2), a substantial fraction of APP was also detected at mitochondria-ER contact sites (MERCS) (Figure 16A). Notably, the levels of full-length APP (APP FL) were not altered in the absence of PGAM5 at either the ER or MERCS (Figure 16B-C).

Because amyloid-β (Aβ) is generated through proteolytic processing of APP C-terminal fragments (APP CTF), we next quantified CTF levels within these compartments. APP CTF abundance remained unchanged in PGAM5 KO mice compared to wild-type controls (Figure 16D-E).

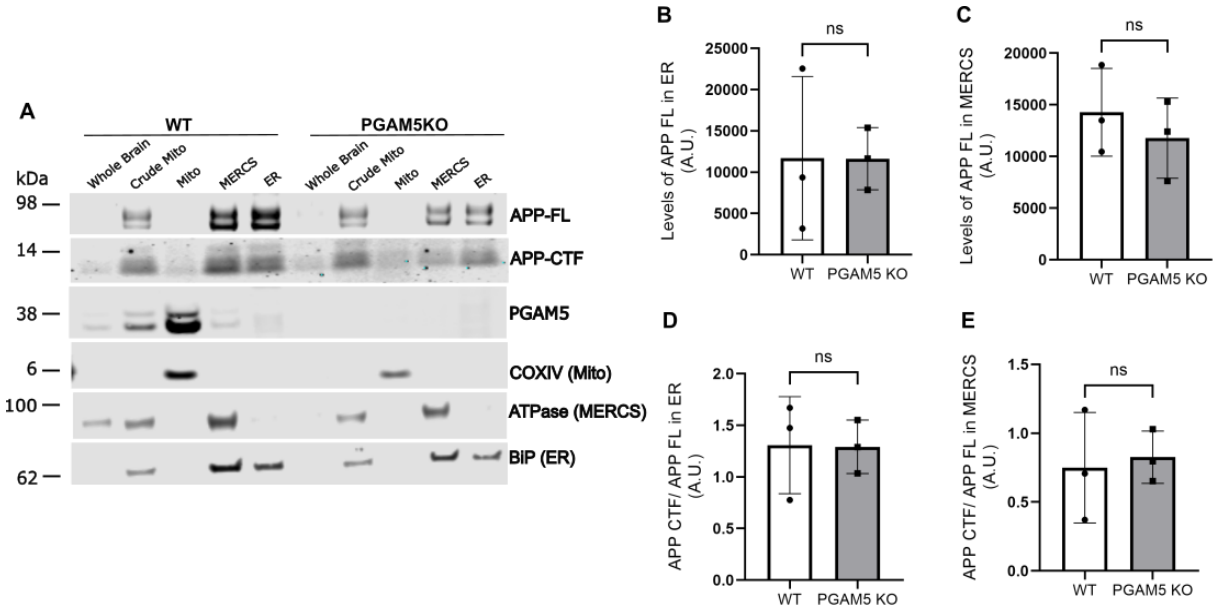

Figure 19. Levels of APP in mitochondria and MERCS isolated from PGAM5 KO mouse brain. A. Western blot showing subcellular localization of APP and PGAM5 in WT (C57Bl6, 3 months old, females) and PGAM5 KO (3 months old, females) mouse brains. The cellular compartments shown are Whole brain, Crude mitochondria, Mitochondria, Mitochondria-ER contact sites (MERCS) and Endoplasmic reticulum (ER). The purity of each sample was validated by its marker protein (COXIV (Cytochrome c Oxidase Subunit 4), Mitochondria; ATPase (Adenosine Triphosphatase), MERCS; BiP (Binding Immunoglobulin Protein), ER). **(B-E).** Graphs showing western blot quantification indicating levels of APP full-length (FL) protein in B. ER and C. MERCS and APP C-terminal fragments (CTF) in D. ER and E. MERCS. Values shown are band intensity means ± SD (n =7). One-way ANOVA tests were performed for each graph, ns (non-significant).

4.2 Contribution of PGAM5 in mitochondrial dysfunction in AD mouse model

We next considered asking whether PGAM5 protein levels are altered in Alzheimer's Disease. To test this, we used an AD mouse model APP NL-G-F. This mouse model avoids APP overexpression but still produces high levels of pathological Aβ due to three mutations related to familial AD (Swedish (NL), Iberian (F), Arctic (G)). These mutations increase total Aβ production (Swedish), increase the ratio of Aβ42/ Aβ40 (Iberian) and promote Aβ aggregation (Arctic). These mice develop early and severe AD pathology including amyloid plaques, inflammation, and synaptic loss[227]. We characterized these APP NL-G-F mouse brain via immunohistochemistry confirming the significant increase in Aβ plaque deposition as compared to WT (Figure 17).

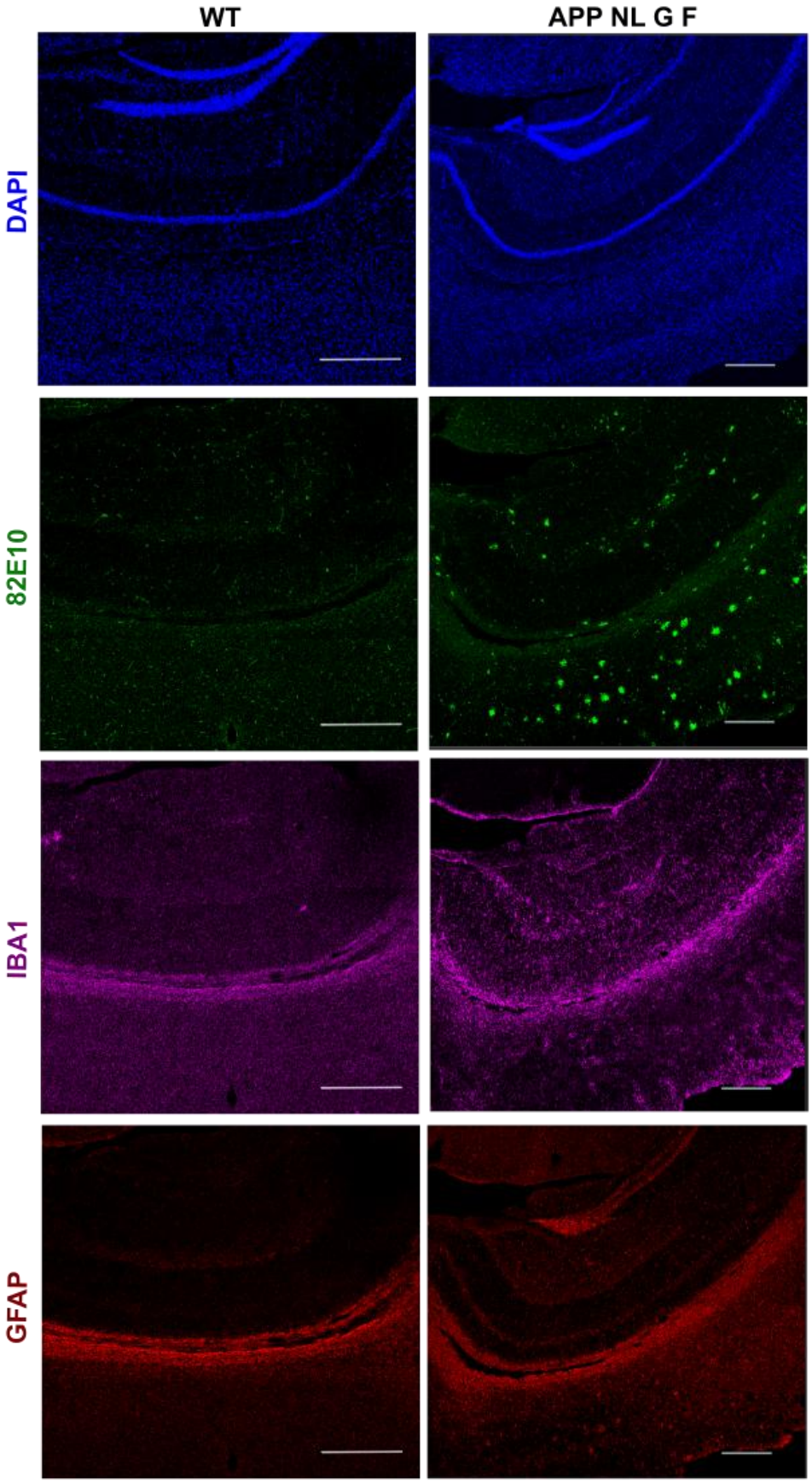
WT
APP NL G F
DAPI
82E10
IBA1
GFAP

Figure 20. Aβ plaque deposition and reactive glia in APP NL-G-F mouse brains. Confocal images of coronal sections of mouse brains showing cortex and hippocampus in wild-type (WT, left) and APP NL-G-F (right) mouse showing nuclear dye (DAPI; blue), Amyloid-β plaques antibody (82E1; green) (Mouse IgG, Immuno-biological, 10323), IBA1 (Microglia marker, Chicken IgG, Encor Biotechnology, CPCA-IBA1) and GFAP (Astrocyte marker, Goat IgG, Encor Biotechnology, GPCA-GFAP) staining. Scale bars, 500μm.

We also carried out some mitochondrial functional assessments by measuring the NADH oxidase and complex 1 activity in the young (4mo) and old (12mo) APP NL-G-F mice brain mitochondria as a measure of electron transport chain efficiency (Figure 18). Although we did not see any changes in the enzymatic activity of the brain mitochondria isolated from these APP NL-G-F mice, the conclusion should be made with caution since the low activity levels can be attributed to the fact that these mitochondria were not freshly isolated but flash frozen and thawed.

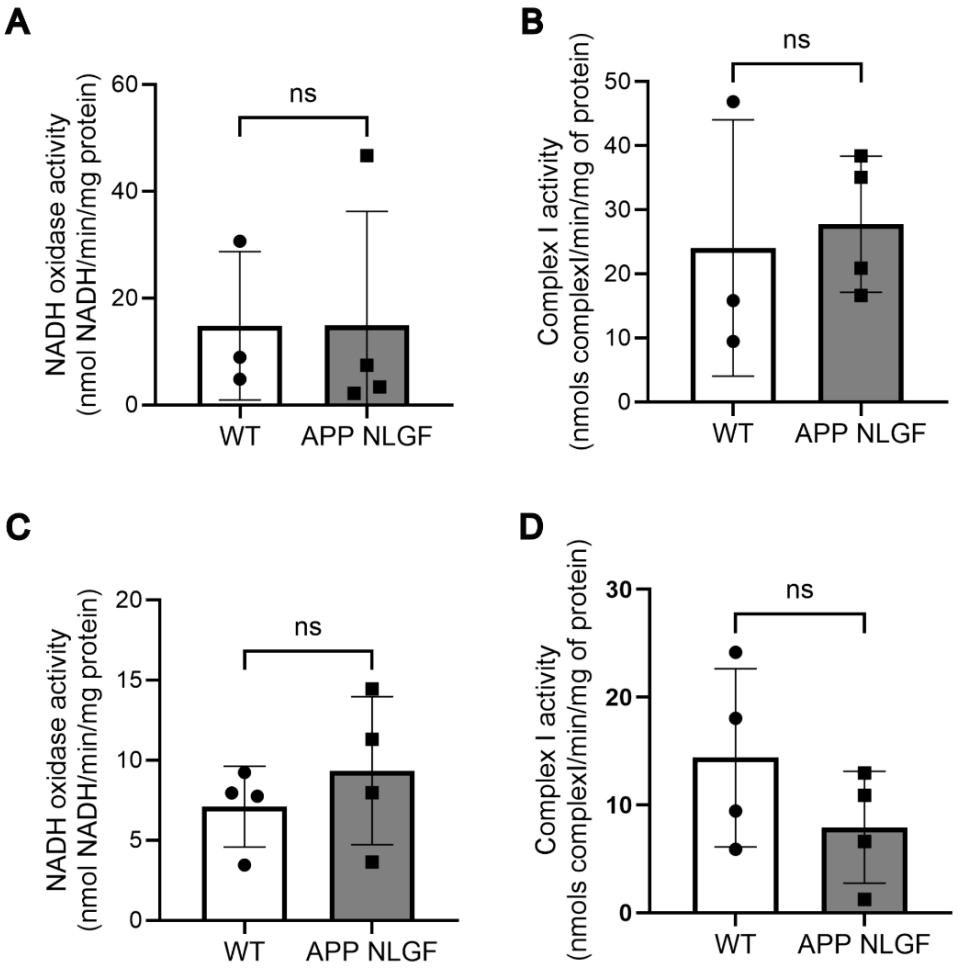

Figure 21. ETC enzyme activities in APP NL-G-F mouse brain mitochondria.

Graphs showing electron transport chain efficiency as indicated by A. NADH oxidase and B. Complex I activity in the mitochondria isolated from 4 mo. old and C. NADH oxidase and D. Complex I activity in the mitochondria isolated from 12 mo. old WT and APP NL-G-F mouse brains. Values shown are means ± SD (n=3-4). Two-tailed paired t-test was performed for each graph, ns (non-significant).

Next, we isolated the subcellular compartments from the whole APP NL-G-F mouse brains. As seen earlier, PGAM5 protein bands were observed only in the crude

mitochondria and mitochondria fractions on the western blots (Figure 19, *other compartments not shown for simplicity*). The western blot and corresponding quantification demonstrated that both in the crude mitochondria as well as mitochondria, levels of cleaved PGAM5 (lower band on the western blot) were significantly decreased in older (11 months) AD mice. No significant differences in PGAM5 cleavage were seen at 3 months old APP NL-G-F mice (Figure 19).

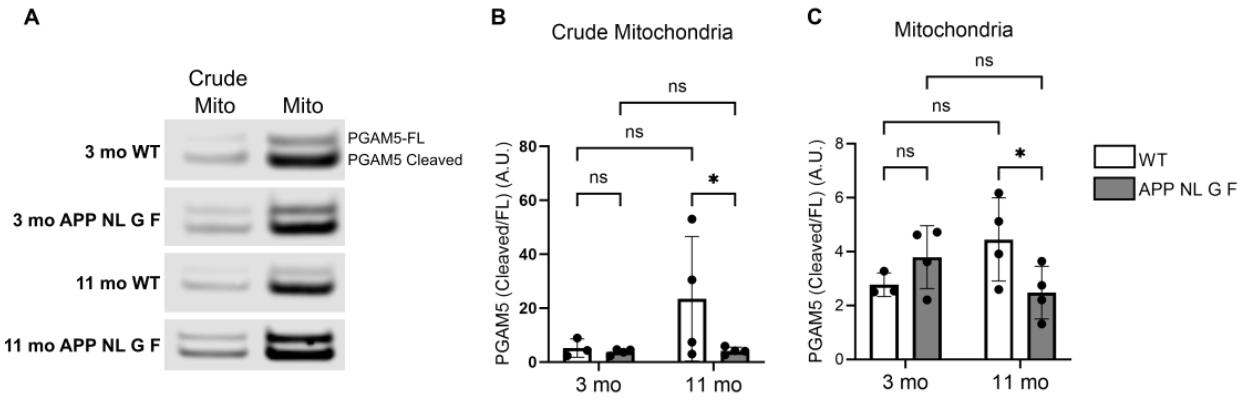

Figure 22. PGAM5 cleavage is impaired in APP NL-G-F mouse brain. A. Western blot and **(B-C).** its quantification showing PGAM5 protein levels (FL; full-length and cleaved) in the crude mitochondria and mitochondria of 3 mo. and 11 mo. old WT (C57Bl6, females) and AD (APP NL-G-F, females) mouse brains. Values shown are band intensity means ± SD (n =4). Two-way ANOVA tests were performed for each graph, * ($P < 0.05$), ns (non-significant).

4.3 Conclusions

The results of this study suggest that the loss of PGAM5 does not significantly alter the localization or early processing of amyloid precursor protein (APP) in the brain. APP remains primarily associated with the endoplasmic reticulum, with a notable portion also present at mitochondria-ER contact sites, and its full-length protein levels are unchanged in PGAM5 KO mice. Similarly, the abundance of APP C-terminal fragments (APP CTF) is unaffected, indicating that PGAM5 does not play a major role in the initial proteolytic steps that generate APP CTF. However, whether PGAM5 deficiency affects subsequent γ-secretase processing or Aβ production remains to be determined.

Although PGAM5 does not affect APP processing, our data suggests its contribution in impaired mitophagy often seen in AD models mimicking the familial form of AD and the brains of SAD patients[228,229]. Mechanistically, PGAM5 cleavage is mediated by the mitochondrial intramembrane protease Presenilin-Associated Rhomboid-Like (PARL), which plays a critical role in mitochondrial quality control. Under normal conditions, PARL cleaves PGAM5 in response to mitochondrial stress and triggers mitophagy[159]. Hence a reduced cleavage of PGAM5 in older AD mice indicates impaired PARL activity. This reduction in PGAM5 cleavage is age-dependent and not observed in younger mice, suggesting a progressive dysfunction. Overall, these findings imply that while PGAM5 does not influence APP processing directly, its impaired cleavage may still contribute to impaired mitochondrial functions, given a rich pool of mitochondrial functions that are mediated by PGAM5 biology.

Chapter 5: Overall discussion

This work highlights a previously unrecognized role of Amyloid precursor protein (APP) within brain mitochondria, expanding the current understanding of its physiological functions beyond its established involvement in amyloid-β production. All members of the APP protein family are highly expressed in the brain, indicating their likely importance in maintaining normal brain function. Furthermore, the evolutionary conservation of APP and its homologs across diverse species underscores their fundamental biological significance. Notably, among these family members, only APP contains the amyloid-β (Aβ) sequence. This distinction suggests that the core physiological roles of APP are unlikely to depend on Aβ itself, but rather on conserved structural domains (e.g. extension domain, acidic domain, E1 and E2) that are shared across the APP protein family.

The findings presented in this work identify a previously uncharacterized interaction between APP and the mitochondrial phosphatase PGAM5 thereby expanding the known repertoire of APP's physiological functions within mitochondria. While APP has traditionally been studied primarily in the context of Aβ generation in Alzheimer's disease, the results discussed here support an expanded role of APP at mitochondria and mitochondria-ER contact sites (MERCS). The observed co-localization of APP and PGAM5 at MERCS highlights these inter-organelle interfaces as critical platforms for signaling pathways. Given that MERCS are already known to coordinate key processes such as calcium signaling, lipid metabolism, and mitochondrial dynamics, the APP-PGAM5 axis may represent an important regulatory mechanism that links protein interaction to essential cellular functions.

By demonstrating that APP directly regulates mitochondrial respiration, this study provides a potential link between amyloid biology and metabolic dysfunction. Rather than acting solely as a precursor to toxic peptides, APP may have a dual role both as a physiological regulator of mitochondrial functions and as a pathological contributor when dysregulated.

Studies have shown that APP affects mitochondrial functions, especially respiration and ATP production but the mechanisms are unknown. Through its binding to the Keap1-binding domain of PGAM5, APP can be regulating mitochondrial respiration and metabolism via PGAM5-Keap1-Nrf2 pathway as indicated by studies done in chapter 2. Further experiments are needed to validate this hypothesis such as immunostainings for Nrf2 to study its co-localization with nucleus and mitochondria in WT and APP KO astrocytes. Subcellular fractionation experiments with whole mouse brains can also indicate if Nrf2 nuclear translocation is impaired in the absence of APP.

In addition, investigating the APP-PGAM5 interaction may provide broader insights into how APP influences other mitochondrial processes, including mitophagy, fission, and fusion. Potential experimental approaches to explore these mechanisms are discussed in the following chapter.

Finally, although Aβ production and other AD pathologies have not yet been examined in a PGAM5 KO model, the observed reduction in PGAM5 cleavage in our AD knock-in model provides a plausible mechanistic basis for the impairment of mitophagy often observed in AD. In this context, PGAM5 emerges as a potential therapeutic target, and its modulation could offer a strategy to alleviate mitochondrial deficits associated with

AD. However, this possibility remains speculative and requires further experimental validation, particularly to define the precise molecular pathways through which PGAM5 influences mitophagy in the disease setting. Moreover, these conclusions should be interpreted with caution due to limitations in the experimental model. The AD knock-in model employed in this study, APP NL-G-F primarily recapitulates amyloid-β pathology and does not encompass other critical hallmarks of human AD, such as neurofibrillary tau tangles. The absence of these features may restrict the extent to which the findings can be generalized to the full spectrum of disease pathology. It is therefore likely that additional human-specific factors including neurofibrillary tau tangles are necessary for a more comprehensive understanding of AD progression. Incorporating such elements into future models will be essential for drawing more definitive conclusions regarding the role of PGAM5 in mitophagy impairment in AD.

Chapter 6: Future directions

The interaction between APP and PGAM5 can be further investigated by assessing changes in PGAM5 mRNA and protein expression under conditions of APP deficiency or overexpression. To this end, we quantified PGAM5 mRNA levels across various cell types isolated from whole brains of wild-type (WT) and APP knockout (APP KO) mice. While PGAM5 mRNA expression remained unchanged across individual cell types, analysis of whole brain lysates revealed a significant increase in PGAM5 mRNA levels in the absence of APP (Figure 20A [input], 20B). Notably, this increase was more pronounced when the analysis was restricted to female samples (Figure 20C), suggesting a potential sex-dependent interaction between APP and PGAM5.

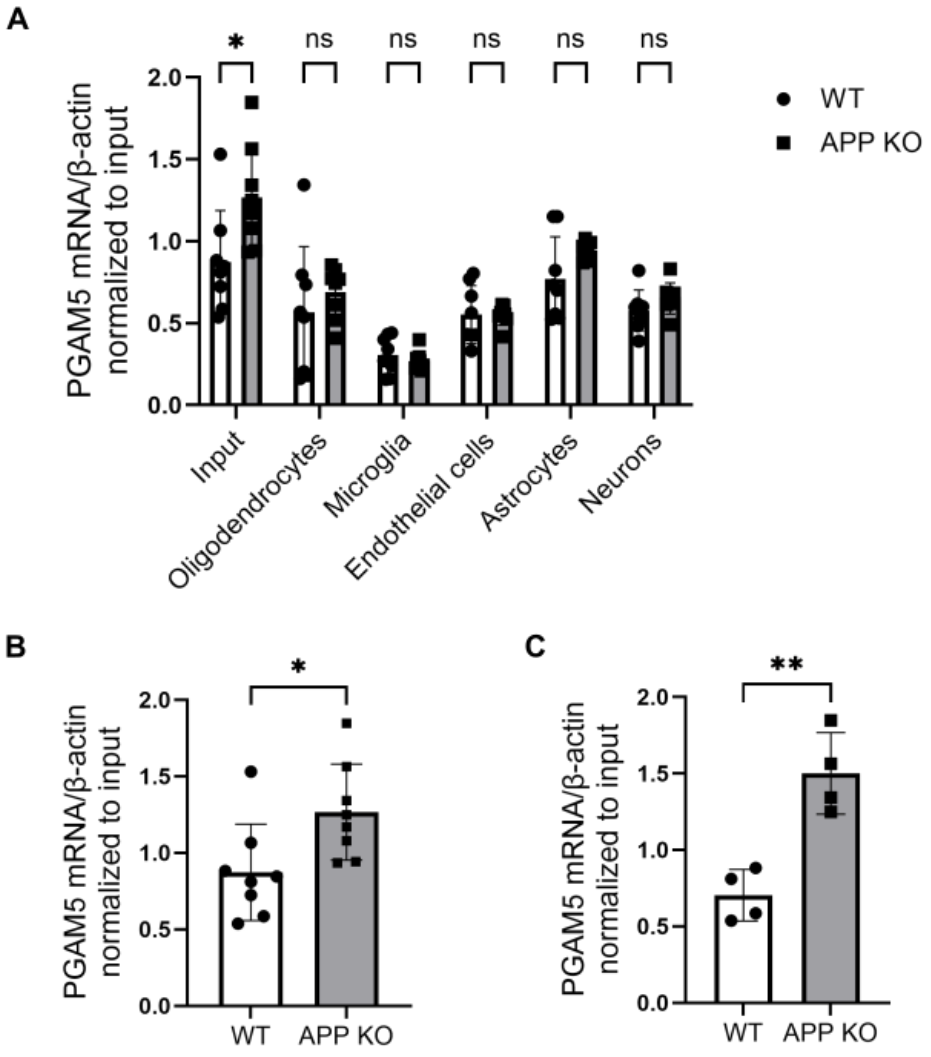

Figure 23. PGAM5 mRNA levels are increased in APP KO mouse brain. Plots showing relative mRNA expression of PGAM5 in **A.** different cell types isolated from WT and APP KO mouse brain and **B.** whole brains measured by RT-qPCR. **C.** Plot showing PGAM5 mRNA levels in female WT and APP KO mouse whole brains. Values shown are the means ± SD (n = 8) and the statistics were performed using two-way ANOVA, followed by Tukey's multiple comparison test. * ($P < 0.05$), ** ($P < 0.01$), ns (non-significant).

Given that APP contains multiple phosphorylation sites including serine and threonine residues located in both the extracellular (S198, S206) and the cytoplasmic domain (T654, S655, T668, S675, T686) and that PGAM5 functions as a serine/threonine phosphatase, it is of interest to investigate whether APP can be a substrate for PGAM5.

To address this, preliminary experiments were conducted using purified sAPPα-Fc and PGAM5Δ54 to assess potential effects on the phosphorylation status of soluble APP, with particular focus on residues S198 and S206. sAPPα-Fc was incubated in the presence and absence of PGAM5Δ54 (Figure 21); however, no detectable changes in phosphorylation levels were observed under these conditions using phosphor-serine antibodies (not shown).

Notably, immunoblot analysis using phospho-serine-specific antibodies (4A3 and 16B4) revealed the presence of a lower molecular weight band (~30 kDa) in the sAPPα-Fc sample which seemed to disappear when incubated with equimolar amounts of PGAM5Δ54. Despite this observation, the identity of the ~30 kDa band remains unclear, particularly given that the expected molecular weight of sAPPα-Fc is approximately 98 kDa, as confirmed by detection with the APP22C11 antibody, which is specific for sAPPα. Future studies can look at the phosphorylation levels of APP using phos-tag gels or radioactive kinase assays using ^{32}P-labeled ATP.

Moreover, PGAM5 mediates mitochondrial functions by regulating the phosphorylation status of its substrates, including BcL-xL, Drp-1, and FUNDC1. A potential study could therefore investigate whether APP influences PGAM5-mediated substrate binding and

phosphorylation activity. This may be achieved by analyzing whole-brain lysates derived from wild-type (WT), APP knockout (KO), and APP overexpression mouse models, followed by probing with phospho-specific antibodies targeting BcL-xL, Drp-1, and FUNDC1.

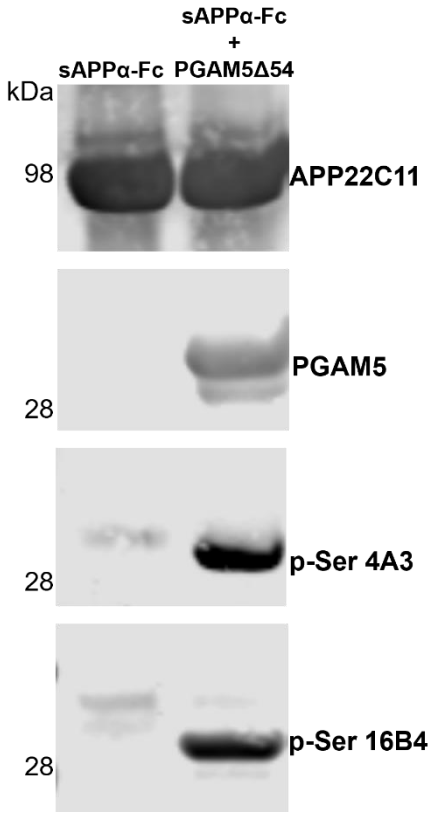

Figure 24. Phosphorylation levels of purified Fc-tagged sAPPα were unaletred by PGAM5Δ54. Western blot showing purified sAPPα-Fc alone and sAPPα-Fc incubated with PGAM5Δ54. sAPPα was detected by APP22C11 antibody (Invitrogen, 14-9749-82) while phosphorylated serines were detected by p-Ser 4A3 (sc-81516, Santacruz) and p-Ser 16B4 (sc-81514, Santacruz).

Structural studies can provide further insight into the interaction between APP and PGAM5. Based on our findings on the domains responsible for this interaction, we utilized AlphaFold2 to predict the structure of these domains in complex, with the aim of pinpointing residues that are in close contact (Figure 22). Table 1 lists the closest atom interactions between APP and PGAM5 in this model where Valine 81 in the Keap1-binding motif (80-NVESGE-85) of PGAM5 was predicted to be in close contact with APP. A distance of 3.42Å suggests a strong hydrophobic (van der Waals) interaction between the two carbons of Valines. Such structural analyses are particularly valuable for guiding mutagenesis studies, enabling the investigation of functional changes in brain mitochondria resulting from targeted mutations that disrupt the APP-PGAM5 interaction.

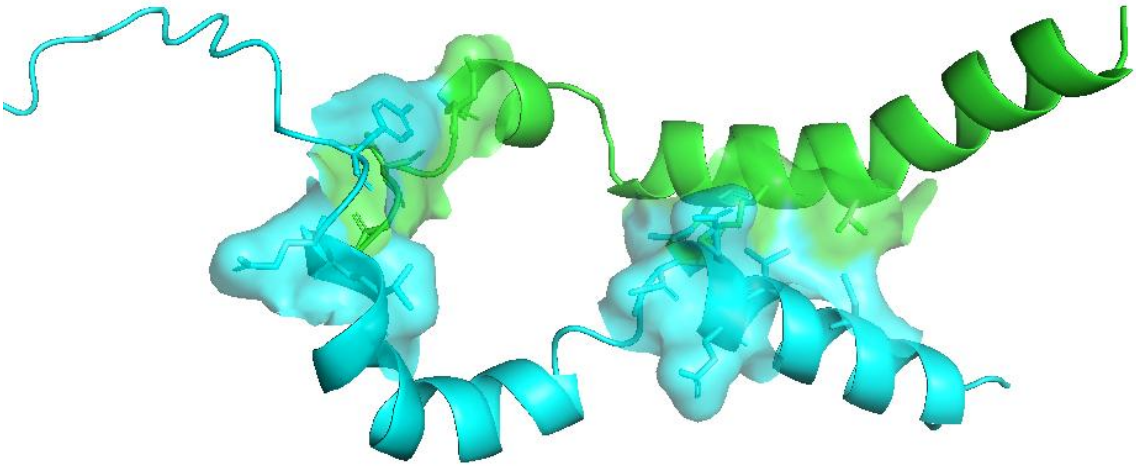

Figure 25. Predicted structure showing interaction between PGAM5 and APP using AlphaFold2. Amino acids 55-94 (UniProt ID: Q96HS1) of PGAM5 (green)

containing multimerization motif and Keap1-binding domain were used with the full-length APP (blue) protein sequence (APP695, UniProt ID: P05067-4).

Chain A- PGAM5	Chain B- APP	Min distance (Å)	Closest atoms
PRO 57	TYR 261	3.75	CB-CE1
GLY 58	TYR 261	3.22	CA-CD2
VAL 59	GLU 259	3.75	CG1-OE1
TRP 60	TYR 261	3.62	NE1-OH
ASP 61	TYR 261	3.48	OD1-OH
LEU 73	VAL 283	3.66	CD1-CG1
ARG 77	SER 282	3.34	NH1-OG
VAL 81	VAL 287	3.42	CG1-CG1

Table 1. Lists of amino acid residue pairs in APP and PGAM5 predicted by AlphaFold2 to be in close contact with each other.

Lastly, to further investigate the role of PGAM5 in Alzheimer's disease, endogenous Aβ levels in whole mouse brain can be measured by multiplex immunoassays in APP NL-G-F knock-in mice with a knock-down or overexpression of PGAM5.

Chapter 7: Supplemental information

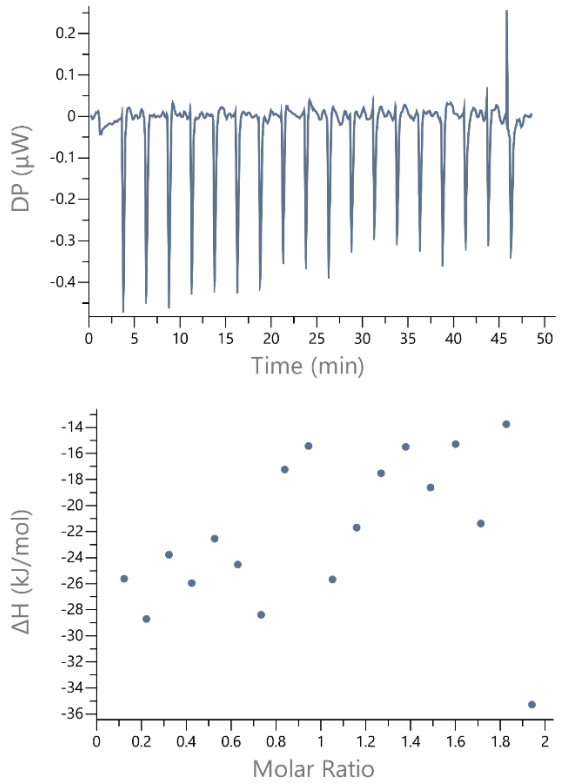

Figure S1. No binding was detected between sAPPα and PGAM5Δ90. Binding curve from isothermal calorimetry experiment done using the sAPPα and PGAM5Δ90 purified proteins (n=1).

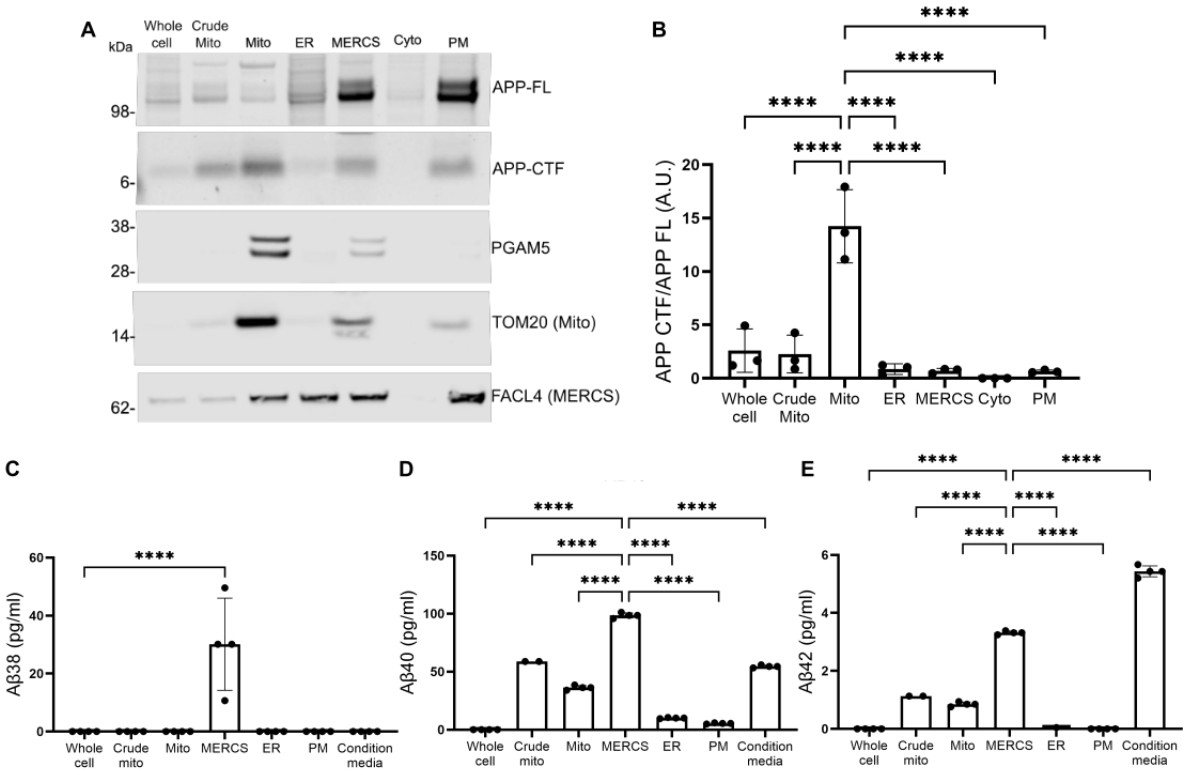

Figure S2. APP C-terminal fragments are enriched in mitochondria and MERCS. A. Western blot showing APP and PGAM5 proteins and B. graph showing quantification APP CTF present in different subcellular compartments of HeLa cells. Values shown are band intensity means ± SD (n =3). One-way ANOVA tests were performed for each graph, ***** ($P < 0.0001$). (C-E). Graphs showing the amounts of C. Aβ38, D. Aβ40 and E. Aβ42 present in different subcellular compartments of HeLa cells, measured by Meso-scale discovery assay (MSD). Values shown are band intensity means ± SD (n =4). One-way ANOVA tests were performed for each graph, ***** ($P < 0.0001$). The cellular compartments shown are Whole cell, Crude mitochondria, Mitochondria, Mitochondria-ER contact sites (MERCS), Endoplasmic reticulum (ER) and Plasma membrane (PM). The purity of mitochondria and MERCS samples were validated by its marker protein (TOM20 (Translocase of Outer Mitochondrial Membrane 20), Mitochondria; FACL4 (Long-chain-fatty-acid—CoA ligase 4)). Condition media was also used as one of the samples in MSD assay.

Magnetic cell-sorting of whole mouse brain

The cell-sorted fractions were prepared as described earlier[230]. Briefly, mice were anesthetized with isoflurane and euthanized by cervical dislocation and decapitation. The brain was dissected and tissue was then transferred to a gentleMACS C-tube and processed as described to obtain different brain cell types[230]. The cell-sorted fractions were validated using RT-qPCR and flow cytometry for cell-specific markers.

RNA extraction and RT-qPCR

RNA was isolated using the Qiagen RNeasy Mini Kit (cat. 74104) and quantified using Nanodrop 1000 spectrophotometer. RNA was converted to cDNA using the High-Capacity cDNA Reverse Transcription Kit (Applied Biosystems 4374966) in a BioRad T100 thermal cycler. RT-qPCR for *Pgam5* was performed using Taqman assay (cat. Mm01205820_g1).

Bibliography

1. 2020 Alzheimer's disease facts and figures. *Alzheimers Dement.* **16**, 391–460 (2020).
2. Alzheimer's Disease Fact Sheet | National Institute on Aging. https://www.nia.nih.gov/health/alzheimers-and-dementia/alzheimers-disease-fact-sheet.
3. Braak, H. & Braak, E. Diagnostic Criteria for Neuropathologic Assessment of Alzheimer's Disease. *Neurobiol. Aging* **18**, S85–S88 (1997).
4. Glenner, G. G. & Wong, C. W. Alzheimer's disease: Initial report of the purification and characterization of a novel cerebrovascular amyloid protein. *Biochem. Biophys. Res. Commun.* **120**, 885–890 (1984).
5. Hardy, J. & Allsop, D. Amyloid deposition as the central event in the aetiology of Alzheimer's disease. *Trends Pharmacol. Sci.* **12**, 383–388 (1991).
6. Kang, J. *et al.* The precursor of Alzheimer's disease amyloid A4 protein resembles a cell-surface receptor. *Nature 1987 325:6106* **325**, 733–736 (1987).
7. Glenner, G. G. & Wong, C. W. Alzheimer's disease: Initial report of the purification and characterization of a novel cerebrovascular amyloid protein. *Biochem. Biophys. Res. Commun.* **120**, 885–890 (1984).
8. 2020 Alzheimer's disease facts and figures. *Alzheimers Dement.* **16**, 391–460 (2020).
9. Parker, W. D., Filley, C. M. & Parks, J. K. Cytochrome oxidase deficiency in Alzheimer's disease. *Neurology* **40**, 1302–1303 (1990).
10. Swerdlow, R. H. & Khan, S. M. A "mitochondrial cascade hypothesis" for sporadic Alzheimer's disease. *Med. Hypotheses* **63**, 8–20 (2004).
11. Shoshan-Barmatz, V., Nahon-Crystal, E., Shteinfer-Kuzmine, A. & Gupta, R. VDAC1, mitochondrial dysfunction, and Alzheimer's disease. *Pharmacol. Res.* **131**, 87–101 (2018).

12. Chakravorty, A., Jetto, C. T. & Manjithaya, R. Dysfunctional Mitochondria and Mitophagy as Drivers of Alzheimer's Disease Pathogenesis. *Front. Aging Neurosci.* **11**, 497777 (2019).

13. Misrani, A., Tabassum, S. & Yang, L. Mitochondrial Dysfunction and Oxidative Stress in Alzheimer's Disease. *Frontiers in Aging Neuroscience* vol. 13 Preprint at https://doi.org/10.3389/fnagi.2021.617588 (2021).

14. Lin, M. T. & Beal, M. F. Mitochondrial dysfunction and oxidative stress in neurodegenerative diseases. *Nature* **443**, 787–795 (2006).

15. Monzel, A. S., Enríquez, J. A. & Picard, M. Multifaceted mitochondria: moving mitochondrial science beyond function and dysfunction. *Nature Metabolism 2023 5:4* **5**, 546–562 (2023).

16. Atamna, H. & Frey, W. H. Mechanisms of mitochondrial dysfunction and energy deficiency in Alzheimer's disease. *Mitochondrion* **7**, 297–310 (2007).

17. Ferrer, I. Altered mitochondria, energy metabolism, voltage-dependent anion channel, and lipid rafts converge to exhaust neurons in Alzheimer's disease. *J. Bioenerg. Biomembr.* **41**, 425–431 (2009).

18. Lopez Sanchez, M. I. G. *et al.* Amyloid precursor protein drives down-regulation of mitochondrial oxidative phosphorylation independent of amyloid beta. *Sci. Rep.* **7**, (2017).

19. Wang, J., Xiong, S., Xie, C., Markesbery, W. R. & Lovell, M. A. Increased oxidative damage in nuclear and mitochondrial DNA in Alzheimer's disease. *J. Neurochem.* **93**, 953–962 (2005).

20. Mao, P. & Reddy, P. H. Aging and amyloid beta-induced oxidative DNA damage and mitochondrial dysfunction in Alzheimer's disease: Implications for early intervention and therapeutics. *Biochim. Biophys. Acta Mol. Basis Dis.* **1812**, 1359–1370 (2011).

21. Dumont, M. *et al.* Reduction of oxidative stress, amyloid deposition, and memory deficit by manganese superoxide dismutase overexpression in a transgenic mouse model of Alzheimer's disease. *The FASEB Journal* **23**, 2459 (2009).

22. Wang, X. *et al.* Amyloid-beta overproduction causes abnormal mitochondrial dynamics via differential modulation of mitochondrial fission/fusion proteins. *Proc. Natl. Acad. Sci. U. S. A.* **105**, 19318–19323 (2008).

23. Wang, X. *et al.* Impaired Balance of Mitochondrial Fission and Fusion in Alzheimer's Disease. *The Journal of Neuroscience* **29**, 9090 (2009).

24. Calkins, M. J., Manczak, M., Mao, P., Shirendeb, U. & Reddy, P. H. Impaired mitochondrial biogenesis, defective axonal transport of mitochondria, abnormal mitochondrial dynamics and synaptic degeneration in a mouse model of Alzheimer's disease. *Hum. Mol. Genet.* **20**, 4515–4529 (2011).

25. Cai, Q. & Tammineni, P. Mitochondrial Aspects of Synaptic Dysfunction in Alzheimer's Disease. *J. Alzheimers Dis.* **57**, 1087 (2017).

26. Briggs, C. A., Chakroborty, S. & Stutzmann, G. E. Emerging Pathways Driving Early Synaptic Pathology in Alzheimer's Disease. *Biochem. Biophys. Res. Commun.* **483**, 988 (2016).

27. Hu, Y. *et al.* Tau accumulation impairs mitophagy via increasing mitochondrial membrane potential and reducing mitochondrial Parkin. *Oncotarget* **7**, 17356 (2016).

28. Green, K. N. & LaFerla, F. M. Linking Calcium to Aβ and Alzheimer's Disease. *Neuron* **59**, 190–194 (2008).

29. Goel, P. *et al.* Neuronal cell death mechanisms in Alzheimer's disease: An insight. *Front. Mol. Neurosci.* **15**, 937133 (2022).

30. Calvo-Rodriguez, M. *et al.* Increased mitochondrial calcium levels associated with neuronal death in a mouse model of Alzheimer's disease. *Nat. Commun.* **11**, 2146 (2020).

31. Csordás, G. & Hajnóczky, G. SR/ER-mitochondrial local communication: Calcium and ROS. *Biochim. Biophys. Acta* **1787**, 1352 (2009).

32. Booth, D. M., Enyedi, B., Geiszt, M., Várnai, P. & Hajnóczky, G. Redox Nanodomains Are Induced by and Control Calcium Signaling at the ER-Mitochondrial Interface. *Mol. Cell* **63**, 240–248 (2016).

33. Schon, E. A. & Area-Gomez, E. Is Alzheimer's disease a disorder of mitochondria-associated membranes? *Journal of Alzheimer's Disease* **20**, 281–292 (2010).

34. Garrido-Maraver, J., Loh, S. H. Y. & Martins, L. M. Forcing contacts between mitochondria and the endoplasmic reticulum extends lifespan in a Drosophila model of Alzheimer's disease. *Biol. Open* **9**, bio047530 (2020).

35. Adami, P. V. M. *et al.* Perturbed mitochondria–ER contacts in live neurons that model the amyloid pathology of Alzheimer's disease. *J. Cell Sci.* **132**, jcs229906 (2019).

36. Moltedo, O., Remondelli, P. & Amodio, G. The Mitochondria–Endoplasmic Reticulum Contacts and Their Critical Role in Aging and Age-Associated Diseases. *Front. Cell Dev. Biol.* **7**, 172 (2019).

37. Leal, N. S. *et al.* Amyloid β-Peptide Increases Mitochondria-Endoplasmic Reticulum Contact Altering Mitochondrial Function and Autophagosome Formation in Alzheimer's Disease-Related Models. *Cells* **9**, 2552 (2020).

38. Völgyi, K. *et al.* Early Presymptomatic Changes in the Proteome of Mitochondria-Associated Membrane in the APP/PS1 Mouse Model of Alzheimer's Disease. *Mol. Neurobiol.* **55**, 7839–7857 (2018).

39. Xie, Q. *et al.* ABT737 reverses cisplatin resistance by regulating ER-mitochondria Ca2+ signal transduction in human ovarian cancer cells. *Int. J. Oncol.* **49**, 2507–2519 (2016).

40. Madreiter-Sokolowski, C. T. *et al.* Resveratrol Specifically Kills Cancer Cells by a Devastating Increase in the Ca2+ Coupling Between the Greatly Tethered Endoplasmic Reticulum and Mitochondria. *Cell. Physiol. Biochem.* **39**, 1404–1420 (2016).

41. Magalhães Rebelo, A. P. *et al.* Chemical Modulation of Mitochondria–Endoplasmic Reticulum Contact Sites. *Cells 2020, Vol. 9,* **9**, (2020).

42. Shi, X., Zhao, M., Fu, C. & Fu, A. Intravenous administration of mitochondria for treating experimental Parkinson's disease. *Mitochondrion* **34**, 91–100 (2017).

43. Chang, C. Y., Liang, M. Z. & Chen, L. Current progress of mitochondrial transplantation that promotes neuronal regeneration. *Translational Neurodegeneration 2019 8:1* **8**, 17- (2019).

44. Del Prete, D. *et al.* Localization and Processing of the Amyloid-β Protein Precursor in Mitochondria-Associated Membranes. *Journal of Alzheimer's Disease* **55**, 1549 (2017).

45. Calì, T., Ottolini, D., Negro, A. & Brini, M. Enhanced parkin levels favor ER-mitochondria crosstalk and guarantee Ca2 + transfer to sustain cell bioenergetics. *Biochimica et Biophysica Acta (BBA) - Molecular Basis of Disease* **1832**, 495–508 (2013).

46. Sathyamurthy, V. H., Nagarajan, Y. & Parvathi, V. D. Mitochondria-Endoplasmic Reticulum Contact Sites (MERCS): A New Axis in Neuronal Degeneration and Regeneration. *Molecular Neurobiology 2024 61:9* **61**, 6528–6538 (2024).

47. Wang, T. & Jia, H. The Sigma Receptors in Alzheimer's Disease: New Potential Targets for Diagnosis and Therapy. *Int. J. Mol. Sci.* **24**, 12025 (2023).

48. De Plano, L. M., Calabrese, G., Rizzo, M. G., Oddo, S. & Caccamo, A. The Role of the Transcription Factor Nrf2 in Alzheimer's Disease: Therapeutic Opportunities. *Biomolecules* **13**, 549 (2023).

49. Jia, H., Zhang, Y. & Huang, Y. Imaging sigma receptors in the brain: New opportunities for diagnosis of Alzheimer's disease and therapeutic development. *Neurosci. Lett.* **691**, 3–10 (2019).

50. Leal, N. S. *et al.* Amyloid β-Peptide Increases Mitochondria-Endoplasmic Reticulum Contact Altering Mitochondrial Function and Autophagosome Formation in Alzheimer's Disease-Related Models. *Cells* **9**, 2552 (2020).

51. Chai, Y. L. *et al.* Mitochondrial Translocase of the Outer Membrane Alterations May Underlie Dysfunctional Oxidative Phosphorylation in Alzheimer's Disease. *Journal of Alzheimer's Disease* **61**, 793–801 (2017).

52. Perreault, S., Bousquet, O., Lauzon, M., Paiement, J. & Leclerc, N. Increased Association Between Rough Endoplasmic Reticulum Membranes and Mitochondria in Transgenic Mice That Express P301L Tau. *J. Neuropathol. Exp. Neurol.* **68**, 503–514 (2009).

53. Hedskog, L. *et al.* Modulation of the endoplasmic reticulum-mitochondria interface in Alzheimer's disease and related models. *Proc. Natl. Acad. Sci. U. S. A.* **110**, 7916–7921 (2013).

54. Area-Gomez, E. *et al.* Upregulated function of mitochondria-associated ER membranes in Alzheimer disease. *EMBO J.* **31**, 4106–4123 (2012).

55. Fernandes, T. *et al.* Structural and Functional Alterations in Mitochondria-Associated Membranes (MAMs) and in Mitochondria Activate Stress Response Mechanisms in an In Vitro Model of Alzheimer's Disease. *Biomedicines* **9**, (2021).

56. Eysert, F. *et al.* Molecular Dysfunctions of Mitochondria-Associated Membranes (MAMs) in Alzheimer's Disease. *Int. J. Mol. Sci.* **21**, 1–29 (2020).

57. Li, X., Yang, Q., Liu, S., Song, S. & Wang, C. Mitochondria-associated endoplasmic reticulum membranes promote mitochondrial fission through AKAP1-Drp1 pathway in podocytes under high glucose conditions. *Exp. Cell Res.* **424**, 113512 (2023).

58. Fernandez-Sanz, C. *et al.* ACTIN Anchors the Highly Oligomeric DRP1 at Mitochondria-Sarcoplasmic Reticulum Contact Sites in Adult Murine Heart: Its Functional Implication. *bioRxiv* 2021.11.29.470468 (2021) doi:10.1101/2021.11.29.470468.

59. McLelland, G. L. *et al.* Mfn2 ubiquitination by PINK1/parkin gates the p97-dependent release of ER from mitochondria to drive mitophagy. *Elife* **7**, e32866 (2018).

60. Wang, X., Su, B., Fujioka, H. & Zhu, X. Dynamin-like protein 1 reduction underlies mitochondrial morphology and distribution abnormalities in fibroblasts from sporadic Alzheimer's disease patients. *Am. J. Pathol.* **173**, 470–482 (2008).

61. Kandimalla, R. *et al.* Reduced dynamin-related protein 1 protects against phosphorylated Tau-induced mitochondrial dysfunction and synaptic damage in Alzheimer's disease. *Hum. Mol. Genet.* **25**, 4881 (2016).

62. Naon, D. *et al.* Critical reappraisal confirms that Mitofusin 2 is an endoplasmic reticulum-mitochondria tether. *Proc. Natl. Acad. Sci. U. S. A.* **113**, 11249–11254 (2016).

63. David, D. C. *et al.* Proteomic and functional analyses reveal a mitochondrial dysfunction in P301L tau transgenic mice. *Journal of Biological Chemistry* **280**, 23802–23814 (2005).

64. Li, X. C. *et al.* Human wild-type full-length tau accumulation disrupts mitochondrial dynamics and the functions via increasing mitofusins. *Sci. Rep.* **6**, (2016).

65. Vance, J. E., Stone, S. J. & Faust, J. R. Abnormalities in mitochondria-associated membranes and phospholipid biosynthetic enzymes in the mnd/mnd mouse model of neuronal ceroid lipofuscinosis. *Biochimica et Biophysica Acta - Lipids and Lipid Metabolism* **1344**, 286–299 (1997).

66. Aaltonen, M. J., Alecu, I., König, T., Bennett, S. A. L. & Shoubridge, E. A. Serine palmitoyltransferase assembles at ER-mitochondria contact sites. *Life Sci. Alliance* **5**, (2021).

67. Roca-Agujetas, V. *et al.* Cholesterol alters mitophagy by impairing optineurin recruitment and lysosomal clearance in Alzheimer's disease. *Mol. Neurodegener.* **16**, (2021).

68. Area-Gomez, E. *et al.* Presenilins Are Enriched in Endoplasmic Reticulum Membranes Associated with Mitochondria. *Am. J. Pathol.* **175**, 1810 (2009).

69. Zampese, E. *et al.* Presenilin 2 modulates endoplasmic reticulum (ER)-mitochondria interactions and Ca2+ cross-talk. *Proc. Natl. Acad. Sci. U. S. A.* **108**, 2777–2782 (2011).

70. Tambini, M. D. *et al.* ApoE4 upregulates the activity of mitochondria-associated ER membranes. *EMBO Rep.* **17**, 27 (2015).

71. Rueter, J., Rimbach, G., Bilke, S., Tholey, A. & Huebbe, P. Readdressing the Localization of Apolipoprotein E (APOE) in Mitochondria-Associated Endoplasmic Reticulum (ER) Membranes (MAMs): An Investigation of the Hepatic Protein–Protein Interactions of APOE with the Mitochondrial Proteins Lon Protease (LONP1), Mitochondrial Import Receptor Subunit TOM40 (TOMM40) and Voltage-Dependent Anion-Selective Channel 1 (VDAC1). *Int. J. Mol. Sci.* **25**, 10597 (2024).

72. Calvo-Rodriguez, M., Hernando-Perez, E., Nuñez, L. & Villalobos, C. Amyloid β oligomers increase ER-mitochondria Ca2+ cross talk in young hippocampal neurons and exacerbate aging-induced intracellular Ca2+ remodeling. *Front. Cell. Neurosci.* **13**, 420256 (2019).

73. Area-Gomez, E. & Schon, E. A. Mitochondria-associated ER membranes and Alzheimer Disease. *Curr. Opin. Genet. Dev.* **38**, 90 (2016).

74. Maurice, T., Grégoire, C. & Espallergues, J. Neuro(active)steroids actions at the neuromodulatory sigma1 (sigma1) receptor: biochemical and physiological evidences, consequences in neuroprotection. *Pharmacol. Biochem. Behav.* **84**, 581–597 (2006).

75. Jin, J. L., Fang, M., Zhao, Y. X. & Liu, X. Y. Roles of sigma-1 receptors in Alzheimer's disease. *Int. J. Clin. Exp. Med.* **8**, 4808 (2015).

76. Arimon, M. *et al.* Oxidative stress and lipid peroxidation are upstream of amyloid pathology. *Neurobiol. Dis.* **84**, 109–119 (2015).

77. Casas-Martinez, J. C., Samali, A. & McDonagh, B. Redox regulation of UPR signalling and mitochondrial ER contact sites. *Cell. Mol. Life Sci.* **81**, 250 (2024).

78. Kunja, C., Kumar, V., Kodam, P., Gopu, C. D. & Maity, S. ER stress sensors at the ER-mitochondrial interface, controlling mitochondrial health in neurodegenerative diseases. *Front. Neurosci.* **19**, 1665272 (2025).

79. Verfaillie, T. *et al.* PERK is required at the ER-mitochondrial contact sites to convey apoptosis after ROS-based ER stress. *Cell Death Differ.* **19**, 1880 (2012).

80. Sassano, M. L. *et al.* PERK recruits E-Syt1 at ER–mitochondria contacts for mitochondrial lipid transport and respiration. *Journal of Cell Biology* **222**, (2023).

81. Branca, C. *et al.* Genetic reduction of Nrf2 exacerbates cognitive deficits in a mouse model of Alzheimer's disease. *Hum. Mol. Genet.* **26**, 4823 (2017).

82. Ramsey, C. P. *et al.* Expression of Nrf2 in Neurodegenerative Diseases. *J. Neuropathol. Exp. Neurol.* **66**, 75 (2007).

83. Neuroprotective effects of transcription factor NRF2 in Alzheimer's disease mice models | VJDementia. https://www.vjdementia.com/video/7nfpfdrk26g-neuroprotective-effects-of-transcription-factor-nrf2-in-alzheimers-disease-mice-models/.

84. Bahn, G. *et al.* NRF2/ARE pathway negatively regulates BACE1 expression and ameliorates cognitive deficits in mouse Alzheimer's models. *Proc. Natl. Acad. Sci. U. S. A.* **116**, 12516–12523 (2019).

85. Luo, L., Martin-Morris, L. E. & White, K. Identification, secretion, and neural expression of APPL, a Drosophila protein similar to human amyloid protein precursor. *The Journal of Neuroscience* **10**, 3849 (1990).

86. Luo, L., Tully, T. & White, K. Human amyloid precursor protein ameliorates behavioral deficit of flies deleted for Appl gene. *Neuron* **9**, 595–605 (1992).

87. Rosen, D. R., Martin-Morris, L., Luo, L. & White, K. A Drosophila gene encoding a protein resembling the human beta-amyloid protein precursor. *Proc. Natl. Acad. Sci. U. S. A.* **86**, 2478 (1989).

88. Lorent, K. *et al.* Expression in mouse embryos and in adult mouse brain of three members of the amyloid precursor protein family, of the alpha-2-macroglobulin receptor/low density lipoprotein receptor-related protein and of its ligands apolipoprotein E, lipoprotein lipase,…. *Neuroscience* **65**, 1009–1025 (1995).

89. Korte, M., Herrmann, U., Zhang, X. & Draguhn, A. The role of APP and APLP for synaptic transmission, plasticity, and network function: lessons from genetic mouse models. *Exp. Brain Res.* **217**, 435–440 (2012).

90. Li, L., Ohman, T., Deeb, S. S. & Fukuchp, K. I. Analysis of mouse intron 7 DNA sequence of the APP gene: comparison with the human homologue. *DNA Seq.* **10**, 219–228 (1999).

91. Beecham, G. W. *et al.* Genome-wide Association Study Implicates a Chromosome 12 Risk Locus for Late-Onset Alzheimer Disease. *Am. J. Hum. Genet.* **84**, 35 (2009).

92. Belyaev, N. D. *et al.* The Transcriptionally Active Amyloid Precursor Protein (APP) Intracellular Domain Is Preferentially Produced from the 695 Isoform of APP in a β-Secretase-dependent Pathway. *Journal of Biological Chemistry* **285**, 41443–41454 (2010).

93. Chau, D. D. L., Ng, L. L. H., Zhai, Y. & Lau, K. F. Amyloid precursor protein and its interacting proteins in neurodevelopment. *Biochem. Soc. Trans.* **51**, 1647 (2023).

94. Masters, C. L. *et al.* Amyloid plaque core protein in Alzheimer disease and Down syndrome. *Proc. Natl. Acad. Sci. U. S. A.* **82**, 4245 (1985).

95. Gabuzda, D., Busciglio, J., Chen, L. B., Matsudaira, P. & Yankner, B. A. Inhibition of energy metabolism alters the processing of amyloid precursor protein and induces a potentially amyloidogenic derivative. *Journal of Biological Chemistry* **269**, 13623–13628 (1994).

96. Allinson, T. M. J., Parkin, E. T., Turner, A. J. & Hooper, N. M. ADAMs family members as amyloid precursor protein alpha-secretases. *J. Neurosci. Res.* **74**, 342–352 (2003).

97. Cai, H. *et al.* BACE1 is the major beta-secretase for generation of Abeta peptides by neurons. *Nat. Neurosci.* **4**, 233–234 (2001).

98. Multhaup, G., Huber, O., Buée, L. & Galas, M. C. Amyloid Precursor Protein (APP) Metabolites APP Intracellular Fragment (AICD), Aβ42, and Tau in Nuclear Roles. *J. Biol. Chem.* **290**, 23515 (2015).

99. Dulubova, I., Ho, A., Huryeva, I., Südhof, T. C. & Rizo, J. Three-Dimensional Structure of an Independently Folded Extracellular Domain of Human Amyloid-β Precursor Protein†,‡. *Biochemistry* **43**, 9583–9588 (2004).

100. Hynes, T. R. *et al.* X-ray crystal structure of the protease inhibitor domain of Alzheimer's amyloid .beta.-protein precursor. *Biochemistry* **29**, 10018–10022 (2002).

101. Rossjohn, J. *et al.* Crystal structure of the N-terminal, growth factor-like domain of Alzheimer amyloid precursor protein. *Nature Structural Biology 1999 6:4* **6**, 327–331 (1999).

102. Wagner, S. L., Siegel, R. S., Vedvick, T. S., Raschke, W. C. & Van Nostrand, W. E. High level expression, purification, and characterization of the Kunitz-type protease inhibitor domain of protease nexin-2/amyloid beta-protein precursor. *Biochem. Biophys. Res. Commun.* **186**, 1138–1145 (1992).

103. Khalifa, N. Ben *et al.* Structural features of the KPI domain control APP dimerization, trafficking, and processing. *The FASEB Journal* **26**, 855–867 (2012).

104. Lee, M. S. *et al.* APP processing is regulated by cytoplasmic phosphorylation. *Journal of Cell Biology* **163**, 83–95 (2003).

105. Zhang, T., Chen, D. & Lee, T. H. Phosphorylation Signaling in APP Processing in Alzheimer's Disease. *Int. J. Mol. Sci.* **21**, (2019).

106. Walter, J., Schindzielorz, A., Hartung, B. & Haass, C. Phosphorylation of the β-Amyloid Precursor Protein at the Cell Surface by Ectocasein Kinases 1 and 2. *Journal of Biological Chemistry* **275**, 23523–23529 (2000).

107. Da Cruz Silva, E. E. F., Da Cruz Silva, E. O. A., Zaia, C. T. & Greengard, P. Inhibition of protein phosphatase 1 stimulates secretion of Alzheimer amyloid precursor protein. *Mol. Med.* **1**, 535–541 (1995).

108. Feyt, C. *et al.* Phosphorylation of APP695 at Thr668 decreases γ-cleavage and extracellular Aβ. *Biochem. Biophys. Res. Commun.* **357**, 1004–1010 (2007).

109. Lu, P. J., Wulf, G., Zhou, X. Z., Davies, P. & Lu, K. P. The prolyl isomerase Pin1 restores the function of Alzheimer-associated phosphorylated tau protein. *Nature* **399**, 784–788 (1999).

110. Wang, Y. & Ha, Y. The X-ray structure of an antiparallel dimer of the human amyloid precursor protein E2 domain. *Mol. Cell* **15**, 343–353 (2004).

111. Kroenke, C. D., Ziemnicka-Kotula, D., Xu, J., Kotula, L. & Palmer, A. G. Solution Conformations of a Peptide Containing the Cytoplasmic Domain Sequence of the β Amyloid Precursor Protein†. *Biochemistry* **36**, 8145–8152 (1997).

112. Gralle, M., Botelho, M. M., De Oliveira, C. L. P., Torriani, I. & Ferreira, S. T. Solution studies and structural model of the extracellular domain of the human amyloid precursor protein. *Biophys. J.* **83**, 3513–3524 (2002).

113. Gralle, M. & Ferreira, S. T. Structure and functions of the human amyloid precursor protein: The whole is more than the sum of its parts. *Prog. Neurobiol.* **82**, 11–32 (2007).

114. Young-Pearse, T. L., Chen, A. C., Chang, R., Marquez, C. & Selkoe, D. J. Secreted APP regulates the function of full-length APP in neurite outgrowth through interaction with integrin beta1. *Neural Dev.* **3**, 1–14 (2008).

115. Rice, H. C. *et al.* Secreted Amyloid-β Precursor Protein Functions as a GABABR1a Ligand to Modulate Synaptic Transmission. *Science* **363**, (2019).

116. Beher, D., Hesse, L., Masters, C. L. & Multhaup, G. Regulation of Amyloid Protein Precursor (APP) Binding to Collagen and Mapping of the Binding Sites on APP and Collagen Type I. *Journal of Biological Chemistry* **271**, 1613–1620 (1996).

117. Tachida, Y. *et al.* O-GalNAc glycosylation determines intracellular trafficking of APP and Aβ production. *Journal of Biological Chemistry* **299**, 104905 (2023).

118. Soba, P. *et al.* Homo- and heterodimerization of APP family members promotes intercellular adhesion. *EMBO Journal* **24**, 3624–3634 (2005).

119. Scheuermann, S. *et al.* Homodimerization of Amyloid Precursor Protein and Its Implication in the Amyloidogenic Pathway of Alzheimer's Disease. *Journal of Biological Chemistry* **276**, 33923–33929 (2001).

120. Barber, D., Salinas-Salinas, C., Houmam, S., Shukla, K. & Rice, H. C. sAPPα Inhibits Neurite Outgrowth in Primary Mouse Neurons via GABA B Receptor Subunit 1a. *eNeuro* **13**, ENEURO.0345-25.2026 (2026).

121. Billnitzer, A. J., Barskaya, I., Yin, C. & Perez, R. G. APP independent and dependent effects on neurite outgrowth are modulated by the receptor associated protein (RAP). *J. Neurochem.* **124**, 123–132 (2013).

122. Bhattacharyya, R. *et al.* Axonal generation of amyloid-β from palmitoylated APP in mitochondria-associated endoplasmic reticulum membranes. *Cell Rep.* **35**, (2021).

123. Copenhaver, P. F. & Ramaker, J. M. NEURONAL MIGRATION DURING DEVELOPMENT AND THE AMYLOID PRECURSOR PROTEIN. *Curr. Opin. Insect Sci.* **18**, 1 (2016).

124. Dawkins, E. & Small, D. H. Insights into the physiological function of the β-amyloid precursor protein: beyond Alzheimer's disease. *J. Neurochem.* **129**, 756 (2014).

125. Tyan, S. H. *et al.* Amyloid precursor protein (APP) regulates synaptic structure and function. *Mol. Cell. Neurosci.* **51**, 43 (2012).

126. Hasebe, N. *et al.* Soluble β-amyloid Precursor Protein Alpha Binds to p75 Neurotrophin Receptor to Promote Neurite Outgrowth. *PLoS One* **8**, e82321 (2013).

127. Erdinger, S. *et al.* Lack of APLP1 leads to subtle alterations in neuronal morphology but does not affect learning and memory. *Front. Mol. Neurosci.* **15**, 1028836 (2022).

128. Von Koch, C. S. *et al.* Generation of APLP2 KO Mice and Early Postnatal Lethality in APLP2/APP Double KO Mice. *Neurobiol. Aging* **18**, 661–669 (1997).

129. Müller, T. *et al.* Modulation of Gene Expression and Cytoskeletal Dynamics by the Amyloid Precursor Protein Intracellular Domain (AICD). *Mol. Biol. Cell* **18**, 201 (2007).

130. Kamal, A., Stokin, G. B., Yang, Z., Xia, C. H. & Goldstein, L. S. B. Axonal Transport of Amyloid Precursor Protein Is Mediated by Direct Binding to the Kinesin Light Chain Subunit of Kinesin-I. *Neuron* **28**, 449–459 (2000).

131. Otero, M. G. *et al.* Proteasome stress leads to APP axonal transport defects by promoting its amyloidogenic processing in lysosomes. *J. Cell Sci.* **131**, (2018).

132. Kamal, A., Stokin, G. B., Yang, Z., Xia, C. H. & Goldstein, L. S. B. Axonal Transport of Amyloid Precursor Protein Is Mediated by Direct Binding to the Kinesin Light Chain Subunit of Kinesin-I. *Neuron* **28**, 449–459 (2000).

133. Tsatsanis, A., Dickens, S., Kwok, J. C. F., Wong, B. X. & Duce, J. A. Post Translational Modulation of β-Amyloid Precursor Protein Trafficking to the Cell Surface Alters Neuronal Iron Homeostasis. *Neurochem. Res.* **44**, 1367 (2019).

134. Hosseinpour Mashkani, S. M., Bishop, D. P., Westerhausen, M. T., Adlard, P. A. & Golzan, S. M. Alterations in zinc, copper, and iron levels in the retina and brain of Alzheimer's disease patients and the APP/PS1 mouse model. *Metallomics* **16**, (2024).

135. Choy, R. W. Y., Cheng, Z. & Schekman, R. Amyloid precursor protein (APP) traffics from the cell surface via endosomes for amyloid β (Aβ) production in the trans-Golgi network. *Proc. Natl. Acad. Sci. U. S. A.* **109**, E2077–E2082 (2012).

136. Schubert, D., LaCorbiere, M., Saitoh, T. & Cole, G. Characterization of an amyloid beta precursor protein that binds heparin and contains tyrosine sulfate. *Proc. Natl. Acad. Sci. U. S. A.* **86**, 2066 (1989).

137. Furukawa, K. *et al.* Increased activity-regulating and neuroprotective efficacy of alpha-secretase-derived secreted amyloid precursor protein conferred by a C-terminal heparin-binding domain. *J. Neurochem.* **67**, 1882–1896 (1996).

138. Cam, J. A. & Bu, G. Modulation of β-amyloid precursor protein trafficking and processing by the low density lipoprotein receptor family. *Mol. Neurodegener.* **1**, 8 (2006).

139. Anandatheerthavarada, H. K., Biswas, G., Robin, M. A. & Avadhani, N. G. Mitochondrial targeting and a novel transmembrane arrest of Alzheimer's amyloid precursor protein impairs mitochondrial function in neuronal cells. *Journal of Cell Biology* **161**, 41–54 (2003).

140. Walls, K. C. *et al.* Swedish Alzheimer Mutation Induces Mitochondrial Dysfunction Mediated by HSP60 Mislocalization of Amyloid Precursor Protein (APP) and Beta-Amyloid. *Journal of Biological Chemistry* **287**, 30317–30327 (2012).

141. Devi, L., Prabhu, B. M., Galati, D. F., Avadhani, N. G. & Anandatheerthavarada, H. K. Accumulation of Amyloid Precursor Protein in the Mitochondrial Import Channels of Human Alzheimer's Disease Brain Is Associated with Mitochondrial Dysfunction. *The Journal of Neuroscience* **26**, 9057 (2006).

142. Vaillant-Beuchot, L. *et al.* Accumulation of amyloid precursor protein C-terminal fragments triggers mitochondrial structure, function, and mitophagy defects in Alzheimer's disease models and human brains. *Acta Neuropathol.* **141**, 39–65 (2021).

143. Schmidt, C. *et al.* Amyloid precursor protein and amyloid beta-peptide bind to ATP synthase and regulate its activity at the surface of neural cells. *Mol. Psychiatry* **13**, 953–969 (2008).

144. Mi, Y., Qi, G., Brinton, R. D. & Yin, F. Mitochondria-Targeted Therapeutics for Alzheimer's Disease: The Good, the Bad, the Potential. *Antioxid. Redox Signal.* **34**, 611 (2021).

145. Lee, S. E. *et al.* Accumulation of APP-CTF induces mitophagy dysfunction in the iNSCs model of Alzheimer's disease. *Cell Death Discovery 2021 8:1* **8**, 1–10 (2022).

146. Belaidi, A. A. *et al.* Marked Age-Related Changes in Brain Iron Homeostasis in Amyloid Protein Precursor Knockout Mice. *Neurotherapeutics* **15**, 1055–1062 (2018).

147. Rao, S. K. *et al.* Differential proteomic and behavioral effects of long-term voluntary exercise in wild-type and APP-overexpressing transgenics. *Neurobiol. Dis.* **78**, 45 (2015).

148. Verma, A. *et al.* Targeting the overexpressed mitochondrial protein VDAC1 in a mouse model of Alzheimer's disease protects against mitochondrial dysfunction and mitigates brain pathology. *Translational Neurodegeneration 2022 11:1* **11**, 1–30 (2022).

149. Matsumoto, K. *et al.* Overexpression of amyloid precursor protein induces susceptibility to oxidative stress in human neuroblastoma SH-SY5Y cells. *J. Neural Transm. (Vienna)* **113**, 125–135 (2006).

150. Pavlov, P. F., Petersen, C. H., Glaser, E. & Ankarcrona, M. Mitochondrial accumulation of APP and Aβ: significance for Alzheimer disease pathogenesis. *J. Cell. Mol. Med.* **13**, 4137 (2009).

151. An, Y. A. *et al.* Dysregulation of Amyloid Precursor Protein Impairs Adipose Tissue Mitochondrial Function and Promotes Obesity. *Nat. Metab.* **1**, 1243 (2019).

152. Montagna, E. *et al.* In vivo Ca2+ imaging of astrocytic microdomains reveals a critical role of the amyloid precursor protein for mitochondria. *Glia* **67**, 985–998 (2019).

153. Wang, Y. *et al.* Lost region in amyloid precursor protein (APP) through TALEN-mediated genome editing alters mitochondrial morphology. *Sci. Rep.* **6**, (2016).

154. Prete, D. Del, Rice, R. C., Rajadhyaksha, A. M. & D'Adamio, L. Amyloid Precursor Protein (APP) May Act as a Substrate and a Recognition Unit for CRL4CRBN and Stub1 E3 Ligases Facilitating Ubiquitination of Proteins Involved in Presynaptic Functions and Neurodegeneration. *J. Biol. Chem.* **291**, 17209 (2016).

155. Wilson, E. L. & Metzakopian, E. ER-mitochondria contact sites in neurodegeneration: genetic screening approaches to investigate novel disease mechanisms. *Cell Death Differ.* **28**, 1804 (2020).

156. Pavlov, P. F. *et al.* Mitochondrial γ-secretase participates in the metabolism of mitochondria-associated amyloid precursor protein. *FASEB J.* **25**, 78–88 (2011).

157. Takeda, K. PGAM5: A Novel Type of Protein Serine/Threonine Phosphatase That Exists in the Mitochondria. *J. Oral Biosci.* **53**, 122–127 (2011).

158. Chaikuad, A. *et al.* Structures of PGAM5 Provide Insight into Active Site Plasticity and Multimeric Assembly. *Structure(London, England:1993)* **25**, 1089 (2017).

159. Sekine, S. *et al.* Rhomboid protease PARL mediates the mitochondrial membrane potential loss-induced cleavage of PGAM5. *J. Biol. Chem.* **287**, 34635–34645 (2012).

160. Ruiz, K. *et al.* Functional role of PGAM5 multimeric assemblies and their polymerization into filaments. *Nature Communications 2019 10:1* **10**, 531- (2019).

161. Qi, Y. *et al.* The dual role of PGAM5 in inflammation. *Exp. Mol. Med.* **57**, 298–311 (2025).

162. Sugo, M. *et al.* Syntaxin 17 regulates the localization and function of PGAM5 in mitochondrial division and mitophagy. *EMBO J.* **37**, EMBJ201798899- (2018).

163. Lu, W. *et al.* Mitochondrial Protein PGAM5 Regulates Mitophagic Protection against Cell Necroptosis. *PLoS One* **11**, e0147792 (2016).

164. Yu, B. *et al.* Mitochondrial phosphatase PGAM5 modulates cellular senescence by regulating mitochondrial dynamics. *Nature Communications 2020 11:1* **11**, 1–17 (2020).

165. Ruiz, K. *et al.* Functional role of PGAM5 multimeric assemblies and their polymerization into filaments. *Nature Communications 2019 10:1* **10**, 1–16 (2019).

166. Yu, B. *et al.* Mitochondrial phosphatase PGAM5 modulates cellular senescence by regulating mitochondrial dynamics. *Nature Communications 2020 11:1* **11**, 2549- (2020).

167. Ma, K. *et al.* Dynamic PGAM5 multimers dephosphorylate BCL-xL or FUNDC1 to regulate mitochondrial and cellular fate. *Cell Death & Differentiation 2019 27:3* **27**, 1036–1051 (2019).

168. Nag, S. *et al.* PGAM5 is an MFN2 phosphatase that plays an essential role in the regulation of mitochondrial dynamics. *Cell Rep.* **42**, 112895 (2023).

169. Bernkopf, D. B. *et al.* Pgam5 released from damaged mitochondria induces mitochondrial biogenesis via Wnt signaling. *J. Cell Biol.* **217**, 1383 (2018).

170. Hong, J. M. & Lee, S. M. Heme oxygenase-1 protects liver against ischemia/reperfusion injury via phosphoglycerate mutase family member 5-mediated mitochondrial quality control. *Life Sci.* **200**, 94–104 (2018).

171. Yang, J. *et al.* Receptor-mediated mitophagy: a new target of neurodegenerative diseases. *Front. Neurol.* **16**, 1665315 (2025).

172. Zeb, A. *et al.* A novel role of KEAP1/PGAM5 complex: ROS sensor for inducing mitophagy. *Redox Biol.* **48**, 102186 (2021).

173. Chen, G. *et al.* A regulatory signaling loop comprising the PGAM5 phosphatase and CK2 controls receptor-mediated mitophagy. *Mol. Cell* **54**, 362–377 (2014).

174. Li, J. *et al.* Phosphoglycerate mutase 5 initiates inflammation in acute kidney injury by triggering mitochondrial DNA release by dephosphorylating the pro-apoptotic protein Bax. *Kidney Int.* **103**, 115–133 (2023).

175. Zhang, J. *et al.* Role of the RIP3-PGAM5-Drp1 pathway in aluminum-induced PC12 cells necroptosis. *Ecotoxicol. Environ. Saf.* **270**, (2024).

176. Wang, Z., Jiang, H., Chen, S., Du, F. & Wang, X. The Mitochondrial Phosphatase PGAM5 Functions at the Convergence Point of Multiple Necrotic Death Pathways. *Cell* **148**, 228–243 (2012).

177. Zhou, H. *et al.* Inhibitory effect of melatonin on necroptosis via repressing the Ripk3-PGAM5-CypD-mPTP pathway attenuates cardiac microvascular ischemia–reperfusion injury. *J. Pineal Res.* **65**, e12503 (2018).

178. Chen, Y. *et al.* Downregulation of phosphoglycerate mutase 5 improves microglial inflammasome activation after traumatic brain injury. *Cell Death Discovery 2021 7:1* **7**, 290- (2021).

179. Kang, T. B., Yang, S. H., Toth, B., Kovalenko, A. & Wallach, D. Caspase-8 Blocks Kinase RIPK3-Mediated Activation of the NLRP3 Inflammasome. *Immunity* **38**, 27–40 (2013).

180. Holze, C. *et al.* Oxeiptosis, a ROS-induced caspase-independent apoptosis-like cell-death pathway. *Nat. Immunol.* **19**, 130–140 (2018).

181. Lo, S. C. & Hannink, M. PGAM5 tethers a ternary complex containing Keap1 and Nrf2 to mitochondria. *Exp. Cell Res.* **314**, 1789–1803 (2008).

182. Safakli, R. N., Gray, S., Bernardi, N. & Smyrnias, I. Unveiling a novel signalling pathway involving NRF2 and PGAM5 in regulating the mitochondrial unfolded protein response in stressed cardiomyocytes. *Int. J. Biochem. Cell Biol.* **178**, 106704 (2025).

183. Zhong, F. *et al.* The KEAP1/PGAM5/AIFM1-Mediated oxeiptosis pathway in Alzheimer's disease. *Brain Res.* **1845**, 149173 (2024).

184. Loboda, A., Damulewicz, M., Pyza, E., Jozkowicz, A. & Dulak, J. Role of Nrf2/HO-1 system in development, oxidative stress response and diseases: an evolutionarily conserved mechanism. *Cell. Mol. Life Sci.* **73**, 3221 (2016).

185. Chiang, S. K., Chen, S. E. & Chang, L. C. The Role of HO-1 and Its Crosstalk with Oxidative Stress in Cancer Cell Survival. *Cells* **10**, 2401 (2021).

186. Lo, S. C. & Hannink, M. PGAM5, a Bcl-XL-interacting Protein, Is a Novel Substrate for the Redox-regulated Keap1-dependent Ubiquitin Ligase Complex. *Journal of Biological Chemistry* **281**, 37893–37903 (2006).

187. Kobayashi, A. *et al.* Oxidative stress sensor Keap1 functions as an adaptor for Cul3-based E3 ligase to regulate proteasomal degradation of Nrf2. *Mol. Cell. Biol.* **24**, 7130–7139 (2004).

188. O'Mealey, G. B. *et al.* A PGAM5-KEAP1-Nrf2 complex is required for stress-induced mitochondrial retrograde trafficking. *J. Cell Sci.* **130**, 3467–3480 (2017).

189. Wang, S., Zhang, J., Zhang, H., Yang, Y. & Wen, Y. Exploration of mitochondrial autophagy related genes in the diagnosis model construction and molecular marker mining of Alzheimer's disease based on multi-omics integration. *Cell. Mol. Biol. (Noisy-le-grand)* **70**, 114–121 (2024).

190. Serrano-Pozo, A., Frosch, M. P., Masliah, E. & Hyman, B. T. Neuropathological alterations in Alzheimer disease. *Cold Spring Harb. Perspect. Med.* **1**, (2011).

191. Ashleigh, T., Swerdlow, R. H. & Beal, M. F. The role of mitochondrial dysfunction in Alzheimer's disease pathogenesis. *Alzheimer's and Dementia* **19**, 333–342 (2023).

192. Pszczołowska, M. *et al.* Mitochondrial disorders leading to Alzheimer's disease—perspectives of diagnosis and treatment. *GeroScience* vol. 46 2977–2988 Preprint at https://doi.org/10.1007/s11357-024-01118-y (2024).

193. Zhang, C., Rissman, R. A. & Feng, J. Characterization of ATP Alternations in an Alzheimer's Transgenic Mouse Model. *J. Alzheimers Dis.* **44**, 375 (2015).

194. Gasparini, L. *et al.* Energy metabolism inhibition impairs amyloid precursor protein secretion from Alzheimer's fibroblasts. *Neurosci. Lett.* **263**, 197–200 (1999).

195. Li, P. A., Hou, X. & Hao, S. Mitochondrial biogenesis in neurodegeneration. *J. Neurosci. Res.* **95**, 2025–2029 (2017).

196. Singulani, M. P. *et al.* Impairment of PGC-1α-mediated mitochondrial biogenesis precedes mitochondrial dysfunction and Alzheimer's pathology in the 3xTg mouse model of Alzheimer's disease. *Exp. Gerontol.* **133**, (2020).

197. Schreiner, B., Hedskog, L., Wiehager, B. & Ankarcrona, M. Amyloid-β Peptides are Generated in Mitochondria-Associated Endoplasmic Reticulum Membranes. *Journal of Alzheimer's Disease* **43**, 369–374 (2015).

198. Wilkins, H. M. & Swerdlow, R. H. Amyloid precursor protein processing and bioenergetics. *Brain Res. Bull.* **133**, 71–79 (2017).

199. Strope, T. A. & Wilkins, H. M. Amyloid Precursor Protein and Mitochondria. *Curr. Opin. Neurobiol.* **78**, 102651 (2023).

200. Strope, T. A. & Wilkins, H. M. The reciprocal relationship between amyloid precursor protein and mitochondrial function. *J. Neurochem.* **168**, 2275–2284 (2024).

201. Wilkins, H. M. Mitochondrial Localized Amyloid Precursor Protein Alters Mitochondrial Function and Mitophagy. *Alzheimer's & Dementia* **19**, e074226 (2023).

202. Strope, T. A. *et al.* Amyloid-β protein precursor modulates mitophagy and mitochondrial function through its cellular localization. *J. Alzheimers Dis.* **107**, 277 (2025).

203. Nag, S., Szederkenyi, K., Yip, C. M. & McQuibban, G. A. PGAM5 cleavage and oligomerization equilibrates mitochondrial dynamics under stress by regulating DRP1 function. *J. Cell Sci.* **138**, jcs263903 (2025).

204. Baird, L. & Yamamoto, M. The Molecular Mechanisms Regulating the KEAP1-NRF2 Pathway. *Mol. Cell. Biol.* **40**, e00099-20 (2020).

205. Tong, K. I. *et al.* Keap1 Recruits Neh2 through Binding to ETGE and DLG Motifs: Characterization of the Two-Site Molecular Recognition Model. *Mol. Cell. Biol.* **26**, 2887 (2006).

206. Ma, S. *et al.* Targeting mitochondrial phosphatase PGAM5 alleviates ferroptosis and acute pancreatitis by upregulating NRF2-mediated FSP1 expression. *Cell Death Dis.* **17**, 252 (2026).

207. Baird, L. & Yamamoto, M. The Molecular Mechanisms Regulating the KEAP1-NRF2 Pathway. *Mol. Cell. Biol.* **40**, e00099-20 (2020).

208. Chiang, S. K., Chen, S. E. & Chang, L. C. The Role of HO-1 and Its Crosstalk with Oxidative Stress in Cancer Cell Survival. *Cells* **10**, 2401 (2021).

209. Lee, W. S., Ham, W. & Kim, J. Roles of NAD(P)H:quinone Oxidoreductase 1 in Diverse Diseases. . **11**, 1301 (2021).

210. Jaber, S. M. *et al.* Idebenone Has Distinct Effects on Mitochondrial Respiration in Cortical Astrocytes Compared to Cortical Neurons Due to Differential NQO1 Activity. *The Journal of Neuroscience* **40**, 4609 (2020).

211. Haefeli, R. H. *et al.* NQO1-Dependent Redox Cycling of Idebenone: Effects on Cellular Redox Potential and Energy Levels. *PLoS One* **6**, e17963 (2011).

212. Gray, J. P., Karandrea, S., Burgos, D. Z., Jaiswal, A. A. & Heart, E. A. NAD(P)H-dependent Quinone Oxidoreductase 1 (NQO1) and Cytochrome P450 Oxidoreductase (CYP450OR) differentially regulate menadione-mediated alterations in redox status, survival and metabolism in pancreatic β-cells. *Toxicol. Lett.* **262**, 1 (2016).

213. Dinkova-Kostova, A. T. & Talalay, P. NAD(P)H:quinone acceptor oxidoreductase 1 (NQO1), a multifunctional antioxidant enzyme and exceptionally versatile cytoprotector. *Arch. Biochem. Biophys.* **501**, 116–123 (2010).

214. Carr, J. F. *et al.* Heme Oxygenase-1 Supports Mitochondrial Energy Production and Electron Transport Chain Activity in Cultured Lung Epithelial Cells. *Int. J. Mol. Sci.* **21**, 6941 (2020).

215. Lu, W. *et al.* Genetic deficiency of the mitochondrial protein PGAM5 causes a Parkinson's-like movement disorder. *Nat. Commun.* **5**, (2014).

216. Wieckowski, M. R. M. R., Giorgi, C., Lebiedzinska, M., Duszynski, J. & Pinton, P. Isolation of mitochondria-associated membranes and mitochondria from animal tissues and cells. *Nat. Protoc.* **4**, 1582–1590 (2009).

217. Güler, B. E., Krzysko, J. & Wolfrum, U. Isolation and culturing of primary mouse astrocytes for the analysis of focal adhesion dynamics. *STAR Protoc.* **2**, 100954 (2021).

218. Li, P. *et al.* The loss of cardiac SIRT3 decreases metabolic flexibility and proteostasis in an age-dependent manner. *GeroScience 2022 45:2* **45**, 983–999 (2022).

219. Mendez Garcia, M. F. *et al.* Increased cardiac PFK-2 protects against high-fat diet-induced cardiomyopathy and mediates beneficial systemic metabolic effects. *iScience* **26**, 107131 (2023).

220. Leopoldo, A. S. *et al.* Cardiac remodeling in a rat model of diet-induced obesity. *Can. J. Cardiol.* **26**, 423 (2010).

221. Zheng, Z. *et al.* Targeting PGAM5-driven mitochondrial integrated stress response slows ALS progression across subtypes. *Neuron* **22**, 185–212 (2026).

222. Liang, M. Z., Ke, T. L. & Chen, L. Mitochondrial Protein PGAM5 Emerges as a New Regulator in Neurological Diseases. *Front. Mol. Neurosci.* **14**, 730604 (2021).

223. Manczak, M., Calkins, M. J. & Reddy, P. H. Impaired mitochondrial dynamics and abnormal interaction of amyloid beta with mitochondrial protein Drp1 in neurons from patients with Alzheimer's disease: implications for neuronal damage. *Hum. Mol. Genet.* **20**, 2495 (2011).

224. Cho, D. H. *et al.* S-nitrosylation of Drp1 mediates beta-amyloid-related mitochondrial fission and neuronal injury. *Science* **324**, 102–105 (2009).

225. Filadi, R. *et al.* Presenilin 2 Modulates Endoplasmic Reticulum-Mitochondria Coupling by Tuning the Antagonistic Effect of Mitofusin 2. *Cell Rep.* **15**, 2226–2238 (2016).

226. Du, F. *et al.* PINK1 signalling rescues amyloid pathology and mitochondrial dysfunction in Alzheimer's disease. *Brain* **140**, 3233–3251 (2017).

227. App NL-G-F Knock-in | ALZFORUM. https://www.alzforum.org/research-models/app-nl-g-f-knock.

228. Mary, A., Eysert, F., Checler, F. & Chami, M. Mitophagy in Alzheimer's disease: Molecular defects and therapeutic approaches. *Mol. Psychiatry* **28**, 202 (2022).

229. Chakravorty, A., Jetto, C. T. & Manjithaya, R. Dysfunctional Mitochondria and Mitophagy as Drivers of Alzheimer's Disease Pathogenesis. *Front. Aging Neurosci.* **11**, 311 (2019).

230. Houmam, S. *et al.* Protocol to sequentially isolate mouse oligodendrocytes, microglia, endothelial cells, astrocytes, and neurons via magnetic cell sorting. *STAR Protoc.* **6**, (2025).